# Modulation of gene expression by chronic stress in astroglia in hippocampus and prefrontal cortex of the rat

Dissertation
for the award of the degree
**"Doctor of Philosophy" (Ph.D.)"**

GGNB Graduate Program "Molecular Physiology of the Brain"
Faculty of Biology of the Georg-August University, Göttingen

submitted by
**Carolina Araya Callís**

born in
San José, Costa Rica

Göttingen, 2012

Members of the thesis Committee:

**Supervisor/Reviewer:**
**Prof. Dr. Gabriele Flügge**
Laboratory of Clinical Neurobiology
German Primate Center, Göttingen

**Reviewer:**
**Prof. Dr. Swen Hülsmann**
Department of Neuro- and Sensory Physiology
University Medical Center, Göttingen

**Prof. Dr. med. Christine Stadelmann-Nessler**
Institute for Neuropathology,
University Medical Center, Göttingen

Oral examination: April 20th, 2012

## Declaration:

I hereby declare that this submission is my own work and that, to the best of my knowledge and belief, it contains no materials previously published or written by another person nor material which to a substantial extent has been accepted for the award of any other degree of the university or other institute of higher education, except where due acknowledgment has been made in the text.

Göttingen, 2012

_____

CAROLINA ARAYA CALLÍS

# TABLE OF CONTENTS

# Abbreviations

| | |
|---|---|
| 5HT: | Serotonin (5-hydroxytryptamine) |
| 5HT1AR: | Serotonin type 1A receptor |
| ACTH: | Adrenocorticotropin hormone |
| AAV: | Adeno-associated virus |
| ACx: | Anterior cingulate cortex |
| AQP4: | Aquaporin 4 |
| BDNF: | Brain derived neurotrophic factor |
| BSA: | Bovine serum albumin |
| cDNA: | Complementary DNA |
| dsDNA: | Double stranded DNA |
| CIT: | Citalopram |
| CNS: | Central nervous system |
| CRH: | Corticotropin releasing hormone |
| CRS: | Chronic restraint stress |
| CSS: | Chronic social stress |
| DA: | Dopamine |
| DAPI: | 4',6-di-amidino-2-phenylindole |
| DCIT: | Desmethylcitalopram |
| DDCIT: | Didesmethylcitalopram |
| DMEM: | Dulbecco's modified eagle medium |
| DMEM/FBS/PSA: | DMEM/Fetal bovine serum/penicilin-streptomycin-amphotericin B |
| EGFP: | Enhanced green fluorescent protein |
| FBS: | Fetal bovine serum |
| GABA: | Gamma-aminobutyric acid |
| GAPDH: | Glyceraldehyde 3-phosphate dehydrogenase |
| GAS: | General adaptation syndrome |
| GC: | Glucocorticoids |

| | |
|---|---|
| GFAP: | Glial fibrillary acidic protein |
| GLAST: | Sodium-dependent glutamate/aspartate transporter 1; EAA1 |
| GLT-1: | Sodium-dependent glutamate/aspartate transporter 2; EAA2 |
| GRs: | Glucocorticoid receptors |
| HBSS: | Hank's buffered salt solution |
| HMB: | Homogenization buffer |
| HPA axis: | Hypothalamic-pituitary-adrenal axis |
| IBA-1: | Ionized calcium binding adaptor molecule 1 |
| IFs: | Intermediate filaments |
| IL: | Infralimbic |
| ITR: | Inverted terminal repeat |
| Kir4.1: | Inward rectifying potassium channel 4.1 |
| LHPA: | Limbic-hypothalamic-pituitary-adrenal |
| LTP: | Long term potentiation |
| mPFC: | medial prefrontal cortex |
| mRNA: | messenger RNA |
| MDD: | Major depressive disorder |
| MRs: | Mineralocorticoid receptors |
| NA: | Noradrenaline |
| NDRG2: | N-myc downregulated gene 2 |
| Ndrg2S: | N-myc downregulated gene 2, short isoform |
| Ndrg2L: | N-myc downregulated gene 2, long isoform |
| NGS: | Normal goat serum |
| NHS: | Normal horse serum |
| NMDA: | N-methyl-D-aspartate |
| PBS: | Phosphate buffered saline |
| PCR: | Polymerase chain reaction |
| PET: | Positron emission tomography |
| PFA: | Paraformaldehyde |
| PL: | Prelimbic |
| PLL: | Poly-L-lysine |
| PS: | Penicillin-streptomycin |
| PVN: | Paraventricular nucleus |
| RIN: | RNA integrity number |

| | |
|---|---|
| Rpl13a: | 60 S ribosomal protein L13a |
| SNAP-25: | Synaptosomal-associated protein 25 |
| SSRI: | Selective serotonin reuptake inhibitor |
| SDHa: | Succinate dehydrogenase complex, subunit A |
| SO: | Stratum oriens |
| SR: | Stratum radiatum |
| UTR: | Untranslated region |
| WST-1: | Water soluble tetrazolium |
| Ywhaz: | Tyrosine 3-monooxygenase/tryptophan 5-monooxygenase activation protein, zeta polypeptide |

# Abstract

It has been suggested that there are causal relationships between alterations in brain glia and major depression. In order to investigate whether a depressive-like state induces changes in brain astrocytes, we analyzed the modulation of astroglia-specific gene expression in the hippocampus of male rats using two models of chronic stress: chronic social stress (5 weeks, daily confrontations with a dominant male) and chronic restraint stress (3 weeks, immobilization 6h/day). Furthermore, the effects of chronic citalopram administration on hippocampal as well as prefrontal cortex (PFC) gene expression were assessed in the chronic social stress experiment.

The expression of six astroglial genes was determined: N-myc-downregulated gene 2 (Ndrg2), glial fibrillary acidic protein (GFAP), glutamate transporter 1 (GLT-1), glutamate and aspartate transporter (GLAST), aquaporin 4 (AQP4) and the inward rectifying potassium channel 4.1 (Kir4.1). Furthermore, protein analyses in the hippocampus were performed by means of quantitative Western blots. Since so far, there was no reference gene validated for the PFC in experiments where animals were subjected to chronic social stress, the first step was to test several commonly used reference genes for expression stability in this part of the brain. In order to study hemispheric effects of stress in the PFC, the left and right hemispheres were analyzed separately.

The results of astroglial gene expression after chronic stress suggest differential regulation depending of the experimental stress paradigm. Chronic restraint stress altered expression of astroglial genes which have a direct effect on neuronal activity: GLT-1 plays an essential role in glutamate clearance from the synaptic cleft, and Kir4.1 is fundamental in keeping low $K^+$ concentrations in the interstitial space. The upregulation of GLT-1 at the mRNA level and the downregulation of Kir4.1 at the protein level, suggest altered glutamate and potassium ion homeostasis after chronic restraint stress.

Also chronic social stress induced profound changes in astroglia. It downregulated GFAP, which might indicate the presence of resting astrocytes. Whether this represents a pathological process or

is an adaptive mechanism that protects the system from overshooting remains to be elucidated. Chronic social stress also upregulated NDRG2 expression which was not due to alterations in the number of astrocytes, but to changes in the amount of NDRG2 expressed per cell. Altered NDRG2 expression might have an impact on cell proliferation.

The observed changes in gene expression in the hippocampus after chronic social stress were not reversed by a 4-weeks treatment with citalopram, in contrast to previous findings in the dorsal raphe nucleus. However, in the hippocampal formation, citalopram reversed the stress-induced changes in two neuronal genes involved in synaptic transmission, the synaptosomal-associated protein 25 (SNAP-25) and syntaxin-1A. Taken together, these results might indicate that citalopram's therapeutic effects depend on the brain region with its specific neurochemical environment as well as features of the target cells. Also, it appears that restoration of normal astroglial gene expression in the hippocampus is not a prerequisite for the therapeutic effects of citalopram. These findings are in concordance with the hypothesis that chronic antidepressant treatments stimulate plasticity of brain cells; however, glial changes may show a different time course in comparison to neuronal alterations.

In regard to the quantification of gene expression in the PFC, it is not possible to draw clear conclusions because expression of several presumptive reference genes was also affected by the chronic stress, at least in the left PFC. Nonetheless, analysis of reference gene stability revealed that cyclophilin was stably expressed in the right PFC.

Furthermore, in an attempt to gain insight into the potential role of Ndrg2, astrocyte cultures were generated. Since NDRG2 has been previously related to processes of cell proliferation and stabilization of cell morphology, the astrocyte cultures were transduced with AAV vectors expressing two isoforms of Ndrg2 (Ndrg2S and Ndrg2L). EGFP-transduced cultures as well as buffer treated ones were used as controls. Subsequently, morphological measurements, proliferation studies and analysis of gene expression were performed on the astrocytes. The results suggest that the EGFP-transduced cultures were not an appropriate control for transduction, as these cultures showed differences compared to the buffer control in terms of morphological parameters and proliferation. Therefore, it was not possible to conclude if the changes in cell proliferation observed after NDRG2 transduction were related to NDRG2 expression or to the transduction procedure *per se*. No significant changes were observed in the morphological parameters measured, and GFAP quantification did not show significant alterations after NDRG2 transduction while there was a high variability in the results from the different experiments.

# 1 Introduction

## 1.1 Stress and depression

### 1.1.1 Major depressive disorder

Major depression is not a single homogeneous affliction, but a complex disorder responsible for one of the major causes of morbidity worldwide. On average, the number of people who suffer from depression at any given time during their lifespan is in the range of 5% to 9% for women and 2% to 3% for men (DSM-IV 1994). Therefore, major depression represents a serious public health problem.

Major depressive disorder (MDD) is a mood disorder characterized by one or more depressive episodes. Each episode lasts at least 2 weeks and several clinical features are observed, such as an unpleasant (*dysphoric*) mood, intense mental anguish, the inability to experience pleasure (*anhedonia),* and a generalized loss of interest in daily activities. Other symptoms may also appear, like disturbances in sleep (either insomnia or hypersomnia), loss of appetite and weight, loss of energy, restlessness, decreased sex desire, cognitive problems (e.g. lack of concentration and memory deficits), pessimistic thoughts, guilt, indecisiveness and sometimes thoughts about dying and suicide. The diagnosis of depression depends on the presence and continuity of several of the symptoms when there is no clear evidence of any traumatic event shortly before the episode (DSM-IV 1994).

Different biological, psychological and social factors contribute to the development of depression. Compiling evidence suggests that, together with a preexisting vulnerability (either genetic predisposition or social environment conditions), stressful-life events can endanger the physiological and psychological integrity of an organism and trigger the development of affective disorders such as depression (Kendler *et al.* 1999). The

interrelation between depression and chronic stress is also manifested in a series of shared neuroendocrine, immune, physiological and neurochemical changes to be discussed later (Fuchs & Flügge 2002).

## 1.1.2 Current theories of depression

During the 1950's, the gradual accumulation of evidence gathered mainly from pharmacological studies suggested a relation between depression and alterations in monoamine concentrations in the central nervous system (CNS). In those days, it was accidentally discovered that the drugs iproniazid (an antimycobacterial with inhibitory properties on monoamine oxidase) and imipramine (a putative antipsychotic drug) had therapeutic antidepressant effects. Among others, these findings stimulated research in the field, and led to the formulation of the first hypothesis about the pathophysiology of affective disorders in 1965. In the so called "The catecholamine hypothesis of affective disorders", J. Schildkraut proposed that, at least in a subgroup of depressive patients, the illness was associated with deficiencies in catecholamine levels as well as other monoamines in the brain (Schildkraut 1965). Further extended, depression resulted from imbalances in serotonin (5-HT), noradrenaline (NA) and dopamine (DA) neurotransmitter systems in the CNS. Further promising support to this theory came with the discovery of the selective serotonin reuptake inhibitors (SSRIs) and their antidepressant properties, as well as with studies of the serotonin type 1A receptors (5-HT1AR).

However, in spite of a clear role of the monoamine systems in depression, there are also unsolved issues that need to be reconsidered. For example, even with the advent of new drugs, less than 50% of patients show signs of improvement at behavioral and cognitive levels after antidepressant treatment. Moreover, the beneficial effects of antidepressants are affected by a wide spectrum of undesired side-effects and treatment relies on chronic administration, suggesting a delayed response to therapy (Lee *et al.* 2010). Also monoamine depletion studies in healthy humans failed to find a causal relationship to depression (Ruhe *et al.* 2007). Therefore, it is clear that depression cannot be reduced to monoamine abnormalities in the brain, since there is no simple direct relationship between the two factors.

Current studies suggest complex relationships between multiple factors and alternative hypotheses have been postulated. For example, the neurotrophin hypothesis of depression

correlates reduced brain derived neurotrophic factor (BDNF) levels with depression, and the normalization of neurotrophic factor concentrations and behavioral improvement with antidepressant therapy (Castren & Rantamaki 2010, Lee *et al.* 2010). On the other hand, the neuroplasticity hypothesis adduces the impairment of plasticity (understood as the ability of the adult and differentiated brain to adapt functionally and structurally to internal and external stimuli) and cell resilience as important key players in major depressive disorder (McEwen *et al.* 2009, Duman 2002, Kempermann & Kronenberg 2003).

Finally, another line of research directs its attention away from neurons and focuses on glial alterations in mood disorders, as some studies have found major structural and functional changes in these cells in MDD patients and in preclinical models of depression (Banasr *et al.* 2010, Miguel-Hidalgo *et al.* 2010, Rajkowska 2000, Rajkowska & Miguel-Hidalgo 2007).

Nevertheless, it is important to remember that a better understanding of the pathological mechanisms underlying mood disorders can only arise by integrating information gathered from different research areas.

### 1.1.3 Hypothalamic-pituitary-adrenal (HPA) axis and the stress response

Since the concept of "stress" will be constantly referred to throughout this dissertation, it is necessary to establish a clear definition. One of the pioneers in the study of stress was the Hungarian endocrinologist, Hans Selye (1907-1982). His experiments in rats on the analysis of the organism's response to different damaging agents led him to develop his theory on stress known as the general adaptation syndrome (GAS) or biologic stress syndrome. He defined the term "stress" as a nonspecific, stereotyped response of the body to any demand made upon it, and GAS as the syndrome that appeared after exposure to such demands. GAS could be characterized by three phases. The first one represents an "alarm reaction", followed by a second stage of adaptation or resistance, and finally, upon persistent high demanding conditions, a third phase of exhaustion as the energy to cope with the stressor is depleted (Selye 1973, Selye 1998). In his studies, Hans Selye also mentions the term homeostasis (from the Greek *homoios = similar* and *stasis = position,* standing), which was originally coined by W.B. Cannon as an extension to C. Bernard's concept of internal environment, and refers to the coordinated physiological processes aimed to maintain the

organism in a steady state (Cannon 1932). Selye points out that to resist different stressors, the organism regulates its reaction in order to keep homeostasis (Selye 1998). Since that time, the concept of stress has been a topic of intense debate, as it has been generally considered as any response of the organism to a noxious stimulus. However, harmful stimuli do not necessarily represent a real threat to homeostasis, as the elicited response might also be part of adaptive changes to deal with the challenging situation (Koolhaas *et al.* 2011). Therefore, according to Koolhaas *et. al.* (2011), the term stress should be restricted to situations characterized by uncontrollability and unpredictability that exceed the natural regulatory capacity of an organism. As a result, a number of deleterious effects at the physiological and psychological level appear due to the incapacity of the organism to prepare an anticipatory response and to normally recover from the neuroendocrine reaction.

These problems are in part related to dysfunction of the limbic-hypothalamic-pituitary-adrenal (LHPA) system. In general physiological terms, its activation contributes to the mobilization and redistribution of energy and oxygen in preparation to respond to a variety of environmental signals (Koolhaas *et al.* 2011) and it is highly dependent on the presence of complex stimuli which require cortical processing to integrate information based on previous experiences (Fuchs & Flügge 2003). The hypothalamic-pituitary-adrenal (HPA) axis involves the activation and release of the hypothalamic peptide corticotropin releasing hormone (CRH) from the paraventricular nucleus. CRH stimulates the anterior pituitary to release adrenocorticotropin hormone (ACTH), which in turn, acts on the adrenal cortex to stimulate the production of glucocorticoids (GC) (for a detailed review see De Kloet *et al.* 1998, Ulrich-Lai & Herman 2009, Mason 1968). GC transport in the blood stream allows them to reach target tissues, such as the hippocampus and the hypothalamus, which work as a negative feedback control of ACTH secretion to turn off the system (Dallman *et al.* 1972). Glucocorticoids (cortisol in humans and corticosterone in rats) act at two different receptor subtypes: the mineralocorticoid receptors (MRs), which show a high affinity for GC, and the glucocorticoid receptors (GRs), which in spite of lower affinity, show high selectivity and are predominantly activated during periods of high GC levels, such as in stress (Reul & de Kloet 1985). Moreover, MRs and GRs are differentially distributed in the brain; MRs are restricted to limbic regions such as the hippocampus, lateral septum and to a lesser extent in amygdala nuclei, the paraventricular nucleus (PVN) and the locus coeruleus. In contrast, GRs are more widely expressed in the brain in different cell types, but are highly present in the hippocampus, PVN and lateral septum. Corticosteroid effects on neuronal function are

dependent on gene transcription activation upon translocation into the nucleus of the receptor bound to the hormone (Joels & Baram 2009).

After chronic stress, the HPA axis becomes hyperactive, and an increased concentration of glucocorticoids causes downregulation of the glucocorticoid receptors in the hippocampus and the inability to maintain homeostasis (De Kloet *et al.* 1998, Meyer *et al.* 2001).

### 1.1.4 Hippocampus and prefrontal cortex (PFC): role in stress and depression

Cognitive and emotional responses to stress depend on the activation of complex interdependent brain circuits (Cerqueira *et al.* 2008). Converging evidence from neuroimaging and neuropathological studies correlate the pathophysiology of depression with alterations in the limbic-cortical-striatal-pallidal-thalamic circuits and the connections between orbital and medial prefrontal cortex (mPFC), amygdala, hippocampus, ventromedial striatum, thalamic nuclei and the ventral pallidum. Moreover, the orbital and medial prefrontal cortex circuits are further associated with two extended circuits. The first one establishes connections with sensory associated areas in charge of sensory integration and affective characteristics of stimuli, while the second one includes further areas in the prefrontal cortex (like the dorsomedial and dorsal anterolateral PFC, cingulate cortex, entorhinal cortex and posterior parahippocampal cortex) and connects to limbic structures to modulate reactions to emotional stimuli (Drevets *et al.* 2008, Ongur & Price 2000, Saleem *et al.* 2008).

Magnetic resonance imaging (MRI) studies and positron emission tomography (PET) studies have provided morphological and functional evidence of brain abnormalities in patients with affective disorders. The results of such analyses show volume reductions as well as diminished glucose metabolism in several brain regions (Drevets *et al.* 2002, Drevets *et al.* 1997, Drevets *et al.* 1992, Botteron *et al.* 2002). Hippocampal volumetric reductions are a common feature of MDD patients (reviewed in Czéh & Lucassen 2007) as well as reductions in gray matter volume in cingulate structures and orbital and ventrolateral areas in the prefrontal cortex (Drevets *et al.* 2008, Ongur *et al.* 1998).

The hippocampus seems to have an indirect role in emotional processing. The presence of a high number of glucocorticoid receptors as well as its role in HPA axis deactivation render it an important target of the effects of chronic stress, and suggest a possible implication of

the hippocampus in stress related pathologies (De Kloet *et al.* 1998, Fuchs & Flügge 2003, Heuser 1998). On the other hand, the role of the prefrontal cortex is related to a number of higher cognitive tasks, such as the processing of emotions and modulation of stress responses. Similar to the hippocampus, the PFC is also a target of glucocorticoid action and contributes to the negative feedback control of the HPA axis (Diorio *et al.* 1993, Sullivan & Gratton 1999).

Preclinical studies with animal models of stress report the disruption of hippocampal-dependent memory (Luine *et al.* 1994) as well as alterations in structural and functional plasticity after chronic stress. A reduction in volume, diminished cell survival and neurogenesis, atrophy and retraction of apical dendrites in hippocampal pyramidal cells, enumerate some morphological changes observed after chronic social stress (CSS) (Czéh & Lucassen 2007, Czéh *et al.* 2001, Fuchs *et al.* 2006, Magarinos *et al.* 1996, Magarinos *et al.* 1997). Deficits in long term potentiation (LTP) in specific hippocampal pathways after chronic restraint stress (CRS) exemplify functional alterations (Pavlides *et al.* 2002). Similarly, there are volume reductions, dendritic architecture remodeling of pyramidal cells as well as reductions in the number of glia and gliogenesis in the prefrontal cortex (Banasr *et al.* 2007, Czéh *et al.* 2007, Czéh *et al.* 2008, Pérez-Cruz *et al.* 2007, Pérez-Cruz *et al.* 2009).

Originally, according to the cytoarchitectonic criterion used to define the PFC in primates, it was believed that lower mammals lacked this structure. However, after performing connectivity studies as well as comparing functional properties of certain brain regions, it was concluded that a region in the frontal part of the rat brain is homologous to the primate PFC. Thus the rat prefrontal cortex was redefined as the cortical area that receives projections from mediodorsal thalamic nuclei (reviewed by Uylings *et al.* 2003). The rat PFC is grossly divided in two regions: the mPFC, which shares characteristics with the human dorsolateral and medial PFC, and the lateral and ventral region (similar to the primate orbitofrontal cortex) (Cerqueira *et al.* 2008). The mPFC is formed by three subdivisions called the infralimbic (IL), prelimbic (PL) and anterior cingulated cortex (ACx) (Krettek & Price 1977). Each of these regions shows anatomical and physiological differences; for example, the dorsal part (ACx) is associated with motor behavior and the PL has been linked to emotional and cognitive processes, while the ventral IL is regarded as a visceromotor center (Heidbreder & Groenewegen 2003).

Furthermore, the PFC exhibits functional lateralization, which plays a role in the modulation of cognitive and emotional responses to stress, together with hippocampal-mediated control of paraventricular nucleus activity (regulates ACTH release from the anterior pituitary gland). In basal conditions, the left prefrontal cortex inhibits the right prefrontal cortex. This mechanism is necessary to keep the balance of PVN function. While PL and ACx as well as the hippocampus decrease PVN activation, IL and amygdala increase PVN function. Therefore, alterations in hemispheric dominance result in PVN activation (Cerqueira *et al.* 2008). Chronic stress induces changes in the hippocampus-PFC network, such as volumetric alterations as well as dendritic retraction of pyramidal neurons in PFC and hippocampus, and impaired long term potentiation within this circuit. As a consequence, there is an impairment of left hemisphere inhibition and dysfunction of the HPA axis after chronic stress (for a detailed review see Cerqueira *et al.* 2008).

## 1.2 Stress paradigms in animals as models of depression

Depression is a complex disorder of multi-factorial origin, which makes it difficult to disentangle the mechanisms underlying this affliction. Stress is a common trigger of depression, and therefore, the use of animal models of depression based on different stress paradigms has become a valuable tool in the study of behavioral and neuroendocrine changes underlying stress-related pathologies. Several stress paradigms have been developed to model depression (Willner 1995, Willner & Mitchell 2002). Among them, two commonly used models are the chronic social defeat (resident/intruder) paradigm (Willner *et al.* 1995, Blanchard *et al.* 2001) and the chronic restraint stress paradigm (McLaughlin *et al.* 2007).

The resident/intruder paradigm of social defeat is based on the naturally occurring territorial behavior of some animal species and social subordination induced by aggressive encounters between the resident and intruder animals (Blanchard *et al.* 2001). Since adult male rats aggressively protect and exclude unfamiliar (intruder) rats from their own territory, these animals can be experimentally used to induce social stress in their counterparts. Also, owing to the social and naturalistic components of the stressor, it is likely that this paradigm elicits a stress response similar to the one observed in humans after stressful life events.

The chronic restraint stress model involves daily immobilization sessions for an extended time period and generates feelings of helplessness due to the inability to escape. While this

type of stressor has a stronger physical component as compared to the first one, it is nonetheless claimed to act primarily as a psychological stressor (McLaughlin *et al.* 2007).

Furthermore, both models of chronic stress exhibit parallels with depression at different levels. Physiological alterations such as body weight reduction as well as signs of HPA axis hyperactivity commonly reported in depressed patients (Weber *et al.* 2000, Heuser 1998) are also induced after both kinds of stress in rats (Abumaria *et al.* 2006, Rygula *et al.* 2005, McLaughlin *et al.* 2007).

Chronic stress has been shown to induce changes in the rat that could be considered behavioral correlates of depressive symptoms in humans. Decreased exploratory behavior (motivational deficits) (D'Aquila *et al.* 2000), increased immobility in the forced swim test (despair) (Porsolt *et al.* 1977) and reduced sucrose preference (anhedonia) (Willner *et al.* 1992) were found after 6 weeks of daily social defeat (Rygula *et al.* 2005). Moreover, antidepressant treatment reversed the negative effects on exploratory behavior and improved reward sensitivity (Rygula *et al.* 2006). Similarly, depressive-like behavior has been observed in chronically restrained rats (3h/d, 21 days) (Naert *et al.* 2010). Also, longer restraint stress sessions (6h/d, 21 days) impaired spatial memory, as shown by a similar number of entries in the novel arm compared to the other arms in the Y-maze test (McLaughlin *et al.* 2007). All together, rat models of chronic social defeat and chronic restraint stress have been used to study central nervous processes that might occur in depression.

## 1.3 Astrocytes and their role in brain function

In 1846, the pathologist Rudolf Virchow was the first to describe cells other than neurons that acted as "connective tissue" in the brain, which he called "Nervenkitt" (nerve glue). Similarly, the term glia, (from the greek γλία, γλοία) also means "glue". But in spite of keeping the original name, the concept of glial cells as passive components in the intricate brain network has radically changed as previously unsuspected and unknown roles have been revealed.

There are two main types of glial cells: microglia, with a different ontogenic origin as other neural cells, represent the macrophages of the brain and spinal cord and scavenge the CNS

for damaged cells, plaques, and infectious agents; and macroglia, which comprise oligodendrocytes, astrocytes and ependymal glia cells.

The most numerous glial cells in the human brain are the astrocytes. In general, the relative number of astrocytes in an organism's brain increases with phylogeny and brain complexity. In simple animals such as *C.elegans,* there is a greater number of neurons compared to astrocytes (in a proportion of 6 to 1) (Sulston *et al.* 1983), whereas in lower mammals, like the rat, the ratio of neurons to astrocytes is 3:1. In the human brain, astrocytes outnumber neurons, as there are 1.4 astrocytes for every neuronal cell (Bass *et al.* 1971, Nedergaard *et al.* 2003). The term "astrocyte" was introduced by Lenhossék (1893) to describe the star-shaped neuroglial cells first discovered by Otto Deiters in the mid 19$^{th}$ century (Ostby *et al.* 2009). Astrocytes are characterized by endfeet that contact the basal lamina around blood vessels and/or pia mater or the vitreous body of the eye. In contrast to ependymoglial cells, astrocytes do not contact the ventricular system (Kettenmann & Ransom 2005).

The astroglia can be classified in protoplasmic and fibrous astrocytes. The protoplasmic astrocytes are found mainly in gray matter and consist of a relatively small soma with several thick processes extending into the neuronal network. These extensions project numerous fine processes that ensheath neuronal somata and dendrites (Theodosis *et al.* 2008). Moreover, each protoplasmic astrocyte establishes its own territory, keeping the extensive network organization by gap junctions and allowing rapid integration of information. Fibrous astrocytes are found in white matter tracts, in the optic nerve, and in the nerve fiber layer of mammalian vascularized retinae. Their somata are often arranged in rows between the axon bundles and extend smooth and long processes. But the surface-to-volume ratio is smaller than protoplasmic astrocytes (Reichenbach & Wolburg 2005).

Far from being passive support cells, astrocytes play a critical role in neuronal function and extracellular homeostasis. They link neuronal activity to energy metabolism and blood flow through the glutamate-glutamine cycle (Van den Berg *et al.* 1969, Waniewski & Martin 1986) and by providing lactate to neurons (for a detailed review see Pellerin & Magistretti 2005). Astrocytes also participate in neural development (survival and differentiation) (Arcangeli *et al.* 1993), migration of neuronal progenitors, regulation of axonal guidance, formation of synapses, brain plasticity, and in regeneration after injury (glial scar) (for a detailed review see Reuss & Unsicker 2005).

Astrocytes play a role in pH control and ionic and neurotransmitter concentration regulation in the extracellular space, ensuring physical and chemical integrity in the CNS. For example, pH regulation by the glial enzyme carbonic anhydrase and an electrogenic $Na^+/HCO_3^-$ co-transport system is essential for neuronal $Ca^{++}$ channel conductance and N-methyl-D-aspartate (NMDA) receptor function. Similarly, the spatial buffering of extracellular $K^+$ ions released by excited neurons guarantees normal neuronal activity (Kuffler *et al.* 1966), and is regulated by at least three mechanisms occurring in astroglia: the astrocytic $Na^+/K^+$ pump, passive cotransport of $K^+$ with other ions and $K^+$ flux through the inward rectifying $K^+$ (Kir) channels (Chen & Nicholson 2000). Furthermore, astrocytes express transporters for different neurotransmission systems (glutamate, glycine, γ-aminobutyric acid (GABA)), which enables the shift of the energetic cost of neurotransmitter uptake away from neurons, avoiding any possible interfering effect on those cells that could arise as a result of the electrogenic uptake system; and keeps glutamate levels under toxic concentrations (Perea *et al.* 2009, Pirttimaki *et al.* 2011, Seth & Koul 2008, Valentine & Sanacora 2009). As a result, astrocytes indirectly modulate synaptic activity at the level of both the amplitude and duration of synaptic transmission.

But astroglia can also directly process and control synaptic information by coordinated bidirectional communication between them and neurons. The classical accepted paradigm that brain function results exclusively from neuronal activity has been challenged as the concept of tripartite synapses has emerged (Araque *et al.* 1999). It has become clear that astrocytes can selectively respond to synaptic activity by spatially regulating elevation of cytosolic $Ca^{2+}$. This can induce the release of gliotransmitters, such as glutamate and adenosine-5'-triphosphate (ATP), and modulate presynaptic neurotransmitter release and postsynaptic efficacy as well as processes such as plasticity and synaptic potentiation (Pirttimaki *et al.* 2011, Fellin & Carmignoto 2004).

Taking all this information together and considering the fact that a single astrocyte might contact a number of ~100 000 synapses, it is clear that astrocytes are cellular elements that process and integrate different synaptic input signals in a well-tuned non linear response that provides the system with a high degree of flexibility (Perea & Araque 2005, Perea *et al.* 2009). It is also not unexpected that astrocytes and other glial cells have been hypothesized to play a role in different neurological disorders, major depression being only one of them (Allaman *et al.* 2011, Mitchelmore *et al.* 2004, Banasr *et al.* 2007).

## 1.4 Glial changes and depression

There is a growing body of information arising from both clinical studies as well as research in animal models of depression about the involvement of glia in the pathophysiology of major depressive disorder.

Histopathological *post mortem* analysis of brain tissue from patients with depression consistently shows cellular composition alterations, including glial cell populations. One study showed a significant reduction in Nissl-stained glial cells number and density in the subgenual prefrontal cortex, whereas neuronal number remained unchanged (Ongur *et al.* 1998). Another study showed that glial fibrillary acidic protein (GFAP) immunoreactivity was diminished in the left orbitofrontal cortex of depressed patients (Miguel-Hidalgo *et al.* 2010). These findings, in combination with alterations in mRNA expression of astrocytic glutamate markers (glial glutamate transporter and glutamine synthetase) detected in the orbitofrontal cortex of *post mortem* samples of MDD patients, suggest altered glutamatergic neurotransmission associated with glial dysfunction in depression (Miguel-Hidalgo *et al.* 2010).

Contrasting results were observed in the hippocampus, where glia density was increased in CA1, CA2, CA3 subfields as well as in the dentate gyrus (Stockmeier *et al.* 2004), but GFAP immunoreactivity in cell bodies and fibers was significantly reduced in the CA1 and CA2 hippocampal regions of patients with major depression and in patients treated chronically with synthetic glucocorticoids (Muller *et al.* 2001). However, it should be considered that GFAP immunoreactivity can only provide a narrow picture of glial changes because it is only present in ~15% of the total volume of an astrocyte (Bushong *et al.* 2002).

The scope of clinical studies is limited and obscured by factors such as sample size or quality, and thus cannot clarify whether these changes are a cause or a consequence of the disorder. Nor do they allow deepening into the molecular mechanisms associated with these changes. However, preclinical studies with animal models of depression have generated valuable information about the etiology of depression as well as the possible changes occurring at the cellular and molecular level.

In the male tree shrew (*Tupaia belangeri),* a decrease in GFAP-positive cell number and cell volume was reported in the hippocampus after chronic social stress (Czéh *et al.* 2006). Similarly, in the prefrontal cortex of this species, cells immunoreactive for GFAP were

reduced after chronic social stress (CSS) in rats (Czéh *et al.* 2007). In both cases, antidepressant therapy inhibited the stress-induced changes in astroglia.

Additionally to the stress-induced alterations at the structural level, disturbances in astrocyte specific gene expression have also been reported (Abumaria *et al.* 2007, Liu *et al.* 2009, Nichols 2003, Reagan *et al.* 2004, Valentine & Sanacora 2009, Zschocke *et al.* 2005). Therefore, the study of stress modulation of gene expression in astrocytes may provide some insight into the mechanisms underlying the pathological changes observed in depression and may contribute to the development of innovative therapies for its treatment.

## 1.5 Glial genes

### 1.5.1 N-myc downregulated gene 2 (Ndrg2)

Ndrg2 belongs to the family of N-myc downregulated genes (Ndrg2), although the mechanisms of Ndrg2 regulation by the transcription factor N-myc are not entirely understood (Okuda & Kondoh 1999, Wielputz *et al.* 2007, Zhang *et al.* 2006). The physiological role of the gene in the organism and especially in brain function is also not clear. It is expressed in a variety of tissues throughout the body; however, in the brain, it is primarily located in glial cells, more specifically in the cytoplasm of astrocytes (Okuda *et al.* 2008). Several studies have indicated this protein's involvement in cell proliferation and differentiation. The analysis of Ndrg2 pattern of expression in mouse embryogenesis revealed an increase during the late stages of development, suggesting a role in tissue differentiation and maintenance (Hu *et al.* 2006). Ndrg2 is found in many regions in the adult brain, with particularly strong mRNA expression in the subgranular zone of the dentate gyrus, which is a neurogenesis active site where astrocytes may promote proliferation and/or differentiation of neuronal progenitor cells (Nichols 2003, Nichols *et al.* 2005). Also, *in vitro* cell culture studies showed increased neurite sprouting, extension and guidance after Ndrg2 induction following nerve growth factor-evoked differentiation in PC12 cells, a neuronal cell line (Takahashi *et al.* 2005a). However, the exact role of Ndrg2 in differentiation vs. proliferation of cells remains unclear. On the one hand, a lack of Ndrg2 decreased myoblast proliferation and supported the onset of myogenesis in skeletal muscle tissue (Foletta *et al.* 2009). But on the other hand, Ndrg2 gene silencing enhanced astrocyte

proliferation in culture, while shortening cell processes and reducing F-actin levels (Takeichi *et al.* 2011).

Furthermore, a large number of studies implicate Ndrg2 in cancer progression and propose a role for it as a tumor suppressor. While low Ndrg2 expression has been detected in colon carcinoma (Kim *et al.* 2009a), transfection of human glioblastoma cells with cDNA encoding Ndrg2 reduced cell proliferation (Deng *et al.* 2003). It is interesting to note that the transcription factor p53, which mediates apoptosis, apparently regulates the transcription of the Ndrg2 gene (Liu *et al.* 2008) (Liu *et al.* 2008).

### 1.5.2 Glial fibrillary acidic protein (GFAP)

The cytoskeleton of eukaryotic cells consists of three different kinds of filament structures which differ in composition and thickness. The microfilaments (or actin filaments) are the tiniest (6-8 nm), followed by the intermediate filaments (IFs) (8-10 nm) and the microtubules (24-26 nm). In the nervous system, IFs are present in both neurons and astrocytes. The glial fibrillary acidic protein, originally isolated from a glial scar of a patient with multiple sclerosis, is the major type III IF expressed in mature astrocytes. Others such as vimentin, nestin and synemin are mainly present in astrocyte precursors and are progressively replaced by GFAP, but are also expressed under pathological conditions (Jing *et al.* 2007). GFAP localizes to the peripheral and CNS. In the brain, it is found in protoplasmic astrocytes of the gray matter, fibrous astrocytes of white matter, radial glia in the cerebellum and tanycytes in the subependymal layer of the ventricles (reviewed in Eng & Ghirnikar 1994).

As a structural component of the cytoskeleton of astrocytes, GFAP is involved in processes such as cell movement (Lepekhin *et al.* 2001) and structural stability and has also been proposed to play a role in cell communication, such as astrocyte–neuron interactions (Nedergaard *et al.* 2003). But it also plays an important role in astrogliosis, which is a spectrum of changes that occur following injury caused by trauma, disease or chemical insult. These alterations are highly dependent on the nature and severity of the injury, and include altered gene expression with remarkably rapid synthesis of GFAP, cellular hypertrophy, as well as cell proliferation and formation of glial scar (Sofroniew 2009, Eng & Ghirnikar 1994). Astrogliosis represents an essential part of the response to insults to the CNS, where it takes part in mechanisms of neural protection and repair as well as regulation

of inflammation; however, chronic astroglial activation could comprise normal astrocyte function and have detrimental effects on brain physiology (Silver & Miller 2004).

Studies on the expression of GFAP after chronic social stress in rats may shed light on the role of astrocytes in depression.

### 1.5.3 Glutamate transporter 1 (GLT-1) and glutamate and aspartate transporter (GLAST)

Glutamate is the major excitatory neurotransmitter released in the brain. However, high concentrations in the synaptic cleft have been known to be associated with neuronal damage (Lucas & Newhouse 1957), which occurs via a mechanism that involves the influx of increased levels of calcium ions ($Ca^{2+}$) and detrimental effects on mitochondrial function, finally leading to cell death (Nicholls & Budd 1998). Therefore, the extracellular concentration of glutamate must be tightly regulated and kept low by the action of glutamate transporters located in the plasma membrane of astrocytes. Two transporters are highly expressed in the brain: GLT-1 (Pines *et al.* 1992) and GLAST (Storck *et al.* 1992). Both are broadly expressed in the CNS and are restricted to astrocytes. GLT-1 is enriched in the hippocampus, lateral septum, cerebral cortex and striatum, while GLAST shows increased density in the Purkinje cell layer of cerebellum, presumably in the Bergmann glia cells, and lower density in other regions of the brain (Lehre *et al.* 1995, Storck *et al.* 1992).

### 1.5.4 Aquaporin 4 (AQP4)

Water homeostasis in the brain is achieved by the aquaporins (AQPs), which represent a family of small, hydrophobic proteins mainly located in the plasma membrane that are involved in bidirectional water movement in the cell (Tait *et al.* 2008). These water channels are widely expressed in different living organisms and in a variety of tissues, where, in order to be functional, are assembled as tetramers (Verkman 2005). Aquaporins are also expressed in the central nervous system, where AQP4 represents the principal type in mammals. In the rat brain, AQP4 was detected in glia limitans, the ependymal lining system, cerebellum, hippocampal dentate gyrus, the supraoptic and paraventricular nuclei of the hypothalamus and, to a lower extent, in the cortex and CA1-CA3 hippocampal layers (Jung *et al.* 1994). Immunohistochemical analysis further localized AQP4 to the end-feet

astrocyte processes that ensheath neuronal elements and blood vessels as well as in ependymal cells (Badaut *et al.* 2002). However, it is not expressed in neurons (Andrew *et al.* 2007). AQP4 is present in two main isoforms, M1 and M23, named after the translation initiation at methionine position 1 or 23, respectively. However, besides differential arrangement in the membrane, no functional differences have been reported (Furman *et al.* 2003).

AQP4 is involved, as previously mentioned, in water flow into the brain across the blood-brain-barrier and out of the brain involving the same path or by ependymal and pial cell transport into the cerebrospinal fluid. But it also plays a role in mechanisms of astrocyte migration and neuronal activity regulation. Studies with AQP4-null mice and AQP4-null cultured cells revealed that lack of the water channel reduced astrocyte migration and was associated with impaired glial scar formation (Saadoun *et al.* 2005). These mice also showed delayed $K^+$ clearance, which could be related to altered neurotransmitter release (Ding *et al.* 2007). Finally, AQP4 has also been found in adult neural stem cells, where it can apparently play a role in proliferation, migration and differentiation (Kong *et al.* 2008).

The study of AQP4 expression in the brain after stress could contribute to finding molecular mechanisms to explain the volumetric changes in certain brain regions observed in depressed patients and animal models of stress, or aid in the identification of other AQP4-dependent altered processes.

### 1.5.5 Inward rectifying channel Kir4.1

In 1993, the first inwardly rectifying $K^+$ (Kir) channel was cloned from a mouse macrophage cell line. Since then, further studies have characterized 16 Kir channel subunits, which have been grouped in seven subfamilies, (Kir1.x-Kir7.x) (reviewed in Olsen & Sontheimer 2008). The term “inwardly rectifying” refers to the property of passing current more readily in the inward direction (into the cell).

The different Kir channels are located in a variety of cell types and differ in terms of degree of rectification, conductance and sensitivity to blockers (Schroder *et al.* 2002). But as a main role, they mediate fast $K^+$ siphoning by passive $K^+$ fluxes through the open channel after neuronal activity (Kofuji *et al.* 2002). Consequently, Kir channels contribute to the maintenance of potassium ion homeostasis (D'Ambrosio *et al.* 1999). Several studies have determined that Kir characteristic currents are abundantly found in astrocytes of the central

nervous system (Akopian *et al.* 1997, Steinhauser *et al.* 1992, Newman 1993, Seifert *et al.* 2009). Specifically, Kir4.1 has been characterized as a weakly rectifying channel in astroglial cells, as concluded from electrophysiological data from wildtype and Kir4.1 knockout mice (Kofuji *et al.* 2000), and molecular expression analyses (Schroder *et al.* 2002). Moreover, immunohistochemistry analysis in the ventral respiratory group located Kir4.1 to astrocytes, where its localization in the cell shifted from the cytoplasm to the end feet processes with developmental maturation (Neusch *et al.* 2006).

Furthermore, besides its role in $K^+$ buffering, it has been suggested that Kir4.1 is also involved in glutamate clearance from the synaptic cleft after neuronal activity (Djukic *et al.* 2007).

## 1.6 Aims of the thesis

The present study aimed to conduct analyses on the effects of chronic stress on astrocyte-specific gene expression in two brain regions important in stress regulation, emotional processing and involved in affective disorders such as depression: namely, the hippocampus and the prefrontal cortex. Moreover, the study also intended to provide insight into the biological relevance of Ndrg2 mRNA and protein regulation after stress.

In the first stage, two different models of stress were tested: chronic restraint stress and chronic social stress. Gene expression analyses were performed in the hippocampus in both models. These experiments showed that genes were differentially modulated at the mRNA level according to the specific stress model. An analysis of protein expression in the restraint stress model was also carried out. At this point, we decided to focus on the results obtained from chronic social stress, as this is a more naturalistic model and represents a better approximation to mimic stress situations in humans.

In the second stage, a chronic social stress experiment with rats was conducted not only to confirm preliminary results at the mRNA level, but also to complement those data with protein quantification analysis data of the hippocampus. This experiment also generated the first set of gene expression analysis results for astrocytes in the prefrontal cortex.

The third stage includes the final experiment in which groups of rats were subjected to chronic social stress and concomitant antidepressant treatment. The aim was to assess the

effect of citalopram, a SSRI, in stress modulated gene expression in the prefrontal cortex and hippocampus.

Finally, in the last phase of the project, Ndrg2, one of the identified stress modulated genes, was selected for further exploration into the implications and physiological significance of changes observed after chronic social stress in the hippocampus. Considering NDRG2's upregulation by chronic social stress and its putative role in cell proliferation and morphology, it was artificially over-expressed in an astrocyte culture by means of a viral vector. Subsequently, cell morphology analyses (immunohistochemistry), as well as proliferation studies were conducted.

# 2 Materials and methods

## 2.1 Experimental animals

Male Wistar rats used in chronic social defeat experiments (Harlan-Winkelmann, Borchen, Germany) weighing between 180-200 g on arrival were housed individually (type II macrolon cages), while male Sprague-Dawley rats used in chronic restraint stress experiments (Harlan-Winkelmann, Borchen, Germany) weighing between 250-300 g on arrival were housed in groups (3/cage) in type IV macrolon cages with food and water available *ad libitum*. The animal facility had a reverse 12h:12h light-dark cycle (light off at 6:00 a.m.) and the temperature was maintained at 21°C. The experiments were conducted during the active phase of the animals, which corresponds to the dark phase, and all experimental manipulations were carried out under dim red light. The animals were randomly assigned into control and stress groups.

Lister Hooded male rats, weighing between 300-350 g (Harlan-Winkelmann, Borchen, Germany) were used as the resident dominant males in the chronic social stress experiments. They were paired with sterilized females and housed in large plastic cages (60 x 40 x 40 cm = l x w x h) in a separate room from the Wistar rats. After arrival, the animals were habituated for two weeks to the animal facilities and were handled daily. All animal experiments were conducted in agreement with the European Communities Council Directive of November 24, 1986, (86/609/ECC), including Position 6106/20 of the EU Council of May 26, 2010, and were approved by the Government of Lower Saxony, Germany.

## 2.2 Chronic psychosocial stress

Wistar rats were assigned into four experimental groups: Control (C), Stress (S), Control-Citalopram (CC) and Stress-Citalopram (SC) (n=15 for C and S, respectively; n=10 for CC

and SC, respectively) (Fig. 1A). Chronic psychosocial stress was induced after the 10 days of habituation period, by means of the resident-intruder paradigm (Rygula *et al.*, 2005).

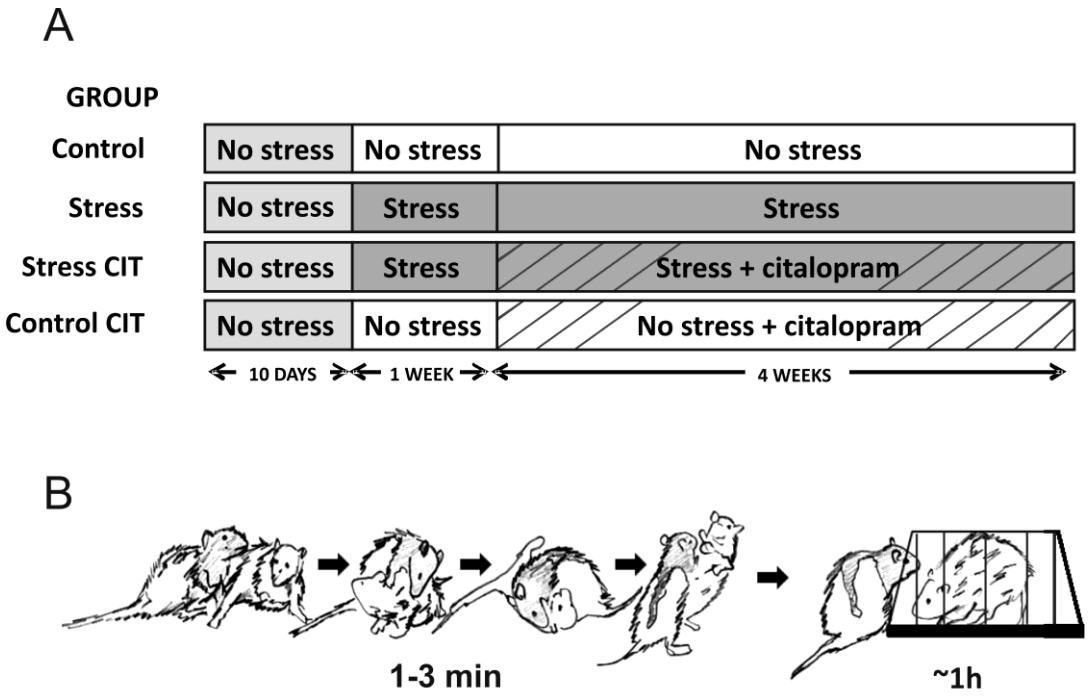


Fig. 1. Chronic psychosocial stress. A) Four groups of male Wistar rats were analyzed: Control, Stress, Control Citalopram and Stress Citalopram. After 10 days of habituation, Stress and Stress CIT animals were subjected to daily social defeat for 5 weeks. Animals in the Stress CIT and Control CIT groups were treated with the antidepressant citalopram daily via the drinking water during four weeks. All animals were sacrificed 24 h after the last stress exposure. B) Social defeat. The intruder is attacked and defeated during the first minutes of physical contact; this is followed by the introduction of the animal into a small cage to protect it from further physical attacks but remaining in olfactory, visual and auditory contact with the dominant male. Finally, after an hour the intruder is returned to its home cage.

The procedure is as follows (Fig. 1B): the intruder is introduced into the resident's home cage after the female has been removed. During the first 1-3 minutes, the resident attacks and defeats the intruder; the latter shows defensive-submissive behavior, freezing behavior and/or flight. From then on, the intruder is placed in a small wire-mesh cage within the resident's home cage for 1 h. In this way, the intruder is protected from further physical injuries, but remains in olfactory, visual and auditory contact with the resident. Afterwards,

the intruder is returned to its home cage. This social defeat procedure was performed every day at 9:00 a. m. Control animals were only handled during the social stress period.

Body weight was registered throughout the 5-weeks experimental period. During the habituation period, body weight was measured three times (on days 2, 5 and 10); afterwards, it was recorded daily prior to social defeat. Body weight gain was calculated as a percentage of the individual baseline body weight at the beginning of the experiment. At the end of the experimental period, 24 h after the last stress exposure, the animals were either decapitated (n= 10 per group) or perfused (n=5, C and S groups). After decapitation, adrenal glands were removed and weighed; weight was expressed as a percentage of body weight. Also, blood samples were collected for corticosterone and testosterone analysis.

## 2.3 Chronic restraint stress

The Sprague Dawley rats were divided into two experimental groups: Control (C) and Stress (S) (n=15 for C and S, respectively) (Fig. 2A). After 10 days of habituation to the animal facility, animals of the stress group were restrained daily for 6 h (9:00-15:00 h) during their activity phase for 21 consecutive days. The restrainer consisted of a well-ventilated polypropylene tube (Fig. 2B). When animals were restrained in the tubes, they had no access to water and food, which was also withheld from the control animals during the restraint session so that the effect of stress on body weight could not simply be a result of limited food and water availability. Body weight was recorded daily before each restraint stress session for the duration of the entire experiment. The animals were sacrificed 24 h after the last stress exposure. After decapitation, the adrenal glands were removed and weighed; weight was expressed as a percentage of body weight. Blood samples were collected for corticosterone and testosterone analysis (kindly conducted by A. Heistermann and Dr. M. Heistermann, German Primate Center, Göttingen, Germany).

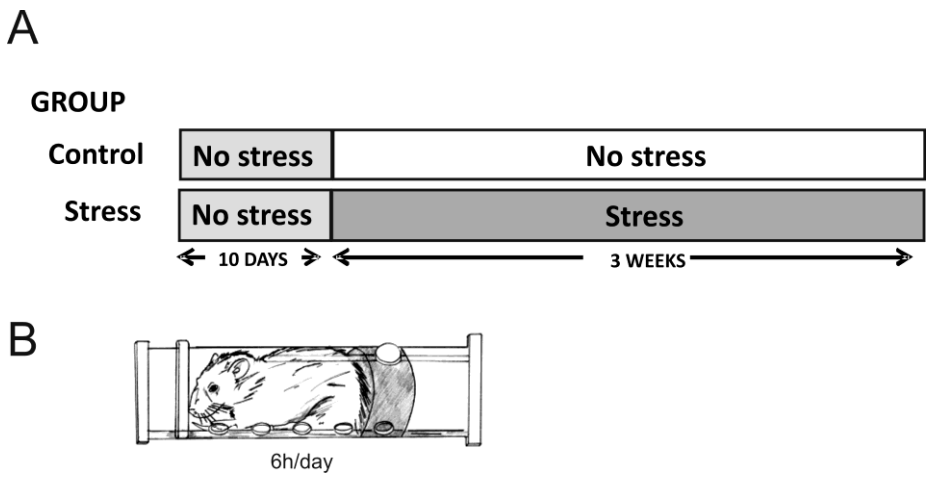


Fig. 2. Chronic restraint stress. A) Two groups of male Sprague Dawley rats were analyzed: Control and Stress. After 10 days of habituation to the animal facility, Stress animals were subjected to 3 weeks of daily restraint stress for 6 h every day. Water and food was withheld during this time from the Control group. B) Rats were restrained in a well-ventilated polypropylene tube.

## 2.4 Chronic administration of citalopram and determination of citalopram and its metabolites in blood

Citalopram (CIT) hydrochloride was kindly supplied by Lundbeck (A/S, Copenhagen, Denmark). In order to reduce stress effects that could be induced by injection, the drug was given orally via drinking water. In accordance with previous experiments (Abumaria *et al.* 2006, Rygula *et al.* 2006), animals were treated chronically with CIT (30 mg/kg) for four weeks starting one week after the beginning of the social stress, while untreated animals received tap water (Fig. 1A). The volume of consumed water was measured daily by weighing the bottles. The amount of drug was adjusted during the experimental period (taking into account body weight and consumed water) and dissolved in the average volume of consumed water (approx. 30 ml/day). The drug solution was prepared freshly every third day and filled into light-protected bottles. The bottles were weighed after preparation (always at 9:00 a.m.) and 24 h later to monitor drug intake. After five weeks of chronic social defeat and concomitant antidepressant treatment, the rats were decapitated and trunk blood as well as brain tissue (neocortex) were collected for the analysis of CIT, DCIT (desmethylcitalopram) and DDCIT (didesmethylcitalopram). Samples were stored at -20 °C and light-protected until assayed for the parent drug and its metabolites. Analysis of CIT,

DCIT and DDCIT was performed by HPLC analysis (kindly performed by Prof. C. Hiemke, University of Mainz, Germany). Data are expressed as ng/ml for blood samples and ng/g of tissue for neocortex samples. In order to compare blood and neocortex cortex values, the ratio of CIT/DCIT and CIT/DDCIT was calculated.

## 2.5 Dissection of the brains

The brains were quickly removed from the crania immediately after decapitation. The dissection of the hippocampus was performed as follows: after the cerebellum and brain stem were removed, a cut between the cortical hemispheres down to the corpus callosum was made. The hemispheres were carefully pried apart and the hippocampal formation was removed using a rounded-tip sterile spatula. Both hippocampi (left and right) were collected. After removing the olfactory bulb, the prefrontal cortex was dissected (levels 5.70 to 4.20 mm from bregma; (Paxinos & Watson 1986), while care was taken to exclude the striatum. The dissected brain regions were immediately frozen over liquid nitrogen and stored at -80 °C for molecular analyses.

## 2.6 Perfusion and brain tissue preparation

Twenty-four hours after the last stress exposure, animals were deeply anesthetized with a mixture of xylazine (50 mg/ml), ketamine (10 mg/ml) and atropine (0.1 mg/ml). Subsequently, the animals were transcardially perfused with cold (4 °C) 0.9% NaCl for 3 minutes followed by cold (4 °C) 4% paraformaldehyde (PFA) in 0.1M phosphate buffer (pH 7.2) for approx. 12 min. The heads were postfixed in fresh 4% PFA at 4°C overnight. The next day, brains were removed from the skulls and immersed in 30% sucrose in phosphate buffer saline (PBS; 0.137 M NaCl, 2.7 mM KCl, 4.3 mM $Na_2HPO_4$•12 $H_2O$, 1.4 mM $KH_2PO_4$; pH=7.2) and incubated at 4°C for two days. The brains were dissected into two blocks that contained the PFC (5.70 to -0.40 mm Bregma: Paxinos and Watson, 1986) or the hippocampal formation (-0.40 to -7.80 mm Bregma; Paxinos and Watson, 1986). The blocks were then frozen on dry ice and stored at -80°C until coronal sectioning was performed on a Leica cryostat (CM3050S) at a thickness of 40 µm.

# 2.7 Quantitative real-time PCR analysis of gene expression

## 2.7.1 Total RNA extraction

Total RNA was isolated from hippocampi and prefrontal cortices using Trizol reagent according to the manufacturer's instructions (Invitrogen, Karlsruhe, Germany). In order to keep half of the homogenate volume for protein analysis, one minor modification was introduced to the procedure: the tissue samples were homogenized in filter sterilized homogenization buffer (HMB) consisting of 150 mM NaCl, 1mM Tris/HCl pH 8.0, 7.0% glycerol and 0.1% Triton-X 100 containing protease inhibitors (Complete Mini, Protease Inhibitor Cocktail Tablets, Roche Diagnostics, Mannheim, Germany). This step was carried out on ice and as fast as possible in order to avoid RNA degradation. After RNA isolation, DNase I digestion was performed and total RNA was purified using phenol/chloroform/isoamylalcohol followed by isopropyl/sodium acetate precipitation (Chomczynski 1993, Chomczynski & Sacchi 1987). Randomly chosen samples were analyzed for RNA integrity using the RNA 6000 Nano LabChip ® kit (Agilent Technologies, Böblingen, Germany). Such samples rendered RNA integrity numbers (RIN) ranging from 7 to 10, which indicate high RNA integrity (Schroeder *et al.* 2006).

## 2.7.2 First strand cDNA synthesis

Complementary DNA (cDNA) was synthesized by reverse transcription of mRNA transcripts with Supercript II (Invitrogen, Karlsruhe, Germany). Briefly, the following components were added to a nuclease free tube: 1 µl of Oligo(dT)$_{12\text{-}18}$ primers (Invitrogen, Carlsbad, CA, 92008, USA), 1 µl dNTP mix (10 mM each) (Bioline, Luckenwalde, Germany), 1 µg of total RNA from each sample and sterile distilled water up to 12 µl total reaction volume. The mixture was heated for 5 min at 65 °C and quickly chilled on ice. Afterwards, 4 µl of 5x first-strand buffer, 2 µl 0.1 M DTT and 1 µl RNase OUT™ (40 units/µl; Invitrogen, Carlsbad) were added into the tube. Contents were mixed gently and incubated at 42°C for 2 min. Then 1 µl (200 units) of SuperScript™ II (Invitrogen) RT was added and gently mixed by pipetting up and down. The mixture was incubated at 42°C during 50 minutes followed by an inactivation step of 15 minutes at 70 °C.

Gene-specific primers were designed using the Primer3 software v2.0 (Rozen & Skaletsky 2000) with amplicons ranging between 50 and 120 bp in length. To ensure no amplification from genomic DNA that might remain in the sample, the forward and reverse primers were intron-spanning; therefore, only amplification from cDNA was possible. Table 1 shows a list of the primers used in this study.

Table 1. List of primers for real-time PCR quantification of gene expression.

| Primers | Forward | Reverse | Product size |
|---|---|---|---|
| **AQP4** | 5’ AGATCAGCATCGCCAAGTCT 3’ | 5’ GGGTGTGACCAGGTAGAGGA 3’ | 89bp |
| **Ndrg2** | 5' GAGATGGTGGCCAGTGAAGAAC 3' | 5' AATGCCCCTGCTTCAATGTG 3' | 51bp |
| **Ndrg2L (Short UTR)** | 5' CTGAGTTAGCTGCCCGAATC 3' | 5' GTGACGGAGCCATAAGGTGT 3' | 73bp |
| **Ndrg2L (Long UTR)** | 5' CAGGACTCGGCTGAGGAG 3' | 5' AGGATTCGGGCAGCTAACTC 3' | 125bp |
| **Cyclophilin** | 5' TCACCATCTCCGACTGTGGAC 3' | 5' AAATGCCCGCAAGTCAAAGA 3' | 51bp |
| **GLT-1** | 5’ CCGAGCTGGACACCATTGA 3’ | 5’ CGGACTGCGTCTTGGTCAT 3’ | 70bp |
| **GLAST** | 5’AATGAAGCCATCATGAGATTGGT 3’ | 5’ CCCTGCGATCAAGAAGAGGAT 3’ | 75bp |
| **GFAP** | 5’ CAGCGGCTCTGAGAGAGATT 3’ | 5’ TGTGAGGTCTGCAAACTTGG 3’ | 101bp |
| **B-actin** | 5' GCGCAAGTACTCTGTGTGGA 3' | 5' ACATCTGCTGGAAGGTGGAC 3' | 64bp |
| **GAPDH** | 5' TGCCACTCAGAAGACTGTGG 3' | 5' GGATGCAGGGATGATGTTCT 3' | 85bp |
| **SDHa** | 5' TCCTCCGATTAAGGCAAATG 3' | 5' ATGGCTCTGCATCGACTTCT 3' | 124bp |
| **Ywhaz** | 5' GATGAAGCCATTGCTGAACTTG 3' | 5' GTCTCCTTGGGTATCCGATGTC 3' | 117bp |
| **Rpl13a** | 5' GAAAGGTGGTGGTTGTACGC 3' | 5' TTTCGGAGAAAGGCCAGATA 3' | 88bp |
| **Kir 4.1** | 5‘ AAGGCAGTGCCCTTAGTGTG 3‘ | 5‘ AGGGCTGAGGAGGAGAGAAC 3‘ | 64bp |

## 2.7.3 Real-time PCR

The quantitative analysis of gene expression was performed using the 7500 real-time PCR from Applied Biosystems together with Quantitect SYBR green technology (Qiagen, Hilden, Germany). The following reaction was performed: 12.5 µl SYBR green (Qiagen), 1µl of each primer (20 µM), cDNA (approx. 100 ng) and sterile distilled water up to 25µl. The real-time cycler conditions for the light cycler were used as follows: an initial PCR activation step lasting for 10 min at 95°C, followed by 40 cycling steps; 15 seconds at 95 °C (denaturation), 30 seconds at 60 °C (annealing) and 1 min at 72 °C (extension). A dissociation curve was generated for all PCR products to confirm that SYBR green emission was specific for a single PCR product (Ririe *et al.* 1997). The relative abundances of the

target mRNA transcripts were normalized against the housekeeping gene cyclophilin in the hippocampus (Alfonso *et al.* 2004), and cyclophilin, β-actin and GAPDH (glyceraldehyde 3-phosphate dehydrogenase) in the prefrontal cortex (Muller *et al.* 2011, Derks *et al.* 2008). Other frequently used reference genes were also tested with the PFC samples: SDHa (succinate dehydrogenase complex, subunit A), Ywhaz (tyrosine 3-monooxygenase/tryptophan 5-monooxygenase activation protein, zeta polypeptide) and Rpl13a (60S ribosomal protein L13a) (Kreth *et al.* 2010, Nelissen *et al.* 2009). In regards to Ndrg2 analysis of gene expression, four isoforms have been reported. Two of the isoforms code for a shorter form of NDRG2 protein (NDRG2S), while the remaining isoforms are translated into the longer version of NDRG2 protein (NDRG2L). Additionally, both Ndrg2S and Ndrg2L proteins are the result of an isoform with a short 5' untranslated region (UTR) and another with a long (UTR) (Boulkroun *et al.* 2002). The general quantification of all isoforms of Ndrg2 was assessed by means of primers located in a sequence in the 3'UTR that is shared by the four isoforms (Fig. 3A). Due to the lack of a unique sequence in the short isoforms, their expression cannot be analyzed independently of the other ones. On the other hand, specific primers to detect both long isoforms were designed by placing one of them in the Ndrg2L specific sequence in the protein coding region. Furthermore, specific primers were designed for the Ndrg2L isoform with a long 5'UTR by placing the forward primer in the 5'UTR unique for this isoform (Fig. 3B).

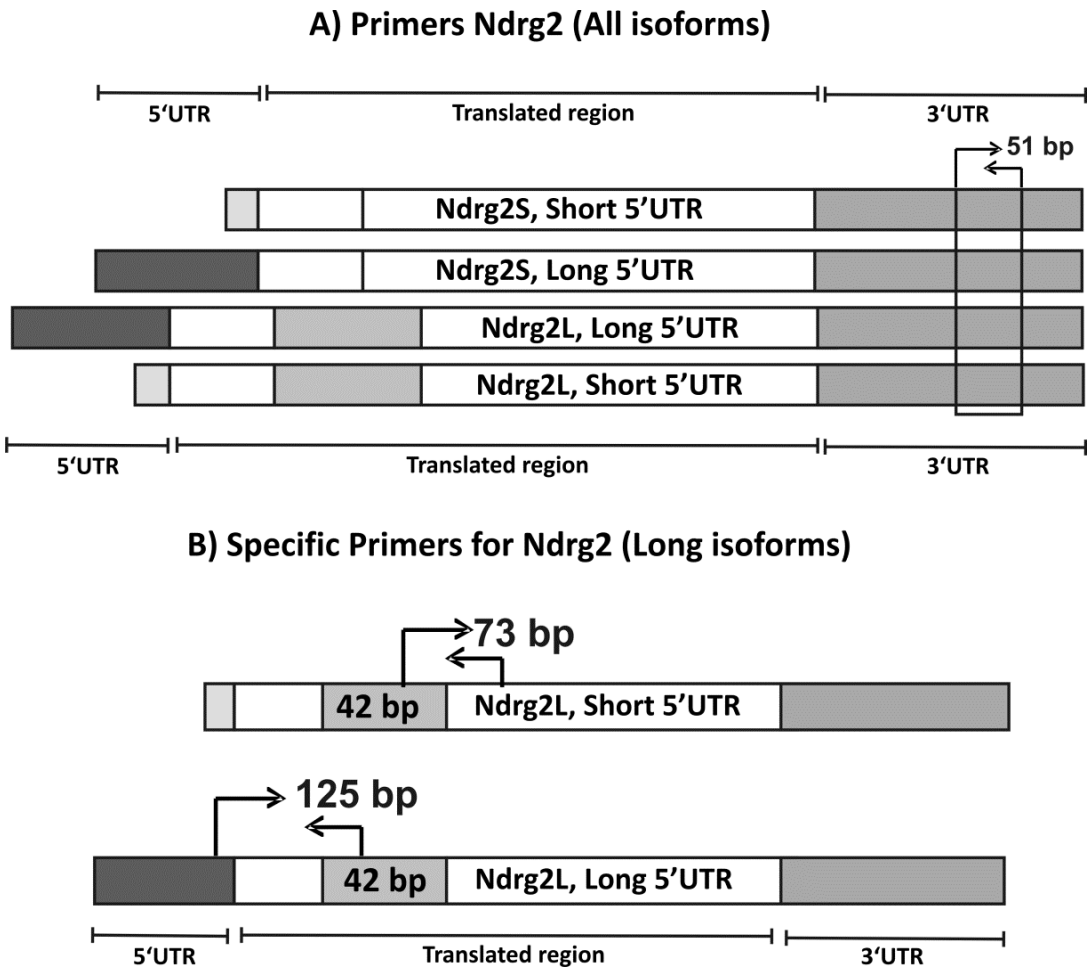


Fig. 3. Ndrg2 isoforms and primer design. A) Primers located in the 3'UTR allow for the analysis of general Ndrg2 mRNA expression, since they amplify a sequence that is common to all four isoforms. B) Specific primers can be designed for the Ndrg2L (Long 5'UTR) isoform by placing the forward primer in a unique sequence in the 5'UTR. Another pair of primers was designed to amplify both long isoforms. It was not possible to design specific primers for the Ndrg2L (Short 5'UTR) isoform since the UTR is too short to place a primer there. Also, the lack of a unique sequence in the short isoforms impedes separate analysis.

In order to assess gene expression stability in the prefrontal cortex, two analyses were performed. Schmittgen and Livak suggest that in the analysis of real-time PCR data by the comparative $C_T$ method (also known as $2^{-\Delta\Delta CT}$), the stability of the reference gene can be measured by calculating the ratio of the average reference gene expression (expressed as $2^{-CT}$) in the treated samples to the control samples. In principle, if the reference gene is not affected by the treatment, the ratio should be close to 1. This simple test provides an approximation of reference gene stability (Schmittgen & Livak 2008) and was performed for all genes tested as reference genes in the prefrontal cortex (GAPDH, β-actin, Cyclophilin, SDHa, Rpl13a and Ywhaz).

Additionally, the Normfinder software was used to find among the reference genes analyzed, which one had the most stable expression to be used for normalization. The program gives a stability value based on intra- and intergroup variations, and for a better performance of the analysis, it is optimal to include the results of at least 5 reference genes (Andersen *et al.* 2004). This analysis was only performed for the first group of PFC samples (experiment R12-09); in the second group (R1-11 experiment), only cyclophilin, β-actin and GAPDH were used as reference genes.

## 2.8 Quantitative Western blot

### 2.8.1 Protein extraction

Samples of hippocampi were homogenized with a Dounce homogenizer (tight pestle) in ice-cold homogenization buffer (HMB) consisting of 150 mM NaCl, 1mM Tris/HCl pH 8.0, 7.0% glycerol and 0.1% Triton-X 100 containing protease inhibitors (Complete Mini, Protease Inhibitor Cocktail Tablets, Roche Diagnostics, Mannheim, Germany). The protein homogenates were centrifuged for 5 minutes at 13,000 rpm, and supernatants were recovered; aliquots were stored at -80 degrees. Protein concentration was measured using the Bio-Rad DC Protein assay (Bio-Rad Laboratories, Hercules, USA).

### 2.8.2 Quantitative Western blot

For electrophoresis, approx. 30 µg/µl protein extracts were loaded on the gel. The protein extracts of hippocampi were denatured for 10 min at 70 °C in Laemmli buffer with dithiothreitol (DTT) and chilled on ice for 5 min. Samples were loaded and electrophoretically separated in 12.5% SDS gels under reducing conditions. Afterwards, the proteins were transferred from the gel to a nitrocellulose membrane (Schleicher and Schuell, Dassel, Germany) via semi-dry electroblotting for 2 h at 1 $mA/cm^2$ in transfer buffer containing 25 mM Tris base, pH = 8.3, 150 mM glycine and 10% methanol. The efficiency and quality of transfer were checked by staining the membrane with 0.5% Ponceaus (in 1% glacial acetic acid) (3 min). Afterwards, the membrane was carefully washed, first with bidist. water and later with PBS-T (0.1 M phosphate buffered saline containing 0.1% Tween 20): three 10-minute washes of each, respectively. The membrane was blocked for 1 h in

5% milk powder in PBS, and incubated with the primary antibody. The antibody concentrations as well as the incubation times were adjusted in order to yield a visible band of the respective protein of interest: AQP4, (Chemicon International, Temecula CA 95590, USA), Ndrg2 (Abnova, Taipei, Taiwan), GFAP (SYSY, Göttingen, Germany), Kir 4.1 (Alomone labs, Jerusalem, Israel), Synaptosomal-associated protein 25 (SNAP-25, SYSY) and syntaxin1A (SYSY) (Table 2). After incubation, the membrane was washed with PBS-T and subsequently incubated with the corresponding peroxidase-labeled secondary antibody (goat anti-rabbit, DakoCytomation, A/S Denmark, or goat anti-mouse, Santa Cruz Biotechnology, USA). After 1 h incubation at RT, the membrane was washed three times with PBS-T and three times with PBS. Finally, the membrane was subjected to enhanced chemiluminescence amplification (ECL) and the bands were visualized on Hyperfilm™ (Amersham Bioscience Ltd, UK). Membranes were subsequently stripped in PBS-S (PBS, 2 % SDS, 0.7 % β-mercaptoethanol) for 2 h and incubated in monoclonal anti-β-actin antibody followed by the corresponding peroxidase-labeled secondary antibody (Santa Cruz Biotech.). The relative optical density of the bands was quantified and analyzed using ImageJ software (Rasband, W.S., ImageJ, U. S. National Institutes of Health, Bethesda, Maryland, USA, http://imagej.nih.gov/ij/, 1997-2011). β-actin was used as an internal loading control for normalization of the optical density of the bands representing the proteins of interest. Data are presented as a percentage of the control.

Table 2. Antibody description and incubation conditions for the Western blots.

| Antibody | Dilution | Incubation | Size (kDa) |
|---|---|---|---|
| AQP4 (Rabbit polyclonal) | 1:1000 | ON/4°C | ~34 |
| Ndrg2 (Mouse polyclonal) | 1:4000 | ON/4°C | ~37 |
| GFAP (Rabbit polyclonal) | 1:500 | ON/4°C | ~55-48 |
| Kir 4.1 (Rabbit polyclonal) | 1:400 | ON/4°C | ~40 |
| SNAP-25 (Mouse monoclonal) | 1:10000 | ON/4°C | ~25 |
| Sintaxin1A (Mouse monoclonal) | 1:1000 | ON/4°C | ~35 |
| B-actin (Mouse Monoclonal) | 1:4000 | 30 min/RT | ~42 |
| Peroxidase conjugated goat anti-rabbit | 1:8000 | 1h/RT | |
| Peroxidase conjugated goat anti-mouse | 1:4000 | 1h/RT | |

RT=Room temperature, ON=Overnight

# 2.9 Immunohistochemistry

## 2.9.1 NDRG2 and AQP4 immunohistochemistry for light microscopy

From a total of 10 animals (5 from group C and 5 from group S), eight floating sections per animal were immunostained and analyzed for NDRG2 expression. The sections were processed in parallel to avoid variations in staining intensity. Sections were washed in PBS and then incubated for 30 min in 1% $H_2O_2$ in PBS to inactivate endogenous peroxidase activity. All washing steps consisted of 3 washes of 10 min each. In order to avoid non-specific binding of the antibody, the sections were incubated after washing in blocking solution for 1 h in 3% normal goat serum (NGS) (Vector Laboratories, Burlingame, CA 94010, USA) in PBS containing 0.3% Triton- X100. Subsequently, the sections were incubated overnight at 4°C with mouse polyclonal anti-NDRG2 antibody (Abnova, dilution 1: 500), in PBS-NGS-T (1% NGS and 0.3% Triton-X100). After washing, the sections were incubated with biotinylated goat anti-mouse IgG (Vector Laboratories; dilution 1:400) in PBS-NGS-T for 2 h. Then the sections were washed and incubated in ABC complex (ABC Kit, Vector Laboratories) in PBS containing 3 % NGS for 1.5 h. Finally, after washing, sections were incubated in 0.025 % 3,3'-diaminobenzidine (DAB, Peroxidase Substrate Kit, Vector Laboratories) with 0.01% $H_2O_2$. The sections were then washed, mounted on glass slides and let dry overnight at 37 °C. The next day, the sections were counterstained with methylgreen, cleared in xylene and coverslipped with Eukitt. A similar protocol was performed for the floating sections of the hippocampus that were immunostained with AQP4 antibody (Chemicon, dilution 1:1000) for qualitative immunohistochemistry.

## 2.9.2 Immunohistochemistry for confocal microscopy

Sections were washed (3 times, 10 min each) in PBS. In order to avoid non-specific binding of the antibody, sections were incubated in blocking solution for 1 h (3 % NGS; 3 % normal horse serum, NHS, Vector Laboratories) in PBS containing 0.3% Triton-X100. Subsequently, sections were incubated overnight at 4°C with mouse polyclonal anti-NDRG2 (Abnova, Taiwan, dilution 1: 500) and rabbit polyclonal anti-GFAP (Synaptic Systems, SySy, Göttingen, Germany; dilution 1: 5,000) in PBS-NGS-NHS-T (3% NGS, 3% NHS, 0.3 % Triton-X100 in PBS). After washing, sections were incubated for 2 h in Alexa

488 and Alexa 594-coupled secondary antibodies (Invitrogen, Eugene Oregon, USA, dilution 1: 500) in PBS-NGS-NHS-T. Finally, sections were rinsed in PBS and shortly in bidist. water before mounted. Microscopy was performed with a LSM Pascal 5 laser scanning confocal microscope (Carl Zeiss, Oberkochen, Germany). High magnification images were obtained with an Apochromat 63x oil objective (Zeiss; NA=1.4).

### 2.9.3 Counting NDRG2 positive cells in the hippocampus

The quantification of NDRG2-immunoreactive cells in the stratum oriens (SO) and stratum radiatum (SR) of the CA1 region in the hippocampus was performed by means of a Zeiss III microscope (Zeiss) and the Neurolucida system Version 7 (Microbrightfield Inc., Williston, USA).

In SO and SR, cells were counted in a delimited area of approximately 90,000 $\mu m^2$ and 185,000 $\mu m^2$, respectively. Data are reported as density (cells/$\mu m^2$) multiplied by 1000. Data from both hemispheres was collected separately in order to assess possible hemispheric effects of chronic stress.

## 2.10 Astrocyte culture experiments

To determine whether the astrocytic gene Ndrg2 plays a role in cell proliferation and morphology, both parameters were analyzed *in vitro* in an astrocyte culture that over-expressed either Ndrg2S or Ndrg2L (Fig. 4) by means of an adeno-associated viral vector (AAV). Plasmids containing the rat Ndrg2 genes (2 isoforms): pIRES2-EGFP-Ndrg2S and pIRES2-EGFP-Ndrg2L (S stands for Short, L stands for Long, and EGFP for enhanced green fluorescent protein) were kindly provided by Dr. M. Yamada (Dept. of Neuropsychopharmacology, National Institute of Mental Health, National Center of Neurology and Psychiatry, Japan) (Takahashi *et al.* 2005a). The adeno-associated viral expression plasmid (GfaABC1D-EGFP) was kindly provided by Dr. S. Kügler (Dept. of Neurology, Medical School, University of Göttingen). The cell culture experiments were performed in Prof. Dr. R. Behr laboratory (Dept. of Stem cell biology, German Primate Center, Göttingen, Germany).


Fig. 4. Four isoforms of the Ndrg2 gene generate two protein products: Ndrg2S and Ndrg2L. The presence of a sequence of 42bp close to the 5' end of the Ndrg2 long isoforms results in Ndrg2L, which encodes a peptide 14 aa longer than Ndrg2S (Takahashi *et al.* 2005a).

In order to produce the vectors AAV-GfaABC1D-Ndrg2S (AAV-Ndrg2S) and AAV-GfaABC1D-Ndrg2L (AAV-Ndrg2L), the EGFP gene sequence was first replaced with Ndrg2S or Ndrg2L sequences in the viral expression plasmid GfaABC1D-EGFP. The final viral plasmids GfaABC1D-Ndrg2S and GfaABC1D-Ndrg2L consisted of a small GFAP promoter, which drove the astrocyte specific expression of Ndrg2S and Ndrg2L, the woodchuck hepatitis virus post-translational regulatory element (WPRE) for enhanced transgene expression and a bovine growth hormone polyadenylation site (bGH) flanked by AAV inverted terminal repeats (ITR) necessary for packing the vector into the viral particles. Finally, the viral plasmids expressing Ndrg2S, Ndrg2L or EGFP (used as a control of transduction) were packed into AAV serotype-6 viral vectors (for a detailed description see 2.10.2.4).

## 2.10.1 Generation of the GfaABC1D-Ndrg2S and the GfaABC1D-Ndrg2L vectors

### 2.10.1.1 Removal of the EGFP gene from the GfaABC1D-EGFP plasmid

All enzymatic digestions were carried out according to manufacturer's instructions. Initially, the integrity of the ITR sequences was verified by a test enzymatic digestion with Sma I (New England Biolabs, Frankfurt am Main, Germany), since corrupted ITR sequences might interfere with packing the plasmid into the viral particles. This procedure was performed for every viral plasmid generated. Agarose gel electrophoresis of the GfaABC1D-EGFP plasmid digestion with Sma I rendered the expected products (size: 3013 bp, 1774 bp, 662 bp). A 0.8% agarose gel was prepared to resolve the bigger bands, while a 2% gel was used for the smaller band.

Subsequently, the EGFP gene sequence was removed. A two-step digestion with AgeI (Biolabs) and HindIII (Biolabs) of 5 µg GfaABC1D-EGFP was performed. Approximately 600 ng of the digestion was loaded and analyzed with agarose gel electrophoresis to confirm the presence and expected size of the digested products (4729 bp and 742 bp, 0.8% and 2% agarose gel respectively). The remaining volume was loaded in a 1% agarose gel and the 4729 bp DNA fragment comprising the main plasmid backbone was cut out of the gel and cleaned (QUIAquick Gel extraction kit, Qiagen). Afterwards, it was treated with the Klenow fragment (33µM dNTPs; Klenow fragment, U/µg of DNA, Biolabs) and incubated at 37 °C for 1 h and heat inactivated for 20 minutes at 75 °C. Finally, the plasmid was religated (T4 DNA Ligase, Biolabs). Electrocompetent SURE cells (Stratagene, La Jolla, CA, USA) were transformed with 20-50 ng/µl of the vector (1.6 kV; 25µF; 200 Ω) and seeded in lysogeny broth (LB)-agar plates: LB medium (1% triptone-peptone, 1% NaCl, 0.5% yeast extract, pH=7.0), 2.0% agar-agar and 100 µg/ml ampicilin. The LB-agar was autoclaved and the antibiotic was added after reaching a temperature of approx. 50°C. Selection of positive clones was done by means of minipreps (Qiagen) and digestions with BclI (New England Biolabs). BclI has a unique restriction site that yields a 4700 bp band if EGFP was removed instead of a 5500 bp band when EGFP is present. The integrity of the ITR sequences was verified as previously described. A larger amount of the plasmid ("midiprep") of the newly generated viral vector plasmid, GfaABC1D, was isolated according to the manufacturer's instructions (Qiagen).

#### 2.10.1.2 Subcloning of Ndrg2S and Ndrg2L into GfaABC1D plasmid

The procedures followed to insert Ndrg2S and Ndrg2L into the viral plasmid GfaABC1D differ from each other due to technical issues. Since Ndrg2S and Ndrg2L were inserted at the unique Xho I and Bam HI restriction sites in the pIRES-EGFP vectors, the first approach was to insert an annealed oligo carrying a Bam HI restriction site next to the 5' end of the gene in the pIRES-EGFP vectors. In that way, Ndrg2S and Ndrg2L could be cut out in a one-step digestion, which reduced problems such as low yield of digested product that could arise from two-step digestion. This approach was successful for subcloning Ndrg2L into the GfaABC1D plasmid. On the other hand, ligation of the annealed oligo with pIRES-EGFP-Ndrg2S failed; therefore, a different approach was followed. Ndrg2S was amplified by PCR, and later ligated to GfaABC1D. The procedure followed for each isoform is depicted in Fig. 5.

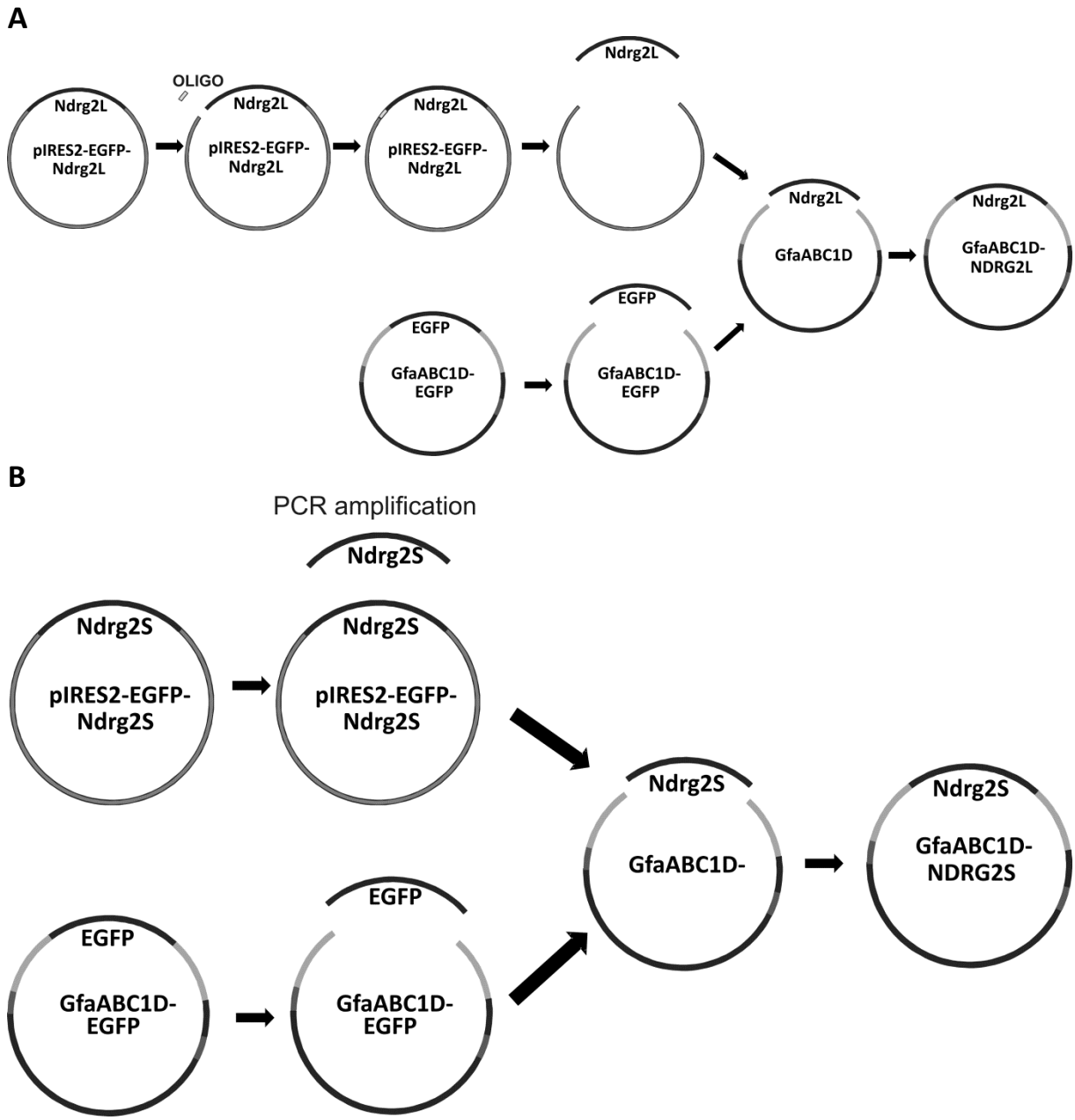


Fig. 5. Schematic representation of the strategies followed to build up the GfaABC1D-Ndrg2L (A) and GfaABC1D-Ndrg2S (B). A) Ndrg2L was cut out of the pIRES-EGFP-Ndrg2L to which an oligo sequence was ligated to introduce a Bam HI restriction site. Then Ndrg2L was ligated into the GfaABC1D vector after EGFP being removed by means of Bam HI digestion. B) Ndrg2S was replicated by means of PCR and introduced in place of EGFP into the GfaABC1D vector.

GfaABC1D-Ndrg2L

The oligo DNA-sequences Oligo-BamHI-BclI-F 5' TCGAGATATTGATCAATATGGATCCATAC 3' and Oligo-BamHI-BclI-R 5' TCGAGTATGGATCCATATTGATCAATATC 3' were first diluted to 200 µM concentration, followed by the annealing reaction: 5 µl OligoF, 5 µl OligoR, 2 µl of 10x annealing buffer

(100 mM TrisHCl, pH=8.0; 10 mM EDTA, 1 M NaCl), 8 µl water. It was heated at 95°C for 4 min and allowed to cool down at RT for 5 to 10 min. After digestion of the pIRES-EGFP-Ndrg2L with XhoI (Fermentas, St. Leon-Rot, Germany), 5 µl of a 10,000 times dilution of the annealed oligo sequences was used for the ligation (T4 DNA Ligase, New England Biolabs). Electrocompetent cells (kindly provided by Prof. Dr. Lutz Walter, Department of Primate Genetics, German Primate Center, Göttingen, Germany) were transformed with 20-50 ng/µl of the vector (1.6 kV; 25µF; 200 Ω) and seeded on LB-K agar plates (LB-agar, 50 µg/ml kanamycin). Positive clones were selected by PCR as briefly described: a colony was picked from the plate with a sterile pipette tip. This tip was first immersed into a tube containing the PCR reaction mix [(1 x GoTaq Polymerase buffer (Promega, Mannheim, Germany), 25 mM $MgCl_2$, 10 mM dNTP's (Bioline), 10 mM forward and reverse primers, 0.1 U GoTaq polymerase (Promega) and sterile water) (forward primer: 5'CGT GTA CGG TGG GAG GTC TA 3' and reverse primer: 5' TCT CCT CAG TGA TCT GCA CCT 3') (Thermocycler (Analytik Jena AG, Jena, Germany); PCR program: 93 °C for 2 min, 35 cycles of 93 °C for 40 s, 50 °C for 40 s 72 °C for 1 min, and 72.0 °C for 5 min)] and afterwards the same pipette tip was inserted into a tube containing LB-K media. Agarose gel electrophoresis allowed the detection of colonies carrying the plasmid with the insertion (PCR product: 146 bp) or colonies with an empty plasmid (PCR product: 126 bp). The positive clone was selected and a "midipred" was performed according to manufacturer's instructions (Qiagen).

Subsequently, the plasmids GfaABC1D and pIRES-EGFP-Ndrg2L-Oligo were digested with Bam HI (Fermentas). The band corresponding to the digested GfaABC1D and Ndrg2L were cut out of the gel, cleaned (QIAquick Gel extraction kit, Qiagen) and Ndrg2L was ligated into the GfaABC1D plasmid (T4 DNA Ligase, New England Biolabs). Electrocompetent SURE cells (Stratagene) were transformed and seeded on LB-A plates. Positive clones were detected by PCR selection (PCR product=271 bp) (primer F: 5' CTG CTT CCC AGA AGT CCA AG 3' and primer R: 5'CAG TGA TCT GCA CCT CCT GA 3'). Primers comprised sequences of GfaABC1D plasmid and Ndrg2L.

GfaABC1D-Ndrg2S

Since the ligation of the annealed oligo failed for pIRES-EGFP-Ndrg2S, a PCR based approach was used to insert Ndrg2S into the GfaABC1D plasmid. Taking advantage of the Bam HI restriction site in the pIRES-EGFP-Ndrg2S vector, a primer carrying a Bam HI restriction site as well as some extra base pairs at the 5' end for the attachment of the

restriction enzyme; and a primer including the Bam HI restriction site at the 3' end were designed (primer F: 5' ATT AAA GGA TCC GCC ACC ATG GCA GAG CTT C 3' and primer R: 5' ACA CCG GCC TTA TTC CAA G 3'). The pIRES-EGFP-Ndrg2S was used as a template and a proofreading polymerase (PFU polymerase kindly provided by Prof. Dirk Görlich (Max-Planck-Institute of Biophysical Chemistry, Göttingen) was used to amplify Ndrg2S according to the following reaction: 1 x PFU Polymerase buffer, 2.5 mM dNTP's, 10 mM F and R primers, 0.1 U PFU Pol, 100 ng DNA template and sterile water. PCR yielded an 1162 bp product which was cut out of a 1% agarose gel and cleaned (QIAquick Gel extraction kit, Qiagen). Next, both Ndrg2S PCR product and GfaABC1D plasmid were digested with Bam HI and ligated (T4 DNA Ligase, Biolabs). Afterwards, electrocompetent SURE cells were transformed and seeded in LB-A plates. Positive clones were detected by PCR selection (PCR product=271 bp). Primers comprised sequences of GfaABC1D plasmid and Ndrg2S (primer F: 5' CTG CTT CCC AGA AGT CCA AG 3' and primer R: 5'CAG TGA TCT GCA CCT CCT GA 3').

Finally, large amounts of GfaABC1D-Ndrg2S and GfaABC1D-Ndrg2L were generated with a 'megaprep' kit according to manufacturer's instructions (Qiagen). The ITRs integrity was checked by enzymatic digestions with Sma I (New England Biolabs) and Bam HI (Fermentas) and analyzed by gel electrophoresis. Molecular weight of the bands was confirmed using three different molecular markers: MPM1: 1kb plus (Fermentas), MPM2: 100 bp (Fermentas), MPM3: 50 bp (Fermentas). Also Ndrg2S and Ndrg2L were sequenced (primer F: 5' CTG CTT CCC AGA AGT CCA AG 3', primer R: 5' GGC ATT AAA GCA GCG TAT CC 3') (SEQLAB Sequence Laboratories GmbH, Göttingen, Germany) and analyzed with CLUSTAL W (version 2.0.12 multiple sequence alignment) (Larkin *et al.* 2007). Fig. 6 shows the basic structure of the viral vectors.

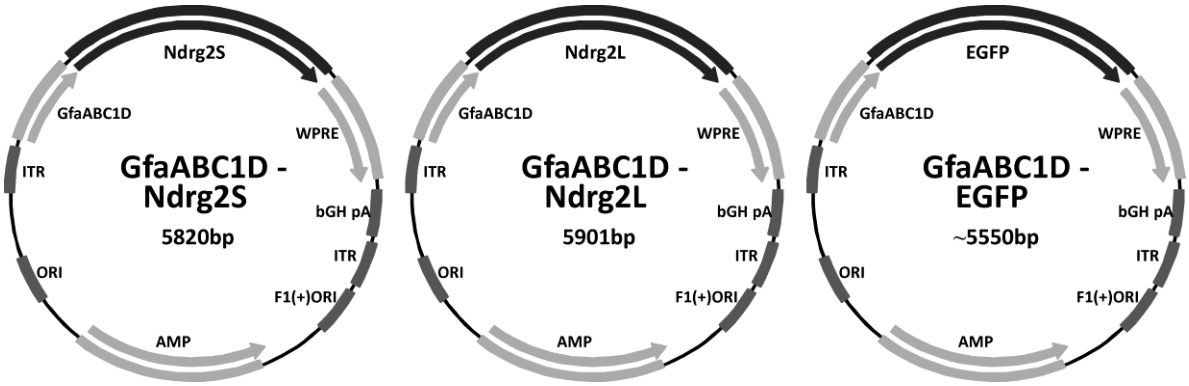


Fig. 6. GfaABC1D plasmids carrying either the short (S) or the long (L) isoform of the Ndrg2 gene, or EGFP. Ndrg2 astrocyte specific expression is driven by a small GFAP promoter (GfaABC1D). ITR= Inverted terminal repeats; WPRE= Woodchuck hepatitis virus post-transcriptional regulatory element; bGH= bovine growth hormone polyadenylation signal. Other sequences: ORI= *E.coli* origin of replication; AMP= Ampicillin resistance gene and F1(+)ORI= F1 phage origin.

### 2.10.1.3 AAV packaging, purification and tittering

The AAV serotype-6 based viral vectors AAV-GfaABC1D-Ndrg2S and AAV-GfaABC1D-Ndrg2L as well as AAV-GfaABC1D-EGFP (control) were produced in collaboration with Dr. Sebastian Kügler (Department of Neurology, Medical School, University of Göttingen) and used for transduction of astrocyte-enriched cultures. A brief description of the protocol is as follows: the final vectors were generated by transient transfection of HEK-293 cells with GfaABC1D-Ndrg2S, GfaABC1D-Ndrg2L or GfaABC1D-EGFP together with pDG2 as a helper plasmid (Fig. 7). The cells were harvested after 2.5 days. Subsequently, the viral particles were purified by means of iodixanol step-gradient centrifugation and fast protein liquid chromatography (Äkta FPLC; Amersham Biosciences, Freiburg, Germany) on 1 ml Q-FF anion-exchange columns (GE Healthcare, Freiburg, Germany), dialysis against excess amounts of PBS and concentration on centrifugal spin concentrators (150 kDa cutoff; Orbital Biosciences, Dulles, VA, USA). Vector genomes were assessed by quantitative PCR and purity was confirmed to be at least 99.5% by sodium dodecyl sulfate–polyacrylamide gel electrophoresis and silver staining.

The produced viruses had the following titer: 1.8 x $10^8$/µl for AAV-GfaABC1D-Ndrg2S, 2.1 x $10^8$/µl for AAV-GfaABC1D-Ndrg2L and 2.7 x $10^8$/µl AAV-GfaABC1D-EGFP.

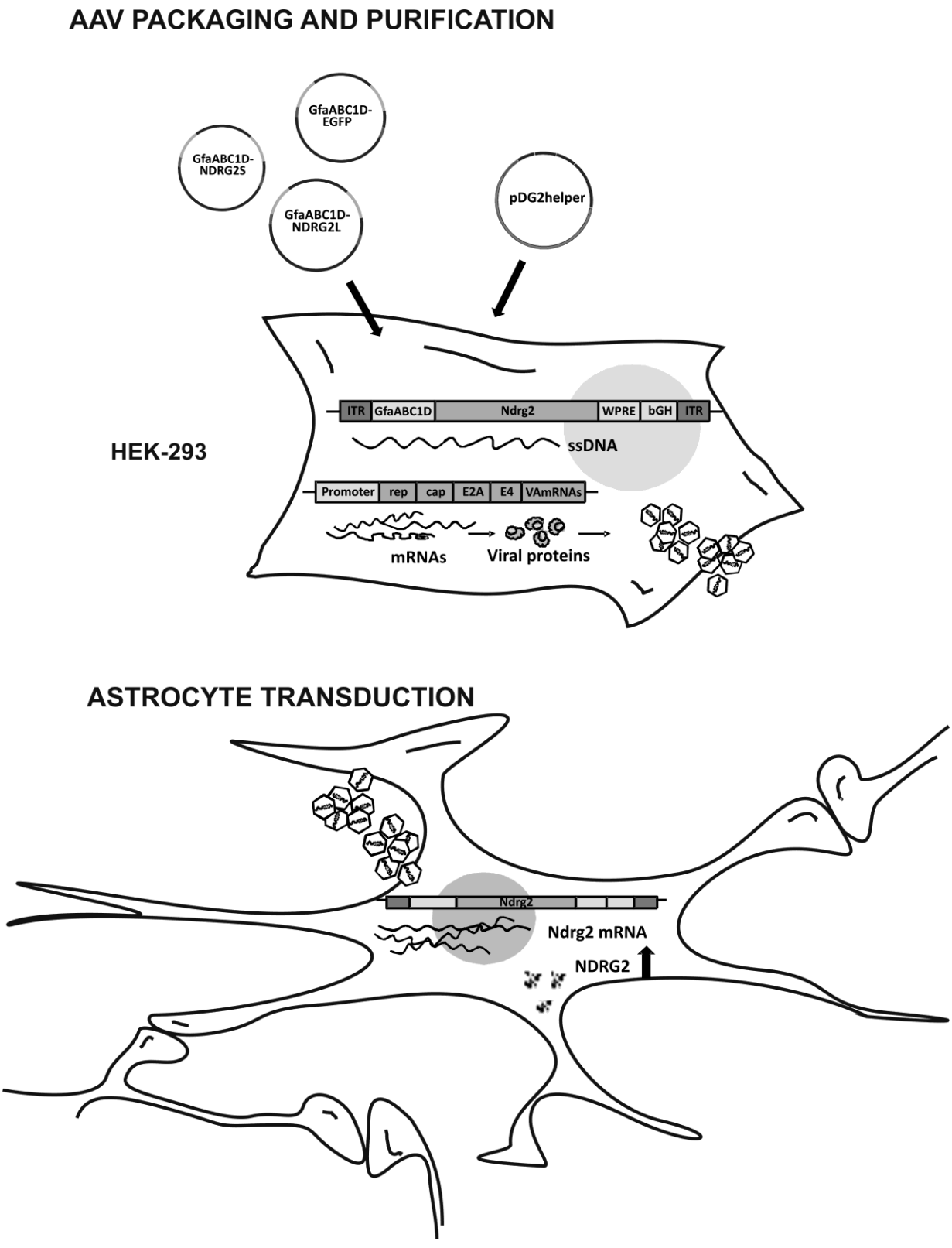


Fig.7. AAV packaging and astrocyte transduction. HEK-293 cells were transfected with GfaABC1D-Ndrg2S, GfaABC1D-Ndrg2L or GfaABC1D-EGFP together with pDG2 as a helper plasmid. The cells were grown and harvested, followed by purification of the viral particles. An astrocyte-enriched culture was transduced with the AAV serotype-6 based viral vectors AAV-GfaABC1D-Ndrg2S, AAV-GfaABC1D-Ndrg2L or AAV-GfaABC1D-EGFP for analysis of NDRG2-induced changes of astrocytes in culture.

## 2.10.2 Cell culture

### 2.10.2.1 Brain dissection

Newborn (at the day of birth or on postnatal day 2) Wistar rat pups were sacrificed by decapitation with scissors. The head was fixed with a cannula on top of a styropor surface and the skin of the skull was opened at the midline of the head, cutting from the base of the skull to the mid-eye area under sterile conditions. After folding back the skin, the cap of the skull was cut from the foramen magnum up to the eye on both sides with small curved scissors. The skull was carefully peeled off with the curved forceps. The brain was removed and immediately transferred to a sterile Petri dish with ice-cold 1 x Hank's balanced salt solution (HBSS), (Invitrogen, Karlsruhe, Germany). After preparation of all brains (n=8), the cerebrum was separated from the cerebellum and brain stem, and the cerebral cortices (grey matter containing the cell bodies), were cut out and placed in a new petri dish with fresh ice-cold 1 x HBSS (Invitrogen). The meninges were gently removed from the individual cortical lobes under a microscope and the cortices were immediately placed on ice into a sterile conical tube (BD Biosciences, Heidelberg, Germany) containing 1 x HBSS (Invitrogen). The cortices were washed twice with 1 x HBSS and finally HBSS was almost completely removed before tissue digestion.

### 2.10.2.2 Tissue digestion

Cortices were dissociated into a cell suspension by adding 5 ml of 0.05% trypsin (Biochrom, Berlin, Germany). It was incubated for 30 minutes at 37°C with constant rotation and short vortex was performed every ten minutes. Trypsination was blocked by adding 8 ml cold (4 °C) Dulbecco's Modified Eagle Medium (DMEM, Invitrogen, Karlsruhe, Germany) containing 10% Fetal Bovine Serum (FBS, Invitrogen) (DMEM/FBS). Further dissociation of the tissue was performed mechanically by pipetting up and down 3-5 times. DNase I (Worthington Biochemical, Lakewood, NJ, USA) digestion was performed (40µl per brain, concentration 0.5 mg/ml) for 1 min at 37°C. If the cell suspension was still not homogeneous, further pipetting up and down was performed. Subsequently, the cell suspension was centrifuged at 800 rpm for 10 minutes at RT; the supernatant was removed and fresh DMEM/FBS/penicillin/streptomycin/amphotericin B (DMEM/FBS/PSA) was added. The cell pellet was resuspended by gentle pipetting up and down. Cells were seeded on 25 $cm^2$ poly-L-Lysine 0.01% (PLL, Sigma-Aldrich, Germany) coated plates (1 h

incubation followed by three washes with bidist. sterile water) (approx. 1 brain per flask). The cell cultures were kept in an incubator (37°C, 5% $CO_2$) for 24-48 h before the first medium change (Fig.8A). Afterwards, the medium was changed every 48 to 72 h until the astrocyte cultures were confluent (after approx. 8-15 days). Clodronate disodium salt (Calbiochem, Darmstadt USA) was added to the medium after the first medium change (0.06 mg/ml) in order to remove microglia.

### 2.10.2.3 Secondary astrocyte cultures

After 7-10 days, the astrocyte cultures were confluent. At this time point, secondary astrocyte cultures were prepared. This step generates a highly enriched astrocyte culture. The cultures were washed three times with PBS with penicillin and streptomycin (PBS/PS). In order to detach the astrocytes from the flask, the cell cultures were incubated for 10 min at 37 °C with the cell dissociating reagent TrypLE$^{TM}$ (Invitrogen, Karlsruhe, Germany) and after 5 and 10 minutes the flask was strongly shaken. Five ml ice cold DMEM/FBS were added to stop the reaction and the cell suspension was transferred to a new sterile 15 ml conical tube (BD Biosciences). The cell suspension was centrifuged for 5 minutes at 300 rpm and the cell pellet resuspended in 1 ml fresh DMEM/FBS/PSA. Cells were counted, seeded in a 24-well PLL-coated plate in a concentration of 5 x $10^4$ cells/ml (final volume per well = 400 µl) and let grow until 90 % confluence. For Western blot analyses, the cells from 1 flask (primary astrocyte culture, 90 % confluence) were seeded in four culture plates (diameter 6 cm) (Fig. 8A-B).

### 2.10.2.4 Astrocyte culture transduction

When secondary astrocyte cultures were 90 % confluent, they were transduced with the Ndrg2 expressing AAV vectors: AAV-GfaABC1D-Ndrg2S, AAV-GfaABC1D-Ndrg2L and AAV-GfaABC1D-EGFP (transduction control). Another control was PBS; these cultures received the same treatment as the transduced ones, but instead of adding the virus to the media, the same amount (µl) of PBS was given to them.

The virus was kept at -150 $^oC$ and thawed on ice before use. For transduction, half of the volume of DMEM/FBS/PSA in each well of the culture plate (approx. 200 µl from a 24 well plate and 2 ml from a 20 $cm^2$ culture plates) was removed and kept in the incubator.

The virus was shortly spun down and the next steps were performed under the hood. The virus was diluted in PBS up to the desired titer so that a 10 µl volume could be applied to the cells. After adding the virus, the plate was shaken gently to homogeneously dilute the virus in the remaining volume of medium. It was left for 5 to 6 h in the incubator. Afterwards, the previously removed volume of medium was returned to the well or plate. A scale of different titers was initially performed to find out the transduction efficiency of the viruses. Three titers were tested: $1 \times 10^{8}$, $1 \times 10^{7}$ and $1 \times 10^{6}$. The titer $1 \times 10^{7}$ resulted in a good yield. For Western blot analyses, each 25 $cm^2$ flask was used to seed four 20 $cm^2$ PLL-coated culture plates. Finally, 4 culture plates originating from different original flasks were transduced for each condition (Ndrg2S, Ndrg2L, EGFP) or treated with PBS (Fig. 8C). Two days after transduction, the cells were fixed with 4% PFA and used for the proliferation assay or protein extraction.

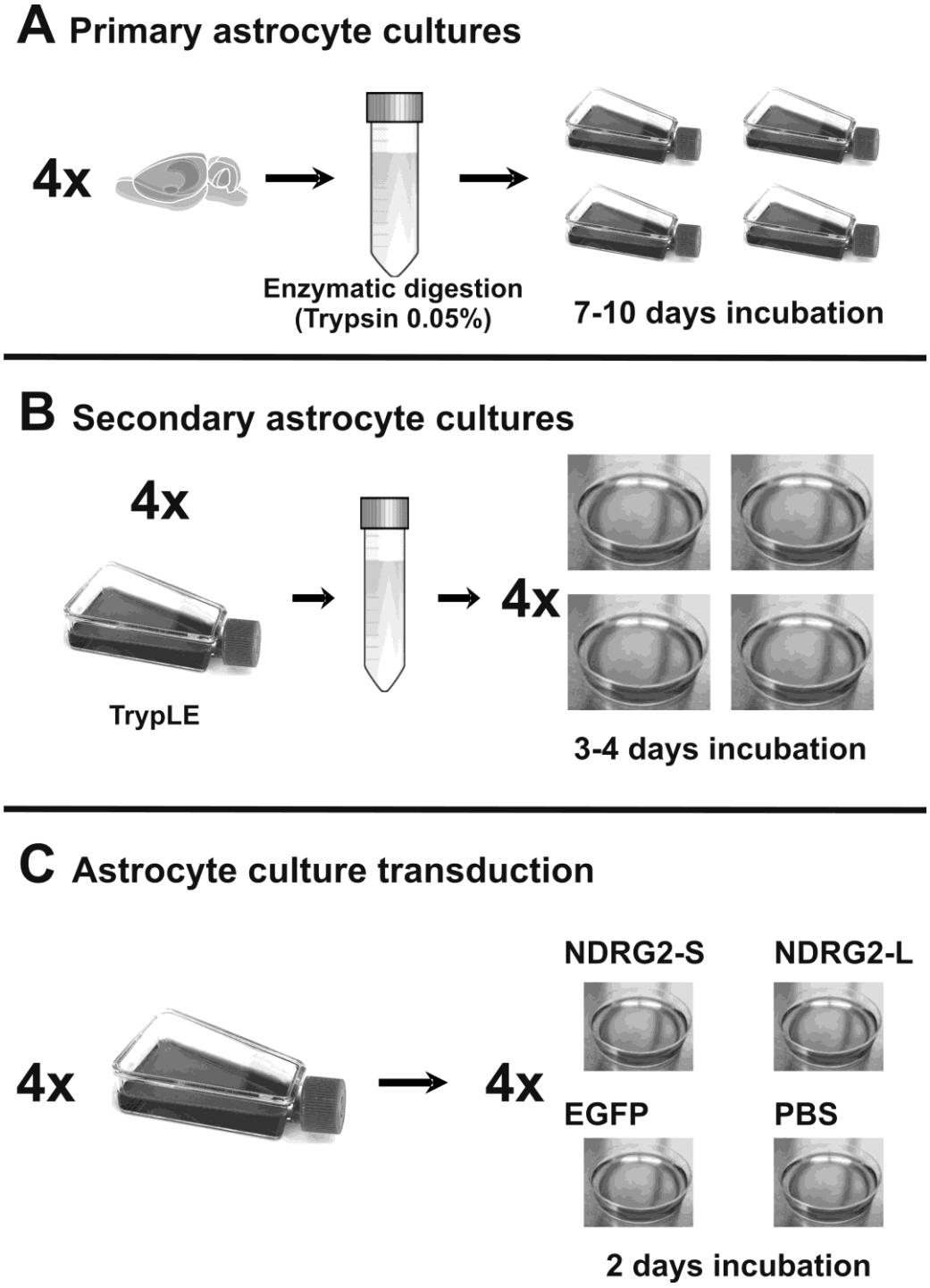


Fig. 8. Astrocyte culture preparation and transduction for Western blot analysis of NDRG2 and GFAP expression. A) Cortices were dissected out of four new born rat brains. After trypsination the cell suspension was centrifuged and resuspended in fresh DMEM/FBS/PSA and seeded in four 25 $cm^2$ culture flasks coated with PLL. After 7 to 10 days of incubation, the astrocyte cultures were approx. 90% confluent. B) Primary cell cultures (90% confluent) were treated with the dissociating reagent TrypLE. Cells were collected and distributed into four 20 $cm^2$ culture plates coated with PLL and allowed to grow for 3-4 days. Each flask was handled independent from the other flasks, but simultaneously. C) Every flask originated four secondary cultures that were differentially transduced with AAV-GfaABC1D-Ndrg2S, AAV-GfaABC1D-Ndrg2L and AAV-GfaABC1D-EGFP or treated with PBS, in order to assure that every transduction shared the same conditions.

### 2.10.2.5 Confirmation of cell culture transduction by Western blot

Secondary astrocyte cultures seeded on 6 cm diameter culture plates were transduced with the Ndrg2 expressing AAV vectors: AAV-GfaABC1D-Ndrg2S and AAV-GfaABC1D-Ndrg2L, as well as with AAV-GfaABC1D-EGFP. As a negative control, PBS was added to one culture. After 48 h, the astrocyte cultures were thoroughly washed with 1 x PBS and treated with TrypLE$^{TM}$ (Invitrogen) to detach the cells. After 5 and 10 min, the plates were strongly shaken in order to resuspend the majority of the astrocytes. Then 5 ml ice cold PBS were added and contents were transferred to a new sterile 15 ml conical tube (BD Biosciences, Heidelberg, Germany). The cell suspension was centrifuged for 5 min at 500 rpm and the cell pellet resuspended in 60 µl homogenization buffer. Western blots were performed as previously described (see section 2.8.2). An amount of 15 µl protein extract was loaded on the gel and NDRG2 expression was analyzed and normalized against β-actin.

### 2.10.2.6 Cell culture fixation

After three washing steps, the astrocyte cultures were fixed with 4% paraformaldehyde (PFA) in 0.1M phosphate buffer (pH 7.2) for 10-30 min. Afterwards, the cultures were washed with PBS.

### 2.10.2.7 Cell culture immunofluorescent staining

In order to confirm astrocyte enrichment, astrocytes were identified by immunofluorescence with the specific marker GFAP and the astrocyte-specific protein NDRG2. The number of GFAP-positive cells was compared to the number of 4',6-diamidino-2-phenylindole (DAPI) positive nuclei. In addition, transduced cell cultures were double stained for NDRG2 and β-catenin (which allows clear identification of cell boundaries).

For immunofluorescence, the astrocyte culture was washed three times in PBS and later permeabilized in 0.04% Triton X for 10 min. Subsequently, it was incubated in PBS-B buffer (3% bovine serum albumin (BSA) in PBS) for 10 min and then the cultures were incubated with the primary antibodies against: NDRG2, GFAP, β-catenin (BD Biosciences) and IBA-1 (Wako, Osaka Japan) (Table 3). After 1 h incubation at 37°C, the astrocyte culture was washed, and incubated in PBS-B containing Alexa 488- and 594-coupled secondary antibodies (Invitrogen, Carlsbad, CA, USA; dilution, 1:500) (Table 3). The

cultures were washed twice in PBS containing DAPI (0.05 ng/ml) and twice more in PBS. After PBS was carefully removed, the cells were covered with Citifluor (EMS, Hatfield, PA, USA). The cell cultures were analyzed using the AxioObserver Z1 inverted phase and fluorescence microscope (Carl Zeiss, Oberkochen, Germany).

Table. 3. Antibody description and incubation conditions for the astrocyte culture.

| Antibody | Dilution | Incubation |
|---|---|---|
| Ndrg2 (Mouse polyclonal) | 1:500 | 1 h / 37 °C |
| GFAP (Rabbit polyclonal) | 1:500 | 1 h / 37 °C |
| B-catenin (Mouse monoclonal) | 1:500 | 1 h / 37 °C |
| IBA-1 (Rabbit polyclonal) | 1:500 | 1 h / 37 °C |
| Alexa 594 (Donkey anti-mouse) | 1:500 | 30 min / 37 °C |
| Alexa 594 (Donkey anti-goat) | 1:500 | 30 min / 37 °C |
| Alexa 594 (Goat anti-guinea pig) | 1:500 | 30 min / 37 °C |
| Alexa 488 (Donkey anti-rabbit) | 1:500 | 30 min / 37 °C |
| Alexa 488 (Donkey anti-mouse) | 1:500 | 30 min / 37 °C |

#### 2.10.2.8 Analysis of astrocyte proliferation and morphology in the astrocyte cultures

In order to test if NDRG2 overexpression had an effect on cell proliferation, the WST-1 assay was used according to manufacturer's instructions (Roche, Molecular Biochemicals, Mannheim, Germany), while the quantification of cell morphology parameters, such as area, perimeter and circularity, were assessed as indicators of the differentiating state of the cells after treatment with the AAV-Ndrg2S, AAV-Ndrg2L, AAV-EGFP or PBS.

*WST-1 cell proliferation assay*

The WST-1 assay enables the quantification of changes in cell proliferation by the determination of formazan soluble dye in cell culture media. Formazan results from the reduction of WST-1 by the mitochondrial dehydrogenase (succinate-tetrazolium reductase) in viable cells (Heni *et al.* 2011). Therefore, an increase in the number of cells is paralleled by an increase in the generation of formazan, which is later quantified by a multiwell spectrophotometer by measuring the absorbance of the dye solution at 440 nm (Takamatsu 1998).

Secondary astrocyte cultures were prepared in 24-well PLL-coated plates. Cells were seeded at a concentration of 5 x $10^4$ cells per well to a final volume of 400 µl/well. After 24-48 h (during which time the cells recovered and attached to the well surface), cells were transduced with AAV-Ndrg2S, AAV-Ndrg2L, AAV-EGFP or treated with PBS as described above. After 48 h of exposure to the virus, the media was replaced with 350 µl fresh media (at 37°C) containing the WST-1 salt (10 µl per well). Following 20 min of incubation under standard culture conditions, the culture plate was shaken thoroughly for one minute in order to homogeneously dissolve the formazan dye in the cell culture medium. Then the medium was removed and pipetted into a microwell plate (96 wells) in 100 µl aliquots (each cell culture was analyzed in triplicate) and quantified in an ELISA reader (Biotek, Winooski, VT, USA) at 450 nm and 630 nm (reference wavelength), according to manufacturer's instructions. A total of 12 secondary cultures were analyzed for each condition (AAV-Ndrg2S, AAV-Ndrg2L, AAV-EGFP, PBS). A well containing the same amount of culture medium with WST-1 was used as a blank position for the microplate reader.

*Cell morphology (area, perimeter and circularity)*

Secondary astrocyte cultures were transduced as previously mentioned (see section 2.10.2.4). After 48 h, the cultures were fixed and were fluorescently immunostained for NDRG2 and β-catenin and nuclei were stained with DAPI. NDRG2 immunofluorescence allows the recognition of transduced astrocytes (enhanced NDRG2 expression). β-catenin shows clear localization to plasma membranes, which permits the determination of cell boundaries necessary for the quantification of cell shape parameters. Cell area (surface included within the cell membrane as determined by β-catenin staining), perimeter (the boundary of the cell) and circularity were quantified using the ImageJ software (Rasband, W.S., ImageJ, U. S. National Institutes of Health, Bethesda, Maryland, USA, http://imagej.nih.gov/ij/, 1997-2011). An average of 55 cells for each condition were included in the analysis. Cells that showed enhanced EGFP or enhanced NDRG2 expression, respectively, were used for the analysis.

## 2.11 Statistics

All data were tested for normality (95% confidence interval). Results are expressed as mean ± SEM. A probability level of 95% was used to determine statistical significance ($p<0.05$). Statistical analyses were performed with Sigma Plot 12.0 (Systat Software Inc., San Jose, California; USA), while graphs were generated with GraphPad 4.0 (GraphPad Software, Inc., San Diego, USA). Statistical analyses and comparisons were performed using two-tailed unpaired Student's *t*-test, one-way analysis of variance (ANOVA) and two-way ANOVA, followed by Student-Newman-Keuls *post hoc* test for examination of group differences. Any values that were 2 standard deviations higher or lower than the mean were excluded from analysis.

# 3 Results

## 3.1 Modulation of glial gene expression by chronic social stress

### 3.1.1 HIPPOCAMPUS

#### 3.1.1.1 Real-time PCR quantification of mRNA expression

*Ndrg2 mRNA expression was modulated by chronic social stress*

Real-time PCR quantitative analysis of mRNA expression showed that Ndrg2 was modulated by stress. Five weeks of chronic social defeat caused a 22% reduction of Ndrg2 mRNA expression in the hippocampus compared to control (Fig. 9A). Statistical analysis using *t*-tests showed a significant effect of stress on its expression ($t_{(12)}$= 4.57, $p$=0.0006). The long isoforms of Ndrg2 were subsequently analyzed (Ndrg2L - Short 5' UTR and Ndrg2L - Long 5' UTR). Surprisingly, none of them showed a significant effect of stress in their mRNA expression ( $t_{(14)}$=0.9196, $p$=0.37 and $t_{(13)}$=0.2430, $p$=0.81 respectively) (Fig. 9B).

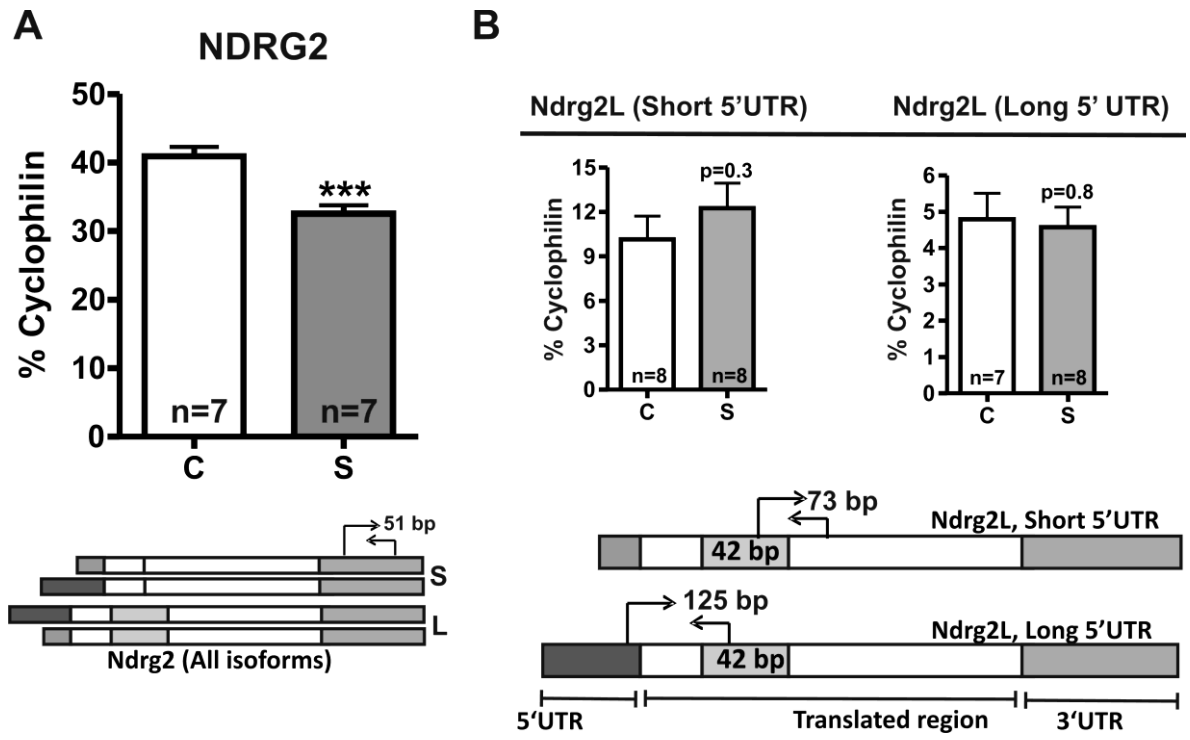


Fig. 9. A) Effect of CSS on the expression of Ndrg2 mRNA. The primers were designed to recognize the three isoforms since they amplify a sequence (51 bp) in the 3'UTR shared by all of them. S=Ndrg2S and L=Ndrg2L. B) Ndrg2 long isoforms in the hippocampus. The primers for Ndrg2L (Long 5' UTR) are specific for that isoform, while the other primers recognize both long isoforms. Data were generated by quantitative real-time PCR. mRNA expression was normalized against the housekeeping gene cyclophilin (presented as a percentage). Significant differences relative to control group are indicated by asterisks (two-tailed un-paired Student's *t*-test: ***$p<0.001$). Data are expressed as mean ± SEM. C=Control, S=Stress.

*Other astroglial genes were not modulated at the mRNA level by chronic social stress*

Quantitative real-time PCR showed that the levels of mRNA encoding GFAP, GLT-1, GLAST and AQP4 were not modulated by five weeks of chronic social stress. Statistical analysis using *t*-tests showed no significant stress-induced effects compared to controls ($t_{(14)}=0.4800$, $p=0.63$; $t_{(13)}=1.404$, $p=0.18$; $t_{(13)}=0.98$, $p=0.34$; $t_{(9)}=1.672$, $p=0.13$) (Fig. 10).

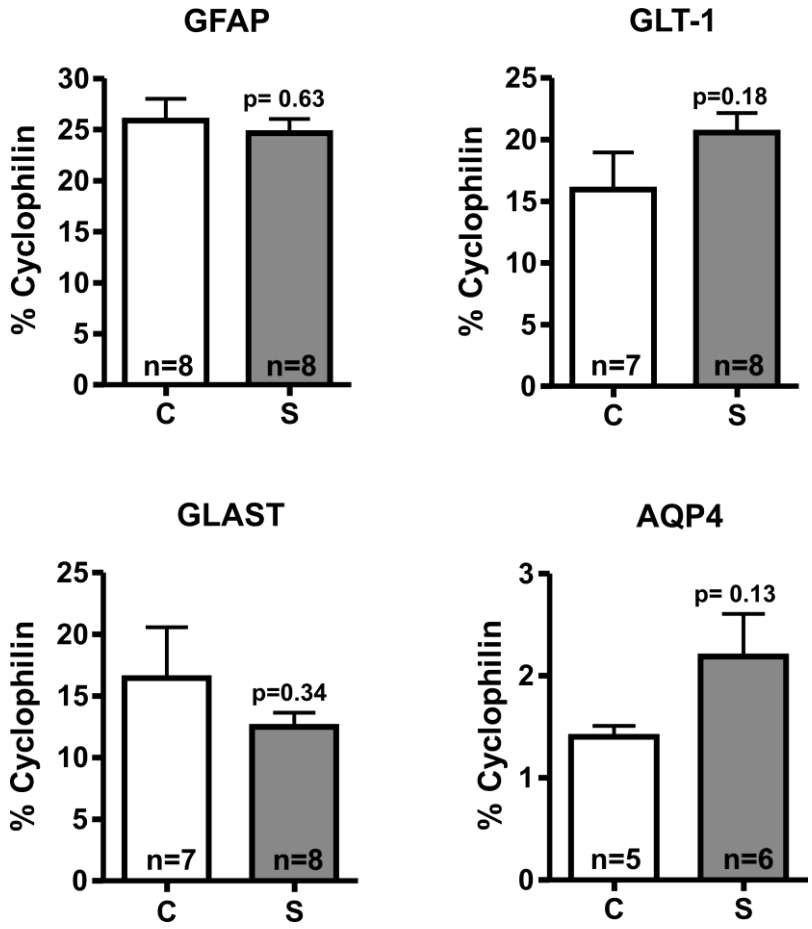


Fig. 10. Effect of chronic social stress on the expression of mRNA encoding GFAP, GLT-1, GLAST and AQP4 in the hippocampus. Data were generated by quantitative real-time PCR with mRNA expression normalized against the housekeeping gene cyclophilin (presented as a percentage). None of the genes showed a significant difference in expression after CSS (two-tailed un-paired Student's *t*-test). Data are expressed as mean ± SEM. C=control, S=stress.

### 3.1.1.2 Western blot quantification of NDRG2 and GFAP protein expression after chronic social stress and concomitant citalopram treatment

As mentioned above (section 1.5.1) NDRG2 is an astrocytic protein expressed in the cytoplasm, as shown by the presence of immunofluorescently double-labeled (NDRG2/GFAP) astrocytes (Fig. 11). Chronic social defeat caused an upregulation of NDRG2 and a downregulation of GFAP protein in the hippocampus (Fig. 12).

Analysis with two-way ANOVA revealed no significant overall effect of stress ($F_{(1,33)}$=2.958, $p$=0.09), but a significant drug effect ($F_{(1,33)}$=7.676, $p$=0.009) on NDRG2 expression. But there was no significant interaction ($F_{(1,33)}$=1.403, $p$=0.24). Post hoc analysis showed that social stress increased the relative optical density of the band corresponding to NDRG2 (~37 kDa) in the Stress group ($p$<0.05) compared to the Control

group. Citalopram administration did not reverse the stress-induced changes (Stress compared to Stress-citalopram group, $p>0.05$) but had an effect in the Control-citalopram group (control vs. control-citalopram group, $p<0.05$) (Fig. 12).

NDRG2 upregulation could be due to an increase in astrocyte cell number in the hippocampus. In order to rule out this possibility, NDRG2-positive astrocytes were counted in two different areas of the hippocampus using the Neurolucida system. The quantification in the stratum radiatum and stratum oriens in CA1 revealed no significant differences between control and stress animals in cell density ($t_{(8)}=0.3351$, $p=0.74$ and $t_{(8)}=0.1738$, $p=0.87$ respectively) (Fig. 13). No hemispheric differences were observed. Data are presented as number of cells per $\mu m^2$ multiplied by a factor of 1,000. NDRG2 labeled cells of stressed animals (Fig. 14; B,D) appeared with a stronger staining when compared to controls (Fig. 14; A,C).

Similarly, expression of GFAP protein was also modulated by chronic social stress. Analysis with two-way ANOVA revealed that five weeks of chronic social defeat and antidepressant treatment showed effects of stress ($F_{(1,31)}=11.275$, $p=0.002$) and drug ($F_{(1,31)}=4.468$, $p=0.043$), but no interaction ($F_{(1,31)}=0.504$, $p=0.483$). The post hoc test showed that there was a decrease in optical density of the band corresponding to GFAP (~55 kDa) in the S, SC and CC groups (**$p<0.01$, **$p<0.01$ and $p=0.065$, respectively, compared to C). Similar to NDRG2, citalopram administration did not normalize GFAP expression (Fig. 12).

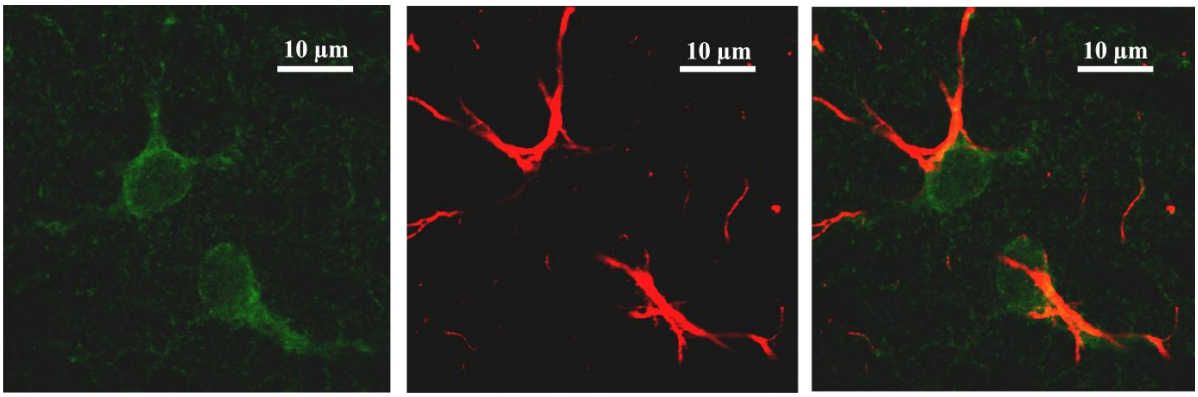


Fig. 11. Co-localization of NDRG2 and GFAP in astrocyte in the stratum radiatum of the hippocampus. Representative confocal microscopy image of astrocytes which express both NDRG2 (left; Alexa 488; green) and GFAP (middle; Alexa 594; red). Overlay image shown on the right. Note that NDRG2 appears to be distributed in the cytoplasm of the cell.

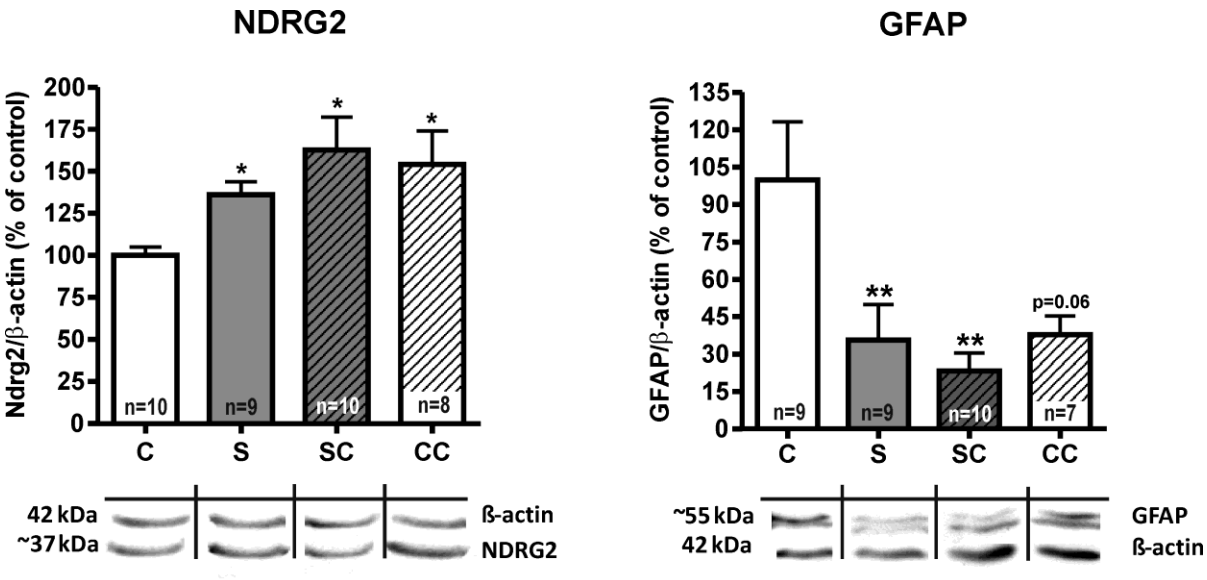


Fig. 12. Effects of chronic psychosocial stress and concomitant citalopram treatment on NDRG2 and GFAP protein expression in the hippocampus. Five weeks of daily social defeat increased the expression of NDRG2 in the hippocampus. Citalopram administration did not reverse the stress-induced effect on NDRG2. Representative Western blots are shown beneath the graphs. Protein expression was normalized against the housekeeping gene β-actin. The results are presented as a percentage of the control group (mean ± SEM). Statistics: two-way ANOVA (Stress x Drug) followed by Student-Newman-Keuls post hoc test: *$p<0.05$, vs. control. C=control, CC=control citalopram, S=stress, SC=stress citalopram. C=control, S=stress.

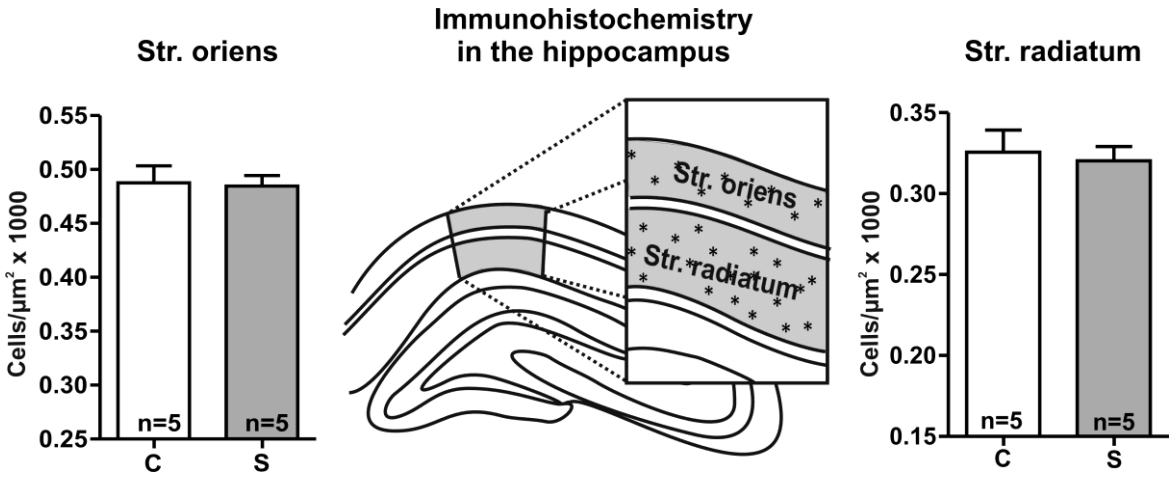


Fig. 13. NDRG2-labeled cell count in stratum radiatum and stratum oriens of CA1. No significant differences in density of NDRG2 labeled cells were observed for either region in control vs. stress rats. The results are presented as number of cells per µm$^2$ by a factor of 1,000 (mean ± SEM). Statistics: two-tailed unpaired Student's *t*-test. C=control, S=stress.

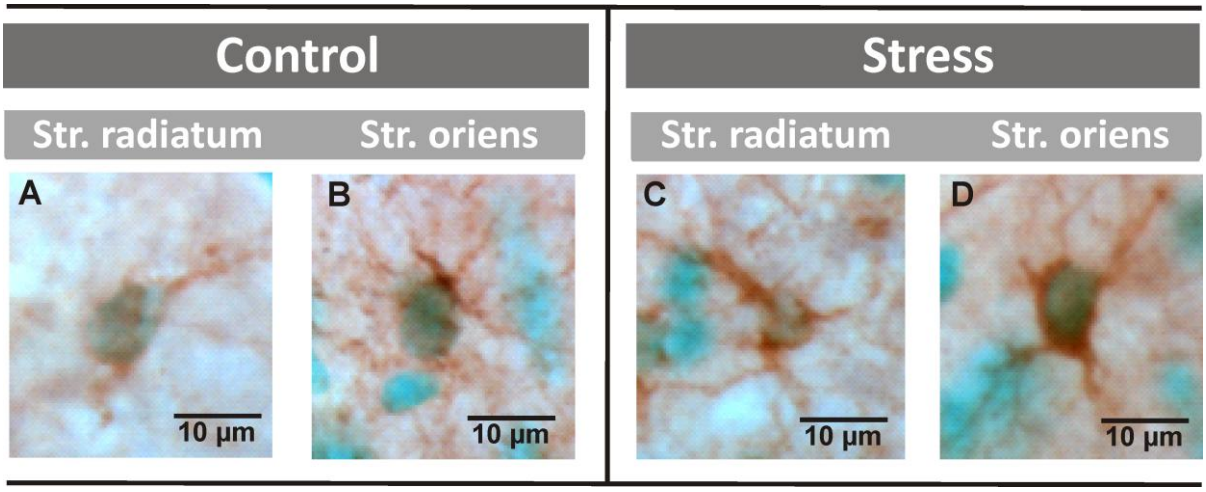


Fig. 14. Representative examples of NDRG2-labeled cells in the stratum radiatum and stratum oriens from sections used for cell quantification in control (A, C) and stress (B, D) animals. There is a stronger NDRG2 immunoreactivity in the Stress group.

Chronic social defeat stress caused also an increase in the synaptic proteins SNAP-25 and syntaxin-1A, but in contrast to the glial genes, citalopram treatment normalized SNAP-25 and syntaxin-1A protein expression in the stressed animals.

As expected, a band in the molecular range of 25 kDa was detected for SNAP-25. Two-way ANOVA revealed no effect of stress ($F_{(1,31)}$=0.04, $p$=0.83) or drug treatment alone ($F_{(1,31)}$= 0.0001, $p$=0.99), but a strong interaction effect: ($F_{(1,31)}$= 27.09, $p$<0.0001). Student-Newman-Keuls *post hoc* test showed that SNAP-25 expression was increased in the S and CC groups ($p$<0.01 for both compared to C). Expression was normalized after citalopram administration in the stress group ($p$<0.01, compared to S) (Fig. 15).

Additionally, the syntaxin-1A band, as expected, was detected at a molecular range of 35 kDa. Two-way ANOVA revealed no interaction ($F_{(1,32)}$=0.15, $p$=0.70), but individual effects of stress ($F_{(1,32)}$=13.03, $p$<0.001) and drug ($F_{(1,32)}$=6.98, $p$<0.05). The *post hoc* test showed that syntaxin-1A was increased after stress ($p$<0.05) and normalized after citalopram treatment ($p$<0.05, compared to S). There was no significant difference between the C and CC group. (Fig. 15).

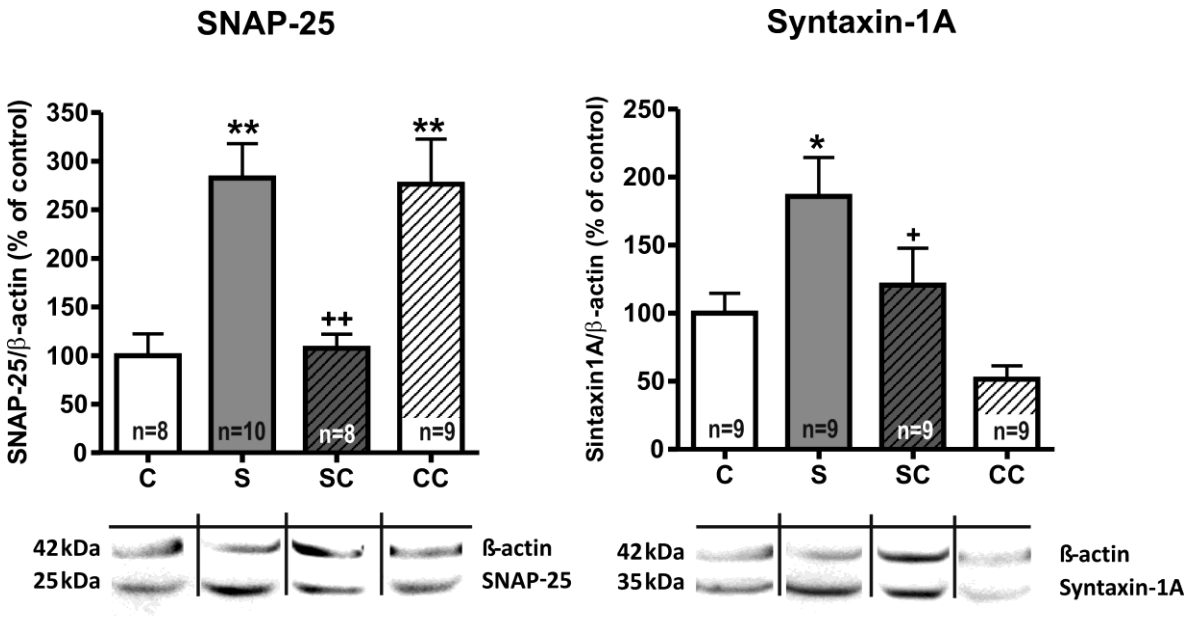


Fig. 15. Effects of chronic psychosocial stress and concomitant citalopram treatment on SNAP-25 and syntaxin-1A protein expression in the hippocampus. Five weeks of daily social defeat increased the expression of both neuronal proteins and citalopram reversed this stress effect. Representative Western blots are shown beneath the graphs. Protein expression was normalized against the housekeeping gene β-actin. The results are presented as a percentage of the control group (mean ± SEM). Statistics: two-way ANOVA (stress x drug) followed by Student-Newman-Keuls post hoc analysis: $*p<0.05$, vs. control, $^{+}p<0.05$, vs. stress. C=control, CC=control citalopram, S=stress, SC=stress citalopram. C=control, S=stress.

## 3.1.2 PREFRONTAL CORTEX

### 3.1.2.1 Determination of mRNA expression by quantitative real-time PCR

Five astroglial genes–Ndrg2, GFAP, AQP4, GLT-1 and GLAST–were quantified for mRNA expression in the prefrontal cortex in two different chronic social stress experiments (R1-11 and R12-09). The results revealed high variability depending on the choice of the reference gene used to normalize the data. Quantification of GFAP mRNA expression exemplifies this variability, as normalization against cyclophilin mRNA suggested an effect of citalopram in the control group, a finding which was not detected when GFAP mRNA was normalized against β-actin or GAPDH. Similarly, when β-actin was used as the reference gene, there was an effect of the stress and citalopram in the citalopram group, which was not observed with cyclophilin or GAPDH (Fig. 16).

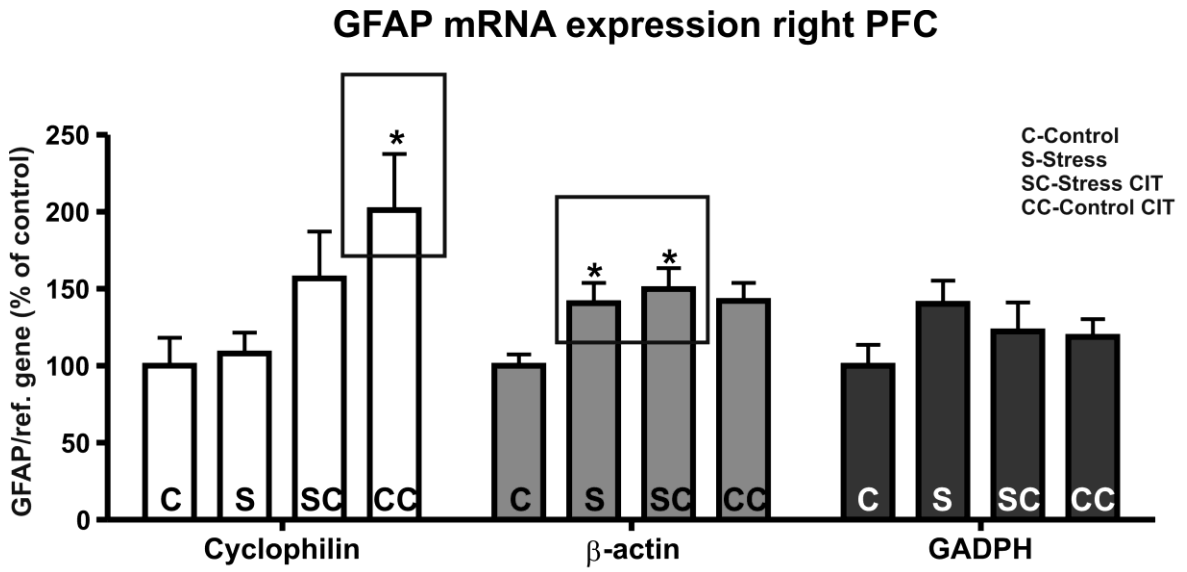


Fig. 16. High variability in GFAP mRNA expression in the right prefrontal cortex depending on the reference gene. GFAP mRNA quantification according to three different reference genes: cyclophilin, β-actin and GAPDH. Results exemplify the effect of the reference gene in normalization of the data. Normalization against cyclophilin suggests an effect in the control citalopram group (compared to control), which is not detected with β-actin or GAPDH. Similarly, when β-actin is used as the reference gene, there is an effect in the stress and the stress citalopram groups (compared to control), which is not observed with cyclophilin or GAPDH as reference genes. Data are presented as a percentage of the control group (mean ± SEM). Statistics: two-way ANOVA (stress x drug) followed by Student-Newman-Keuls post hoc analysis: *$p$<0.05, vs. control. C=control, CC=control citalopram, S=stress, SC=stress citalopram. C=control, S=stress.

There were also inter-experiment differences in PFC gene expression. For a detailed expression profile see Table 4 for the left prefrontal cortex and Table 5 for the right prefrontal cortex. The comparison of GLAST expression in the left hemisphere in R1-11 and R12-09 is one example of such discrepancy (Table 4). Only GLT-1 mRNA expression showed stress-induced downregulation in both chronic social stress experiments in the left PFC (quantitative real-time PCR determination was performed twice for both experiments). Furthermore, GFAP in the left hemisphere and Ndrg2 in the right hemisphere showed no effect of stress on their expression in either experiment. The rest of the results are highly variable.

Table 4. mRNA quantification of gene expression in the left prefrontal cortex.

| PFCL | Experiment | Ref. gene | Control | Control CIT | Stress | Stress CIT |
|---|---|---|---|---|---|---|
| **Ndrg2** | **R12-09** | Cyclophilin | 100 ± 11.1 | | 70 ± 6.2 * | |
| | **R1-11** | Cyclophilin | 100 ± 4.1 | 111 ± 5.1 | 127.1 ± 5.5 * | 124.2 ± 7.3 |
| | **R12-09** | β-actin | 100 ± 6.5 | | 100 ± 16.6 | |
| | **R1-11** | β-actin | 100 ± 8.0 | 95.3 ± 9.8 | 93.2 ± 7 | 130.7 ± 23.1 |
| | **R12-09** | GADPH | 100 ± 7.5 | | 98 ± 8.2 | |
| | **R1-11** | GADPH | 100 ± 6.7 | 116 ± 9.8 | 111,2 ± 6.8 | 106.7 ± 5.3 |
| **GFAP** | **R12-09** | Cyclophilin | 100 ± 9.4 | | 80.37 ± 11,8 | |
| | **R1-11** | Cyclophilin | 100 ± 6.3 | 130± 18.8 | 112 ± 10.1 | 107 ± 7.1 |
| | **R12-09** | β-actin | 100 ± 10.4 | | 94.2 ± 4.3 | |
| | **R1-11** | β-actin | 100 ± 6.9 | 107.7 ± 13.7 | 84.1 ± 7.5 | 112.6 ± 8.2 |
| | **R12-09** | GADPH | 100 ± 10.5 | | 86.5 ± 11,27 | |
| | **R1-11** | GADPH | 100 ± 5.5 | 127.1 ± 16.7 | 98.3 ± 8.2 | 86 ± 5.8 |
| **AQP4** | **R12-09** | Cyclophilin | 100 ± 11.6 | | 68.9 ± 11,6 | |
| | **R1-11** | Cyclophilin | 100 ± 17.4 | 66 ± 14.8 | 54.4 ± 8.1 * | 54.89 ± 8.5 |
| | **R12-09** | β-actin | 100 ± 10.1 | | 94 ± 15.5 | |
| | **R1-11** | β-actin | 100 ± 12.3 | 73 ± 10.0 | 70 ± 13.4 | 64 ± 12.4 |
| | **R12-09** | GADPH | 100 ± 13.3 | | 92.7 ± 19.1 | |
| | **R1-11** | GADPH | 100 ± 18.3 | 76 ± 13.8 | 58 ± 10.1 | 58.4 ± 15.3 |
| **GLT-1** | **R12-09** | Cyclophilin | 100 ± 7.7 | | 53 ± 6.2** | |
| | **R1-11** | Cyclophilin | 100 ± 20 | 78 ± 10.0 | 73 ± 10.7 | 68 ± 5.2 |
| | **R12-09** | β-actin | 100 ± 8.2 | | 71.5 ± 7.6* | |
| | **R1-11** | β-actin | 100 ± 9.2 | 81 ± 8.4 | 69 ± 4.7* | 82 ± 10.1 |
| | **R12-09** | GADPH | 100 ± 9.4 | | 57.6 ± 9** | |
| | **R1-11** | GADPH | 100 ± 13.2 | 87 ± 8.9 | 69 ± 6.9* | 70 ± 6.1 |
| **GLAST** | **R12-09** | Cyclophilin | 100 ± 6.6 | | 91,8 ± 7.5 | |
| | **R1-11** | Cyclophilin | 100 ± 13.6 | 102.9 ± 11,3 | 65.18 ± 9.1 * | 50.39 ± 4.5 ** |
| | **R12-09** | β-actin | 100 ± 8.1 | | 136 ± 12.22 * | |
| | **R1-11** | β-actin | 100 ± 5.4 | 88.7 ± 6.2 | 65 ± 4.7 *** | 59 ± 7.4 *** |
| | **R12-09** | GADPH | 100 ± 9.6 | | 106.6 ± 8.7 | |
| | **R1-11** | GADPH | 100 ± 7.2 | 105 ± 12.4 | 64.7 ± 4.8 ** | 53 ± 6.5 ** |

Data are presented as a percentage of the control group (mean ± SEM). Statistics: two-way ANOVA (stress x drug) followed by Student-Newman-Keuls post hoc analysis *$p$<0.05, **$p$<0.01, ***$p$<0.001.

Table 5. mRNA quantification of gene expression in the right prefrontal cortex.

| PFCR | Experiment | Ref. gene | Control | C ± Cit | Stress | S ± Cit |
|---|---|---|---|---|---|---|
| **Ndrg2** | **R12-09** | Cyclophilin | 100 ± 18.5 | | 117.2 ± 12.6 | |
| | **R1-11** | Cyclophilin | 100 ± 5.5 | 76.3 ± 10.2 | 86.13 ± 3.3 | 92.3 ± 5.5 |
| | **R12-09** | β-actin | 100 ± 16.6 | | 113 ± 8.5 | |
| | **R1-11** | β-actin | 100 ± 14.6 | 74.63 ± 10.9 | 127.0 ± 16.7 | 144. 6 ± 24.9 |
| | **R12-09** | GADPH | 100 ± 12.3 | | 119 ± 12 | |
| | **R1-11** | GADPH | 100 ± 15.4 | 52 ± 7.2 | 116.5 ± 13.9 | 101 ± 20.1 |
| **GFAP** | **R12-09** | Cyclophilin | 100 ± 14.6 | | 93.87 ± 12.71 | |
| | **R1-11** | Cyclophilin | 100 ± 18.23 | 201.1 ± 36.5 * | 108 ± 13.5 | 156.8 ± 30.3 |
| | **R12-09** | β-actin | 100 ± 14.87 | | 78.8 ± 3.1 | |
| | **R1-11** | β-actin | 100 ± 7.4 | 142.2 ± 11.72 | 140.7 ± 13.11 * | 149.9 ± 13.44 * |
| | **R12-09** | GADPH | 100 ± 12.3 | | 83 ± 6.4 | |
| | **R1-11** | GADPH | 100 ± 13.3 | 118.8 ± 11.58 | 140.3 ± 14.9 | 122.4 ± 18.81 |
| **AQP4** | **R12-09** | Cyclophilin | 100 ± 18.6 | | 77 ± 4.9 | |
| | **R1-11** | Cyclophilin | 100 ± 28.9 | 184 ± 39.7 | 142 ± 25 | 162 ± 24 |
| | **R12-09** | β-actin | 100 ± 13.6 | | 89 ± 8.3 | |
| | **R1-11** | β-actin | 100 ± 26.7 | 170.7 ± 9.2 | 235 ± 36.9 | 268 ± 32.73 |
| | **R12-09** | GADPH | 100 ± 13.7 | | 92 ± 7.3 | |
| | **R1-11** | GADPH | 100 ± 32.9 | 86.3 ± 15.6 | 164 ± 25.6 | 167.4 ± 30 |
| **GLT-1** | **R12-09** | Cyclophilin | 100 ± 8.9 | | 156 ± 21.3 * | |
| | **R1-11** | Cyclophilin | 100 ± 18.7 | 122 ± 26.4 | 94 ± 11.6 | 101 ± 13.3 |
| | **R12-09** | β-actin | 100 ± 10.3 | | 181 ± 34.8 * | |
| | **R1-11** | β-actin | 100 ± 14.3 | 85 ± 14.9 | 122 ± 17.6 | 104 ± 11.7 |
| | **R12-09** | GADPH | 100 ± 6.4 | | 199 ± 34.4 * | |
| | **R1-11** | GADPH | 100 ± 21.6 | 50 ± 9.5 | 96 ± 13.5 | 67 ± 9.7 |
| **GLAST** | **R12-09** | Cyclophilin | 100 ± 8.3 | | 99.25 ± 7.6 | |
| | **R1-11** | Cyclophilin | 100 ± 17.2 | 114 ± 24.6 | 86 ± 3.7 | 94.48 ± 18 |
| | **R12-09** | β-actin | 100 ± 9.6 | | 98.6 ± 11.35 | |
| | **R1-11** | β-actin | 100 ± 9.6 | 107 ± 11.5 | 138 ± 17.0 | 114.6 ± 10.3 |
| | **R12-09** | GADPH | 100 ± 7.9 | | 94 ± 9.8 | |
| | **R1-11** | GADPH | 100 ± 8.2 | 71.3 ± 6.4 | 98.9 ± 9.5 | 77.2 ± 7.8 |

Data are presented as a percentage of the control group (mean ± SEM). Statistics: two-way ANOVA (stress x drug) followed by Student-Newman-Keuls post hoc analysis,*$p<0.05$.

*Ratio ($2^{-CT}$ stress samples average / $2^{-CT}$ control samples average)($2^{-CT}$ S / $2^{-CT}$ C) as a measurement of reference gene expression stability after chronic social stress in the prefrontal cortex*

The calculation of the ratios: $2^{-CT}$ S / $2^{-CT}$ C for experiment R12-09 revealed generally stable reference gene expression in the right hemisphere, but high instability of reference gene expression in the left prefrontal cortex (Table 6). According to the data, cyclophilin would

be the best reference gene choice in order to enable comparisons of gene expression after stress and analysis of hemispheric differences in gene expression.

Table 6. Ratios ($2^{-CT}$ S / $2^{-CT}$ C) in the prefrontal cortex after chronic social stress.

| Gene | Ratio S/C (PFC right) | Ratio S/C (PFC left) |
|---|---|---|
| **GAPDH** | 0.85 | 0.60 |
| **β-actin** | 0.97 | 0.57 |
| **Cyclophilin** | 0.90 | 0.70 |
| **SDHa** | 0.86 | 0.60 |
| **Rpl13a** | 0.96 | 0.51 |
| **Ywhaz** | 1.23 | 0.56 |

*NormFinder analysis for assessment of gene expression stability in the prefrontal cortex after chronic social stress and antidepressant treatment*

To further explore which gene may serve as a reliable reference gene for quantification of mRNA expression in the two hemispheres of the prefrontal cortex, mRNA expression of different housekeeping genes (cyclophilin, β-actin, GAPDH, SDHa, Ywhaz and RPL13a) was quantified in left and right PFC of Control and Stress animals and results were subjected to NormFinder analysis. The test ranks the candidate genes according to their expression stability and allows identification of the best reference gene from the candidates (Andersen *et al.* 2004). The analysis revealed that on the average, cyclophilin and Ywhaz were the most stable genes for both prefrontal cortices. For the left hemisphere, cyclophilin results in a stability value of $6.96 \times 10^{-8}$, while Ywhaz had a value of $1.32 \times 10^{-7}$. In the right hemisphere, the respective stability values were $1.99 \times 10^{-7}$and $2.40 \times 10^{-7}$. Also in both hemispheres, β-actin was the least stable expressed gene as shown by high ratios. However, other methodological factors apparently had effects on the reproducibility of the data, as discussed below (section 4.1.1.3).

## 3.1.3 Assessment of physiological indicators of the stress response to chronic social defeat

### 3.1.3.1 Body weight

Five weeks of daily social defeat caused a reduction in body weight gain in the stressed rats as compared to controls after the 2nd ($p<0.05$), 3rd ($p<0.01$), 4th ($p<0.001$) and 5th ($p<0.001$) weeks of social defeat (Fig. 17). Citalopram had no effect on body weight gain in control animals, but stressed animals treated with the drug gained less weight compared with controls after 1 ($p<0.01$), 2 ($p<0.001$), 3 ($p<0.001$), 4 ($p<0.001$) and 5 ($p<0.001$) weeks of stress. Two-way ANOVA (treatment x time) revealed a significant effect of treatment ($F_{(15,276)}=5.675$, $p<0.0001$), time ($F_{(3,276)}=70.83$, $p<0.0001$) and an interaction effect ($F_{(5,276)}=319.8$, $p<0.0001$).

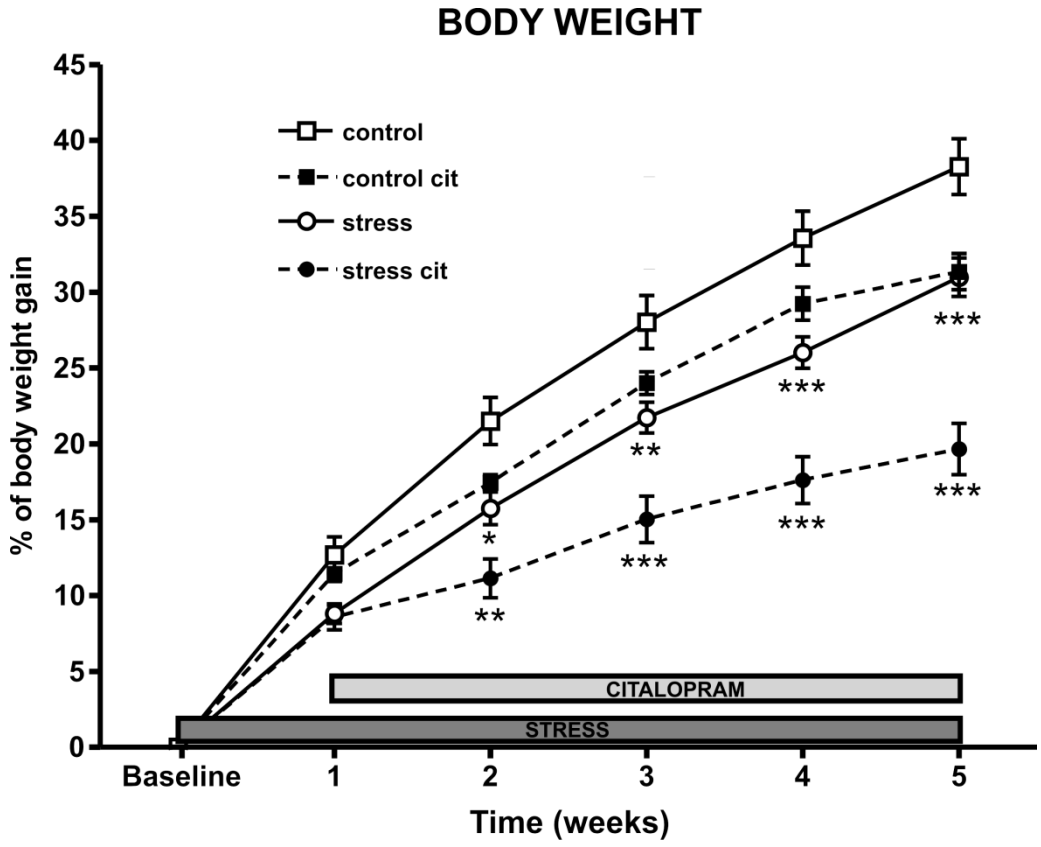


Fig. 17. Effect of chronic psychosocial stress on body weight gain in the experimental animals. Repeated social defeat reduced body weight gain compared to control rats. Results are expressed as a percentage of body weight gain (mean ± SEM). Statistics: Two-way ANOVA for repeated measures, stress x weeks followed by Student-Newman-Keuls post test analysis. **$p<0.01$, ***$p<0.001$compared to control.

### 3.1.3.2 Adrenal glands

Chronic social defeat caused an increase in adrenal gland weight in the stressed animals. Analysis with two-way ANOVA (stress x drug) showed a significant effect of stress on adrenal gland/body weight ratio ($F_{(1,32)}$=11.310, $p$=0.002), but no effect of drug administration ($F_{(1,32)}$=0.297, $p$=0.6) and no interaction ($F_{(1.32)}$=1.805, $p$=0.2) (Fig. 18). Student-Newman-Keuls post test showed no within group differences.

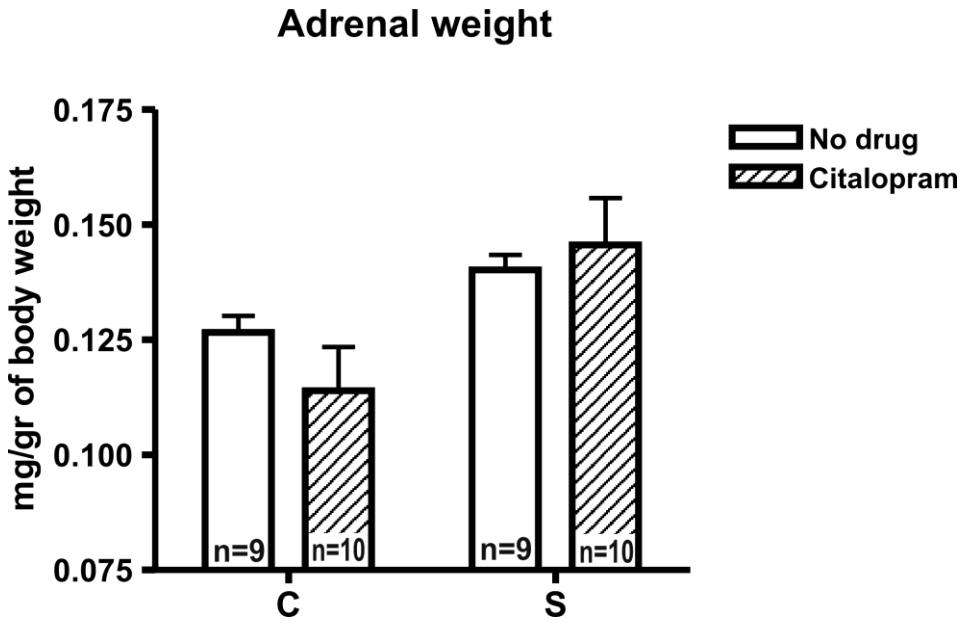


Fig. 18. Effect of chronic psychosocial stress on relative adrenal weight in the experimental animals. Stress caused a significant increased in adrenal gland size. Statistics: Two-way ANOVA (stress x drug) showed a significant stress effect **$p$<0.01. Student-Newman-Keuls post test showed no within group differences. Data are expressed as mean ± SEM.

### 3.1.3.3 Corticosterone and testosterone determination in trunk blood

Both stress and CIT resulted in effects on plasma corticosterone concentration in the animals. Analysis with two-way ANOVA (stress x drug) showed a significant effect of stress ($F_{(1,29)}$=6.848, $p$<0.05) and drug ($F_{(1,29)}$=25.74, $p$<0.001) on corticosterone plasma levels (Fig. 19). The *post hoc* test showed that the corticosterone plasma levels were

increased in the Stress + Citalopram group ($p$<0.001) and Control + Citalopram group ($p$<0.01), but not in the Stress group as compared to the Control group ($p$>0.05).

On the other hand, stress and CIT had no effects on testosterone levels in the animals. Analysis with two-way ANOVA (stress x drug) showed no significant effects of stress or drug, but a significant effect for drug x treatment interaction ($F_{(1,33)}$=5.76, $p$<0.05) (Fig. 19). The *post hoc* test showed that testosterone plasma levels were decreased in the Control + Citalopram group ($p$<0.05), but no effect was shown in the Stress or Stress + Citalopram groups as compared to the Control group ($p$<0.05). Nevertheless statistical analysis with a *t*-test showed a significant difference between C and S groups ($t_{(17)}$=2.30, $p$=0.03).

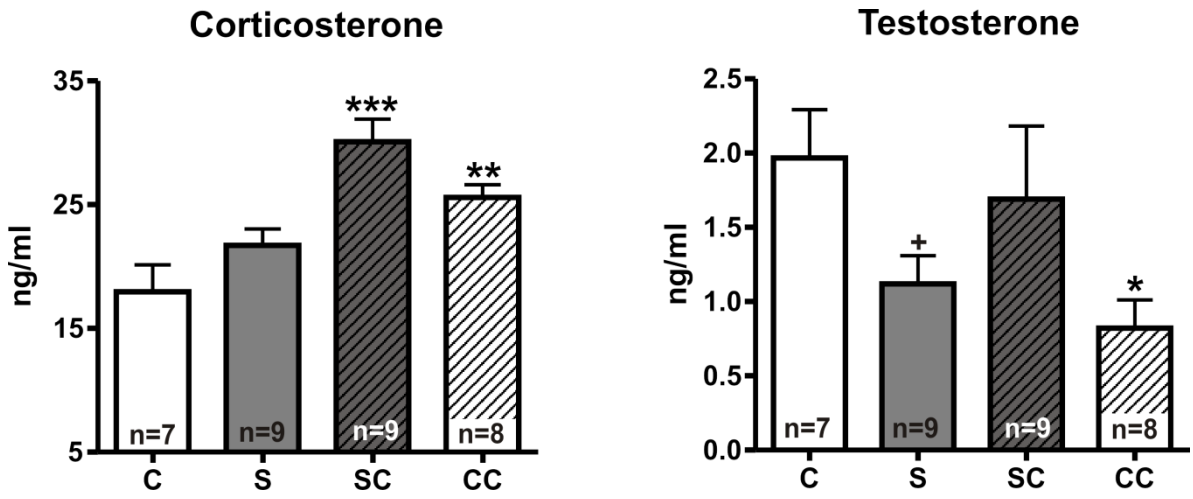


Fig. 19. Effect of chronic psychosocial stress on plasma corticosterone and testosterone levels. Statistics: Two-way ANOVA (stress x drug) followed by Student-Newman-Keuls post hoc analysis. *$p$<0.05, **$p$<0.01 and ***$p$<0.001 compared to C. Two-tailed unpaired Student's *t*-test; $^{+}p$<0.05 compared to C. C=control, CC=control citalopram, S=stress, SC=stress citalopram. Data are expressed as mean ± SEM.

## 3.1.4 Serum and brain tissue concentration of citalopram and its metabolites

The average concentrations of CIT, DCIT and DDCIT in plasma were in the range of values reported previously in a study using the same citalopram dose (Abumaria *et al.*, 2007). No significant differences in concentrations were observed between control and stress animals (Table 7). In plasma, the average CIT to DCIT ratio was 0.55 and CIT to DDCIT ratio was 0.46, while in the cortex the CIT to DCIT ratio was 2.10 and the CIT to DDCT ratio was

2.96, showing a significantly higher concentration of citalopram in the neocortex as compared to blood.

Table 7. Citalopram and its metabolites in blood and neocortex.

| | CONTROL CITALOPRAM | | STRESS CITALOPRAM | |
|---|---|---|---|---|
| Compound | Blood (ng/ml) | Brain (ng/g) | Blood (ng/ml) | Brain (ng/g) |
| CIT | 99.9 ± 14.5 | 674.0 ± 137.3 | 84.3 ± 8.9 | 535.0 ± 86.55 |
| DCIT | 180.5 ± 17.5 | 301.5 ± 21.04 | 191.4 ± 18.5 | 339.0 ± 29.6 |
| DDCIT | 231.2 ± 8.5 | 226.0 ± 9.21 | 243.5 ± 16.8 | 228.0 ± 16.05 |

Data are presented as mean ± SEM. No significant differences between CC and SC (two-tailed unpaired Student's *t*-test).

# 3.2 Modulation of gene expression by chronic restraint stress

## 3.2.1 HIPPOCAMPUS

### 3.2.1.1 Real-time PCR quantification of mRNA expression

*GLT-1 and Ndrg2 mRNA expression was modulated by chronic restraint stress*

Real-time PCR quantitative analysis of mRNA expression showed that levels of GLT-1 and Ndrg2 were modulated by restraint stress. Three weeks of chronic restraint stress significantly increased GLT-1 mRNA expression relative to controls (*t*-test, $t_{(18)}$=2.201, $p$=0.04) in the hippocampus, while there was a trend for downregulation of Ndrg2 (*t*-test, $t_{(17)}$=2.035, $p$=0.0578) (Fig. 20).

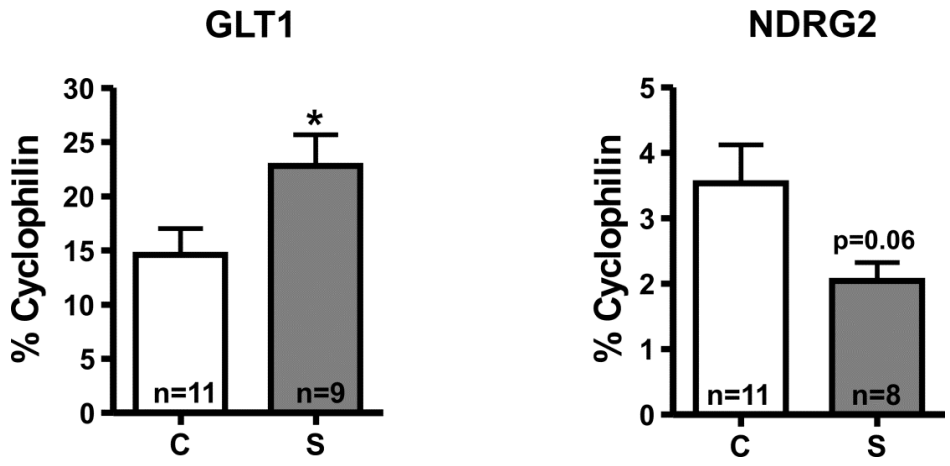


Fig. 20. Effects of chronic restraint stress on the expression of GLT-1 and Ndrg2 in the hippocampus. Data were generated by quantitative real-time PCR with mRNA expression normalized against the housekeeping gene cyclophilin (presented as a percentage). Significant differences are indicated by asterisks (two-tailed unpaired Student's *t*-test: **p*<0.05). Data are expressed as mean ± SEM. C=control, S=stress.

*Other astroglial genes were not modulated at the mRNA level by chronic restraint stress*

Real-time PCR quantitative analysis of mRNA expression showed that levels of GFAP, GLAST, AQP4 and Kir4.1 in the hippocampus were not modulated by three weeks of chronic restraint stress. Statistical analysis using *t*-tests showed no significant stress-induced effects on their expression compared to their respective controls ($t_{(18)}$=1.569, $p$=0.13; $t_{(18)}$=0.4385, $p$=0.67; $t_{(17)}$=0.5986, $p$=0.56; $t_{(26)}$=1.480, $p$=0.15 for GFAP, GLAST, AQP4 and Kir4.1, respectively) (Fig. 21).

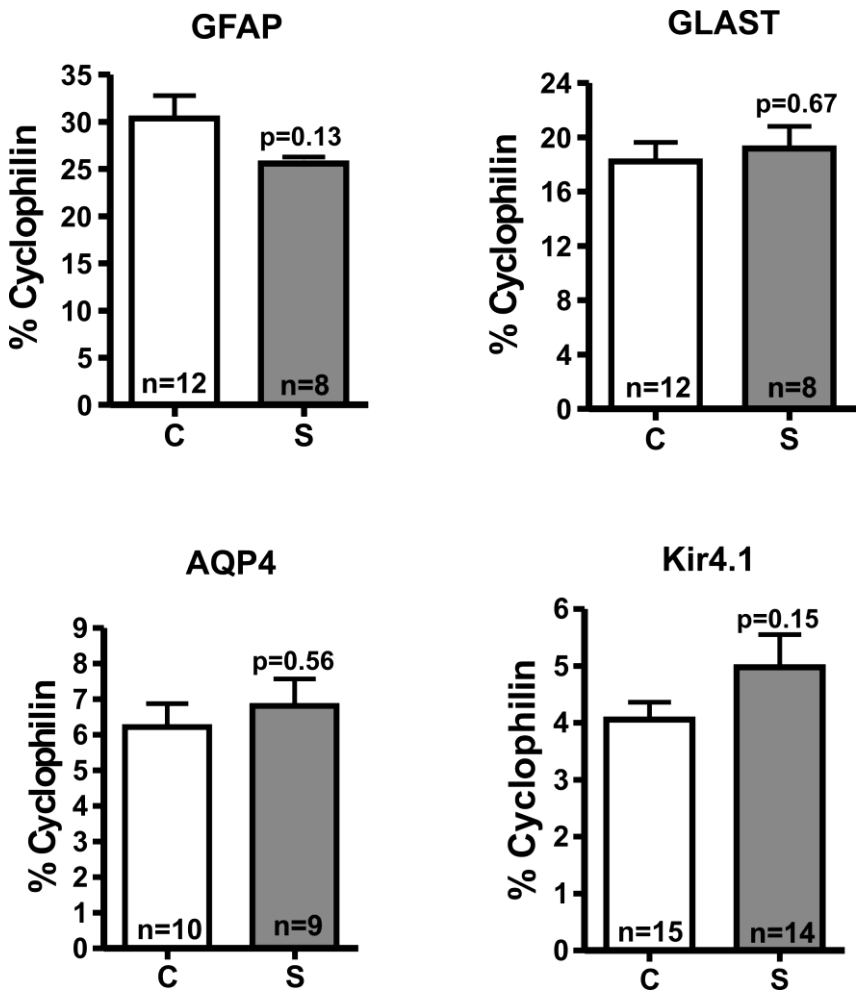


Fig. 21. Effect of chronic restraint stress on the expression of GFAP, GLAST, AQP4 and Kir4.1 in the hippocampus. Data were generated by quantitative real-time PCR with mRNA expression normalized against the housekeeping gene cyclophilin (presented as a percentage). None of the genes showed a significant difference in expression compared to controls after chronic restraint stress (two-tailed unpaired Student's *t*-test). Data are expressed as mean ± SEM. C=control, S=stress.

### 3.2.1.2 Western blot quantification of NDRG2, Kir4.1 and GFAP protein in rats after chronic restraint stress

Chronic restraint stress caused no significant changes in NDRG2 or GFAP expression, but a downregulation of Kir4.1 protein expression in the hippocampus.

Statistical analysis with *t*-tests revealed that stress did not modulate NDRG2 (~37kDa) expression ($t_{(14)}$=1.305, $p$=0.21) or GFAP ($t_{(12)}$=1.297, $p$=0.22), but caused a significant decrease in the optical density of the bands corresponding to the potassium channel Kir4.1 (~43kDa) ($t_{(13)}$= 3.476, $p$=0.0041) (Fig. 22).

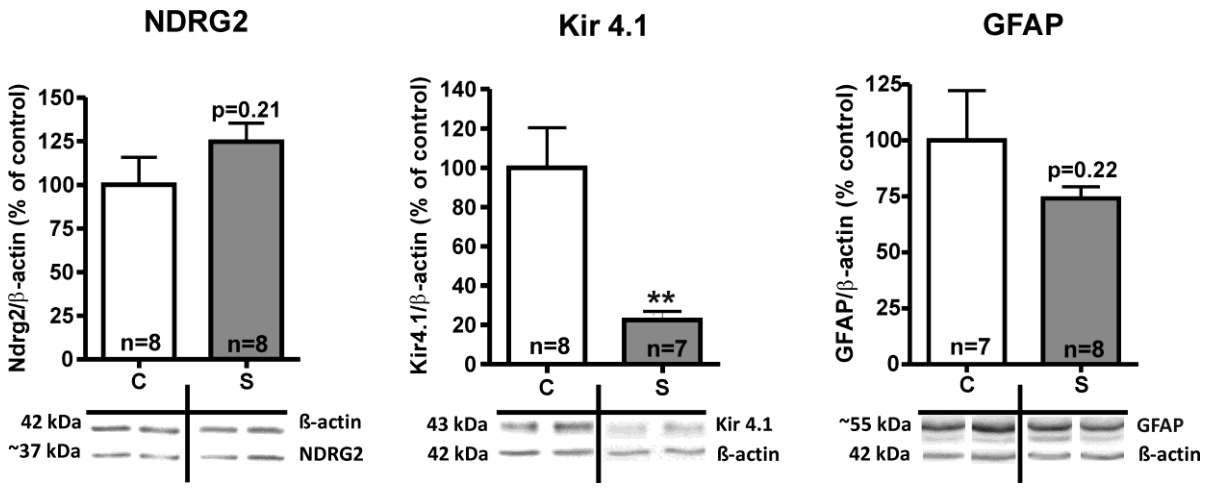


Fig. 22. Effects of chronic restraint stress on NDRG2, Kir4.1 and GFAP protein expression in the hippocampus. Three weeks of chronic restraint stress did not modulate NDRG2 and GFAP expression in the hippocampus, but caused a downregulation of Kir4.1. Representative Western blot gel bands are shown beneath the graphs. Protein expression was normalized against the housekeeping gene β-actin. The results are presented as a percentage of the control group (mean ± SEM). Statistics: two-tailed unpaired Student's *t*-test, $^{**}p<0.01$, vs control. C=control, S=stress.

### 3.2.1.3 Western blot quantification of AQP4 protein in rats after chronic restraint stress and cellular localization by immunohistochemistry

Chronic restraint stress caused no significant changes in AQP4 (~36 kDa) expression in the hippocampus compared to control ($t_{(23)}$=0.3015, $p$=0.76) (Fig. 23A). AQP4 is expressed in astrocyte endfeet that ensheath neuronal elements and blood vessels (Fig. 23B-D).

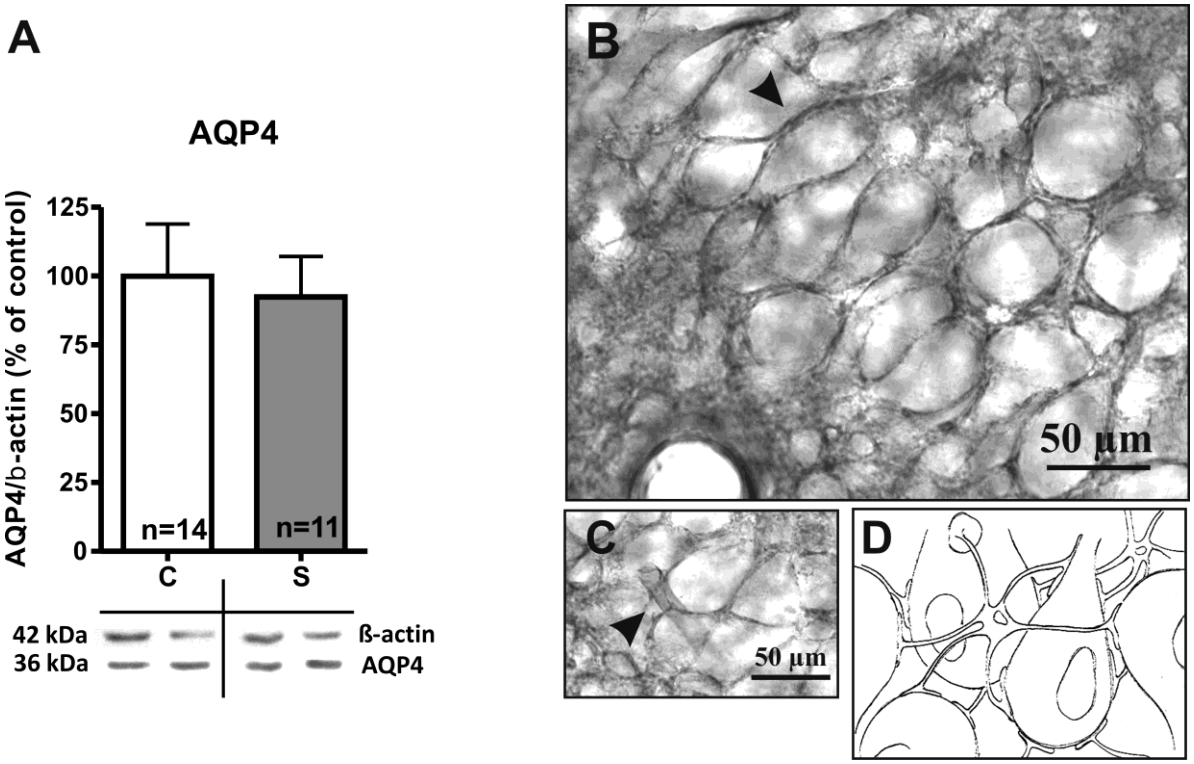


Fig. 23. AQP4 protein expression in the hippocampus after chronic restraint stress. A) AQP4 was not modulated by chronic restraint stress (two-tailed unpaired Student's *t*-test). Data are expressed as mean ± SEM. C=control, S=stress. B) In CA1 area in the hippocampus, AQP4 localizes to endfeet processes that ensheath neuronal elements (thick arrow) and C) blood vessels (thick arrow). D) Graphical representation of an astrocyte's endfeet contacting several neuronal cell bodies.

## 3.2.2 Assessment of physiological indicators of the stress response to chronic restraint

### 3.2.2.1 Body weight

Three weeks of chronic restraint stress decreased body weight gain in the stressed rats as compared to controls after the 1st ($p<0.01$), 2nd ($p<0.01$) and 3rd ($p<0.001$) weeks of restraint (Fig. 24). Two-way ANOVA (stress x weeks) revealed a significant effect of stress ($F_{(1,81)}=7.721$, $p=0.0007$), time ($F_{(3,81)}=176.2$, $p<0.0001$) and an interaction effect ($F_{(3,81)}=16.18$, $p<0.0001$).

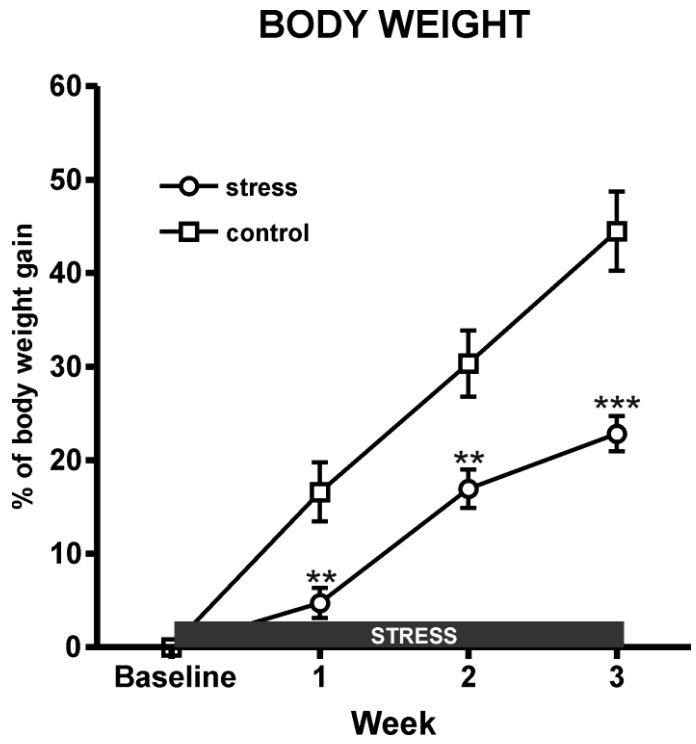


Fig. 24. Effect of chronic restraint stress in body weight gain in the experimental animals. Repeated restraint stress reduced the body weight gain in stressed rats compared to control rats. Results are expressed as percentage of body weight gain (mean ± SEM). Statistics: Two-way ANOVA repeated measures, (stress x weeks) followed by Student-Newman-Keuls post test analysis.

### 3.2.2.2 Adrenal glands, corticosterone and testosterone

Chronic restraint stress increased adrenal gland weight in the stressed animals. Statistical analysis with a *t*-test showed a significant effect of stress on adrenal gland/body weight ratio ($t_{(27)}$=6.341, $p$<0.0001). On the other hand, there was a slight, but non-significant increase in corticosterone levels. Testosterone levels were also not significantly altered (Table 8).

Table 8. Effects of chronic restraint stress on adrenal weight, corticosterone and testosterone levels. Adrenal weight is expressed as a percentage of body weight at the end of the experiment.

| | Control | Stress |
|---|---|---|
| **Adrenal glands** | 0.1379 ± 0.0043 | 0.1733 ± 0.0034***↑ |
| **(mg/gr of body weight)** | n=15 | n=14 |
| **Corticosterone** | 18.20 ±2.61 | 20.84 ± 3.06 |
| **(ng/ml)** | n=14 | n=12 |
| **Testosterone** | 3.55 ± 0.42 | 4.42 ± 0.86 |
| **(ng/ml)** | n=15 | n=14 |

Data are presented as mean values ± SEM. (Statistics: two-tailed unpaired Student's *t*-test, ***$p$<0.0001)

## 3.3 Astrocyte culture experiments

### 3.3.1 Generation of the GfaABC1D-Ndrg2S and the GfaABC1D-Ndrg2L vectors

The sequence identity of the viral plasmids was confirmed by enzymatic digestions with SmaI and BamHI. Ndrg2 (S and L) sequence was also corroborated by sequencing. Digestion with SmaI rendered five products, as shown by: a big band of 3013 bp, followed by a band of 1170 bp or 1213 bp (corresponding to Ndrg2S or Ndrg2L, respectively) and three smaller bands of 964 bp, 673 bp and 11 bp (not visible). Digestion with BamHI generated two fragments: 4734 bp and 1097 or 1140 bp (Ndrg2S or Ndrg2L, respectively) (Fig. 25).

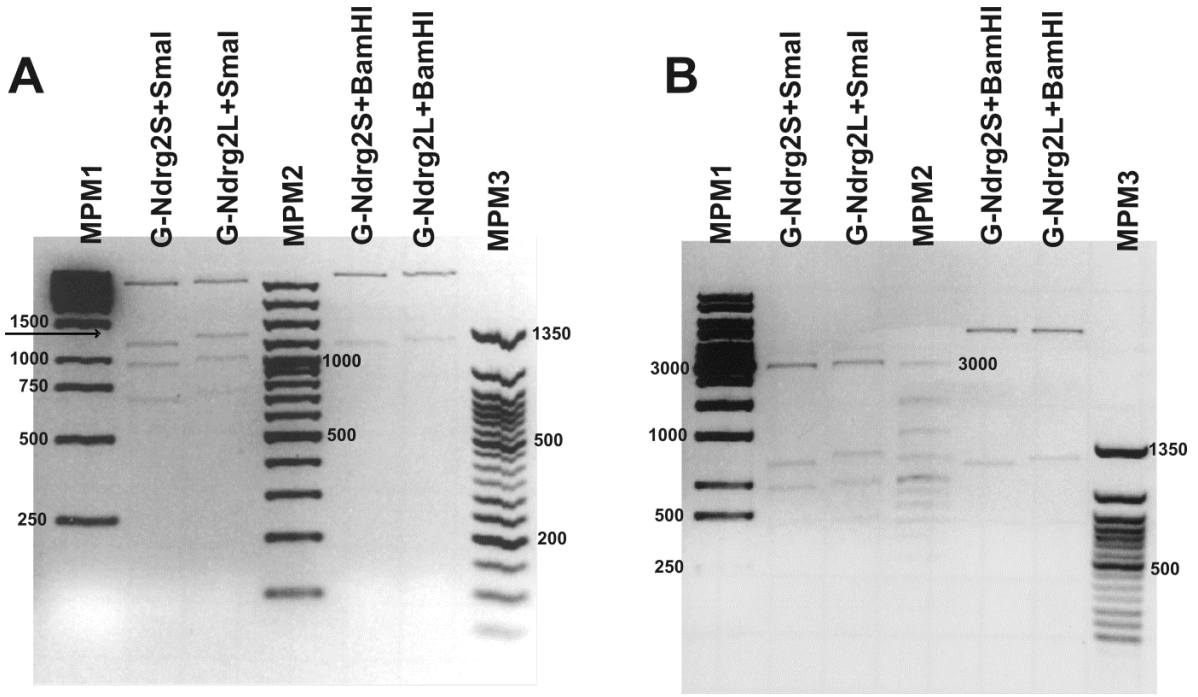


Fig. 25. Enzymatic digestion of plasmids GfaABC1D-Ndrg2S and GfaABC1D-Ndrg2L with SmaI and BamHI. Digestion products were run in two gels: 1% (A) and 2% (B). The size of the bands was compared against three different molecular weight markers (MPM1, MPM2 and MPM3). Digestion with SmaI rendered 5 bands: 3013 bp, 1170 bp or 1213 bp (Ndrg2S or Ndrg2L, respectively (arrow)), 964 bp, 673 bp and 11 bp (not visible). Two bands were the products of the digestion with BamHI (4734 bp and 1140 or 1097 bp for Ndrg2S and Ndrg2L, respectively). Molecular weight is expressed in base pairs.

## 3.3.2 Astrocyte-enriched cultures

Secondary astrocyte cultures were characterized by immunofluorescent staining with the astroglial marker GFAP and the astrocyte-specific protein NDRG2. Additionally, the cultures were stained with the microglial marker IBA-1 in order to discard the presence of microglia. The number of positive GFAP and NDRG2 cells was compared to the number of DAPI positive nuclei in order to estimate the percentage of astrocytes in the culture. Furthermore, staining with markers for oligodendroglia (RIP) and neuronal markers (mitogen activated protein, MAP) (data not shown) was also performed to exclude the presence of other cells in the culture. Results showed a high number of cells positive for GFAP and NDRG2, while only a small number of cells were IBA-1 positive (approx. 3%), indicating that the cultures were highly enriched in astrocytes (>90%) (Fig. 26). There was no positive staining for oligodendrocytes or neurons.

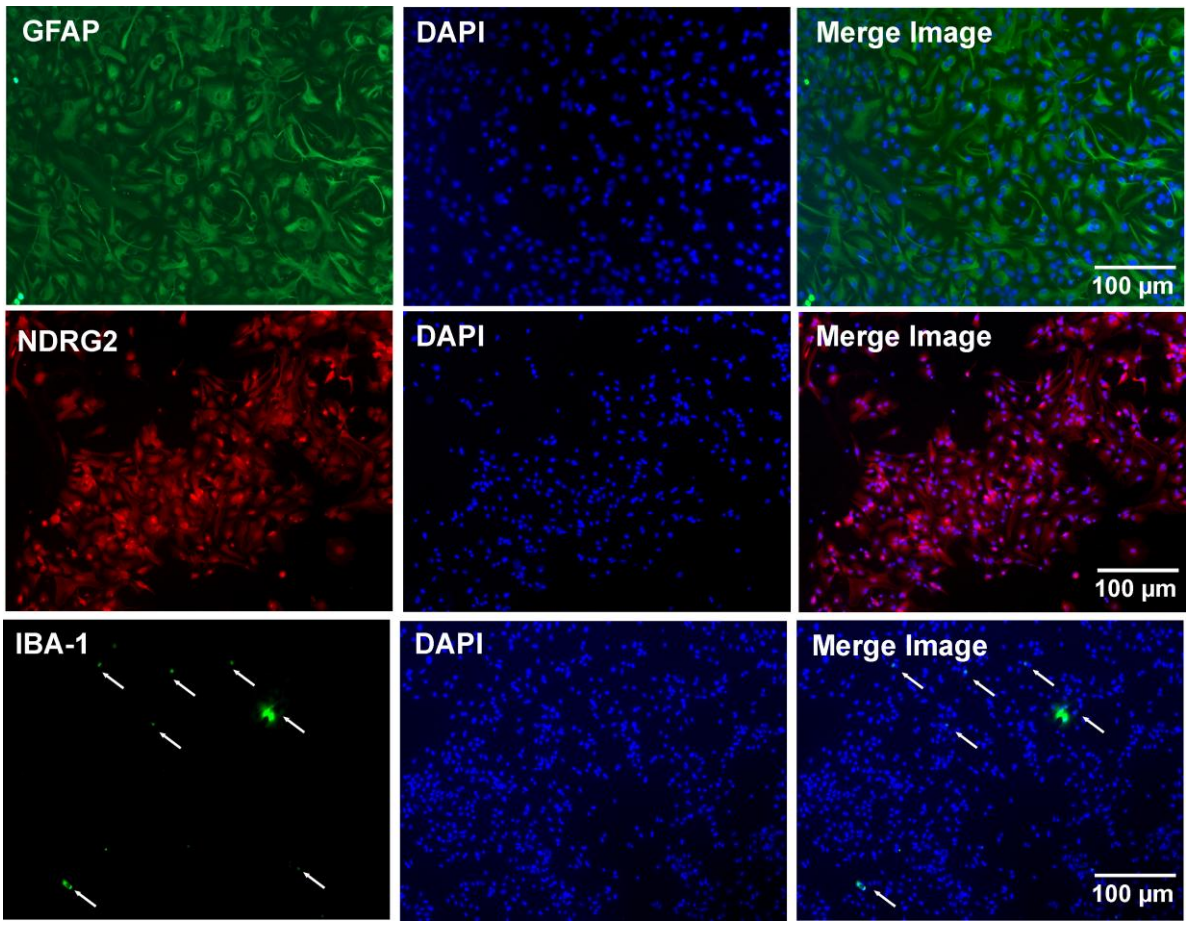


Fig. 26. Enriched astrocyte cultures. Three separate secondary astrocyte cultures were double stained with DAPI (blue) together with antibodies against GFAP (green), NDRG2 (red) or IBA-1(green). The arrows show IBA-1 immunoreactive cells (microglia).

### 3.3.3 Transduction of the astrocytes cultures

Cell cultures enriched in astrocytes were used for transduction with adeno-associated viral vectors carrying the two different isoforms of Ndrg2:, Ndrg2S (short isoform; 1990 bp, 357aa), and Ndrg2L (long isoform; 2032 bp, 371 aa). Astrocyte cultures were transduced as described above (see section 2.10.2.4) with AAV-Ndrg2S, AAV-Ndrg2L. AAV-EGFP (AAV with sequence for green fluorescent protein) served as a negative control to differentiate between transduction-induced changes and NDRG2-induced alterations. Additionally, some cultures were incubated with only PBS without any virus in order to exclude any possible effect that could arise from the manipulation of the cultures during the transduction procedure.

Immunofluorescent images as well as Western blots confirmed NDRG2 overexpression in the cultures (Figs. 27, 28). Considering the role that has been proposed for NDRG2 in cell proliferation and differentiation, the experiments conducted here aimed to assess whether NDRG2 upregulation had a visible effect in astrocyte proliferation or morphology.

Western blot analysis of protein expression also revealed enhanced NDRG2 protein expression in the cultures transduced with AAV-Ndrg2S, AAV-Ndrg2L and AAV-EGFP in comparison to PBS. However, statistical analysis showed no significant AAV-mediated overexpression of NDRG2 in the cultures transduced with the short isoform ($t_{(5)}$=1.794, $p$=0.13) or the long isoform ($t_{(4)}$=1.128, $p$=0.32). Cell cultures transduced with AAV-EGFP also seemed to induce higher expression of NDRG2; however, the increase was not statistically significant ($t_{(5)}$=1.033, $p$=0.72) (Fig. 27).

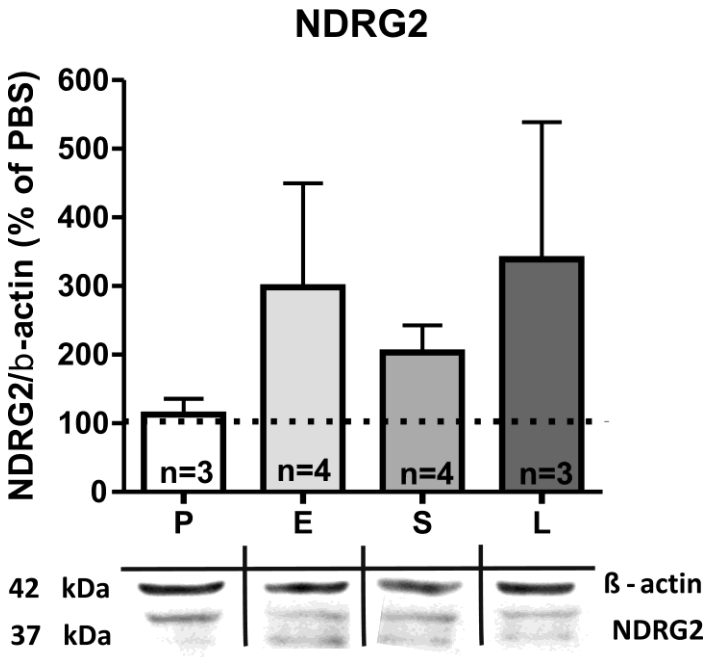


Fig. 27. Western blot analysis of NDRG2 protein expression in astrocyte cultures transduced with AAV-Ndrg2S, AAV-Ndrg2L and AAV-EGFP and compared against cultures that were not transduced (PBS). Representative Western blot gel bands are shown beneath the graph. The results are presented as a percentage of the control group (PBS) (mean ± SEM). Statistics: two-tailed unpaired Student's *t*-tests revealed no significant differences in NDRG2 protein expression in the cultures transduced with AAV-Ndrg2S, AAV-Ndrg2L and AAV-EGFP compared to PBS. P=PBS, E= AAV-EGFP, S= AAV-Ndrg2S, L= AAV-Ndrg2L.

The cultures were identified by immunofluorescent staining with DAPI, NDRG2 and β-catenin (localized mainly in the plasma membrane) for the analysis of cell morphology. The staining allowed clear visualization of the cell boundaries and revealed that the astrocyte cultures were transduced with the adeno-associated viruses AAV-Ndrg2S, AAV-Ndrg2L and AAV-EGFP, as shown by an increase in NDRG2 (red) and EGFP (green) expression in a group of cells in comparison to non-transduced cells and the PBS negative cultures (Fig. 28).

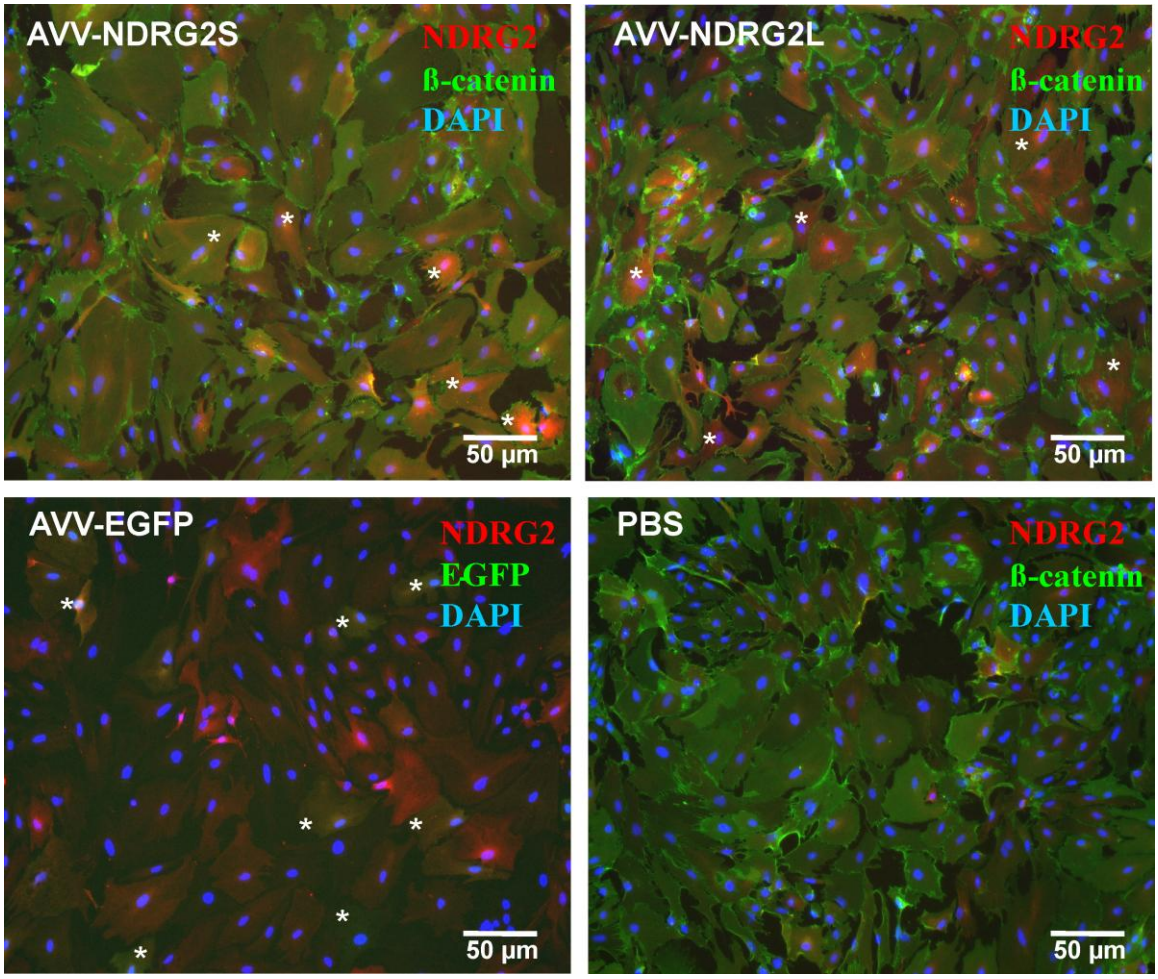


Fig. 28. Astrocyte cultures were transduced with AAV-Ndrg2S, AAV-Ndrg2L and AAV-EGFP. The cultures were stained for NDRG2 (red), β-catenin (green in the AAV-Ndrg2 transduced cultures and red in the AAV-EGFP cultures) and DAPI (blue). Examples of transduced cells which show an enhanced fluorescence are marked with asterisks (*).

### 3.3.4 Analysis of cell proliferation and morphology in astrocyte cell cultures transduced with Ndrg2

Astrocyte-enriched secondary cultures were transduced with AAV-Ndrg2S, AAV-Ndrg2L and AAV-EGFP or just PBS was added to the medium as previously described (see section 2.10.2.4). The WST-1 proliferation assay showed significantly reduced cell proliferation in the astrocyte cultures transduced with AAV-Ndrg2S ($t_{(21)}$=6.174, $p$<0.0001), AAV-Ndrg2L ($t_{(21)}$=4.850, $p$<0.0001) and AAV-EGFP ($t_{(22)}$=5.507, $p$<0.0001) compared to the PBS control (Fig. 29).

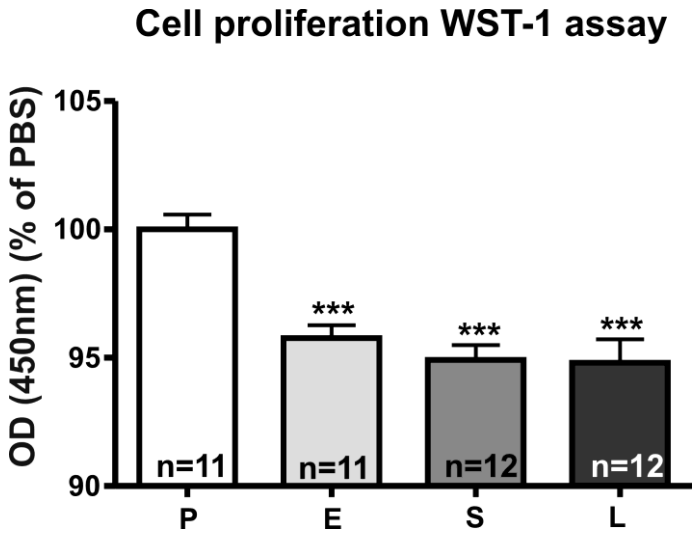


Fig. 29. Analysis of cell proliferation in astrocyte-enriched cultures transduced with AAV-Ndrg2S, AAV-Ndrg2L and AAV-EGFP and compared against cultures that were not transduced (PBS). The results are presented as a percentage of the control group (PBS) (mean ± SEM). Statistics: two-tailed unpaired Student's *t*-test revealed significant differences in cell proliferation in the cultures transduced with AAV-Ndrg2S, AAV-Ndrg2L and AAV-EGFP compared to PBS. ***$p<0.0001$. P=PBS, E= AAV-EGFP, S= AAV-Ndrg2S, L= AAV-Ndrg2L.

Regarding the assessment of morphological parameters in the astrocyte-enriched secondary cultures, transduction with AAV-Ndrg2L caused a non-significant reduction in cell perimeter and area, accompanied by a higher circularity value (meaning that the cells were more spherical than the control ones) ($t_{(111)}$=1.463, $p$=0.14; $t_{(110)}$=1.809, $p$=0.07 and $t_{(109)}$=1.125, $p$=0.26 for perimeter, area and circularity, respectively). Transduction of the short isoform of Ndrg2 caused no effect in any of the parameters measured (perimeter: $t_{(107)}$=1.075, area: $p$=0.28; $t_{(106)}$=0.1670, $p$=0.86 and cell circularity: $t_{(107)}$=1.385, $p$=0.17 respectively). Furthermore, transduction with AAV-EGFP had a significant effect on cell circularity. Astrocytes positive for EGFP expression were less circular (irregular shape) than control cells ($t_{(109)}$=2.017, $p$=0.04) and showed a non-significant increase in cell perimeter and area ($t_{(108)}$=1.758, $p$=0.08 and $t_{(108)}$=0.7685, $p$=0.44) (Fig. 30).

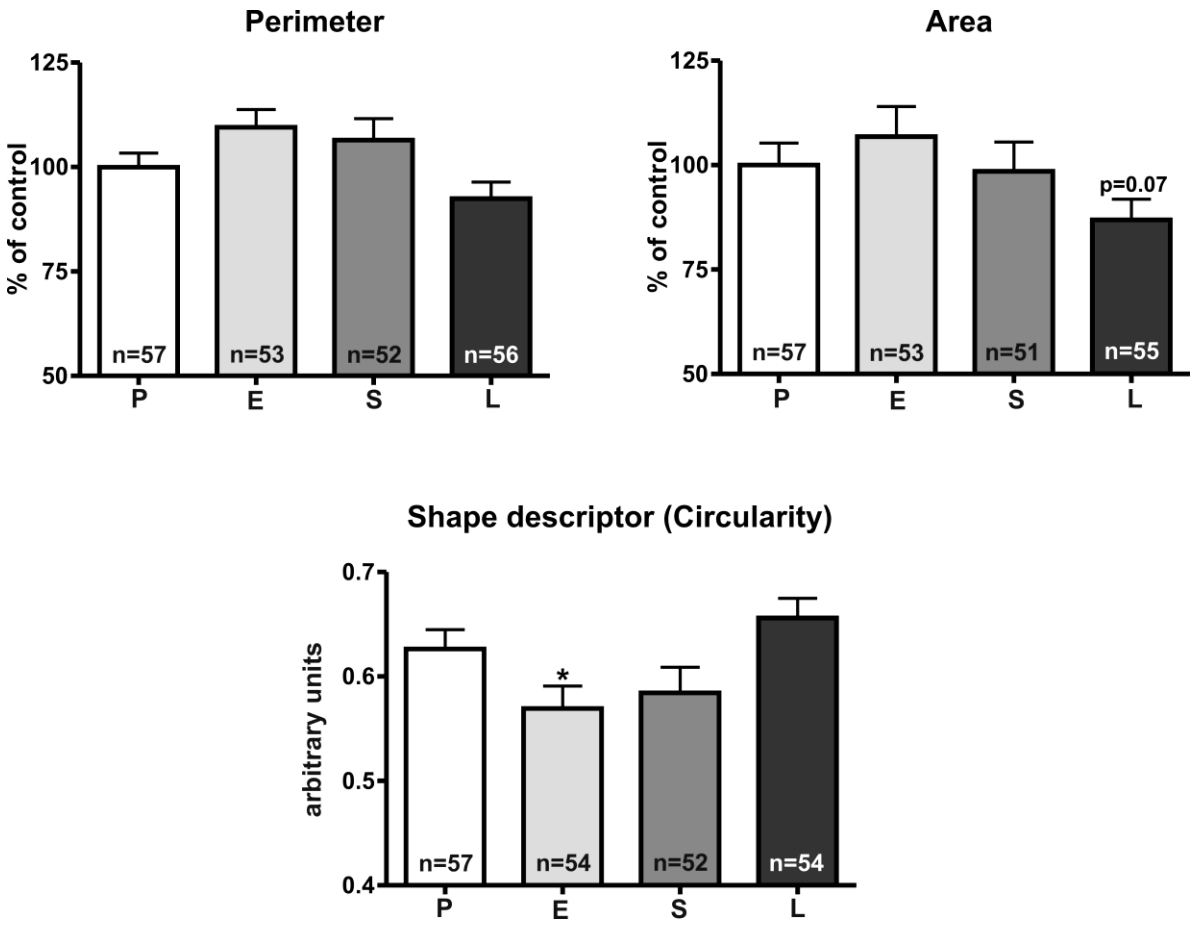


Fig. 30. Measurement of morphological parameters in AAV-Ndrg2S, AAV-Ndrg2L and AAV-EGFP-transduced cells compared with cultures that were not transduced (PBS). The results are presented as a percentage of the control group (PBS) (mean ± SEM). Statistics: two-tailed unpaired Student's *t*-test revealed a significant effect of AAV-EGFP transduction on cell shape, and a trend to a reduced area after AAV-Ndrg2L transduction. *$p$<0.05. P=PBS, E= AAV-EGFP, S= AAV-Ndrg2S, L= AAV-Ndrg2L.

## 3.3.5 Analysis of GFAP expression in cell cultures transduced with AAV-Ndrg2S, AAV-Ndrg2L and AAV-EGFP

Western blot analysis of GFAP expression revealed a non-significant increase in the optical density of the band representing GFAP in the cultures transduced with AAV-Ndrg2S compared to the PBS control ($t_{(5)}$=2.391, $p$=0.06). There were no significant changes in GFAP expression in the astrocyte cultures transduced with the long Ndrg2 isoform ($t_{(5)}$=1.094, $p$=0.32) or with EGFP ($t_{(6)}$=0.3691, $p$=0.72) (Fig. 31).

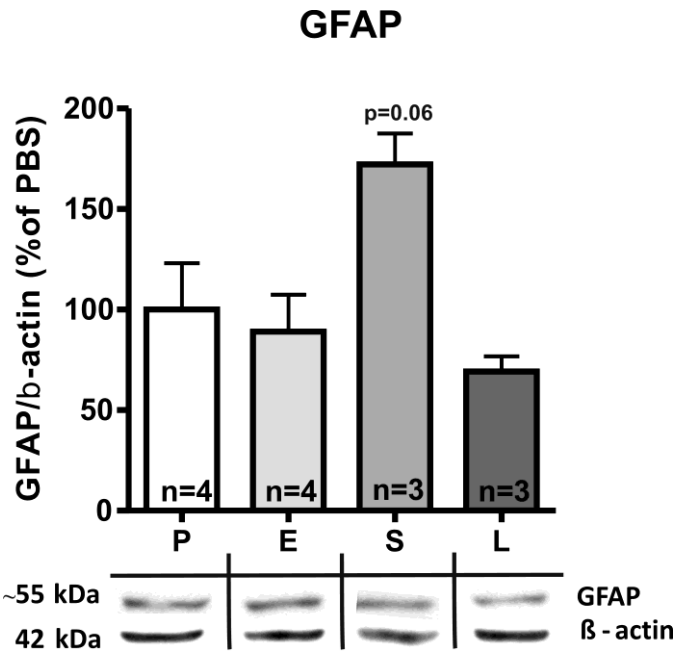


Fig. 31. Western blot analysis of GFAP protein expression in astrocyte cultures transduced with AAV-Ndrg2S, AAV-Ndrg2L and AAV-EGFP and compared against cultures that were not transduced (PBS). Representative Western blot gel bands are shown beneath the graph. The results are presented as a percentage of the control group (PBS) (mean ± SEM). Statistics: two-tailed unpaired Student's *t*-test revealed no significant differences in GFAP protein expression in the cultures transduced with AAV-Ndrg2S, AAV-Ndrg2L and AAV-EGFP compared to PBS. P=PBS, E= AAV-EGFP, S= AAV-Ndrg2S, L= AAV-Ndrg2L.

.

# 4 Discussion

## 4.1 Methodological aspects

### 4.1.1 Quantitative real-time PCR

Quantitative real-time PCR has become the method of choice to perform analyses that aim to evaluate the effect of a specific condition or treatment on gene expression (Vandesompele *et al.* 2002). Clarifying the extent of changes in expression of specific gene sets enables a better understanding of the mechanisms behind certain biological processes and the changes that lead to pathology. Nevertheless, given the high sensitivity of the method and the complexity of the molecular reactions that it includes, several aspects must be taken into account in order to achieve reproducible, precise and accurate data. Real-time PCR is a variant of the conventional PCR method which allows the quantification of gene expression by detection of a fluorescent reporter whose signal increases exponentially (until it reaches a plateau) as the amount of PCR product accumulates with each cycle (Kubista *et al.* 2006, Ponchel *et al.* 2003).

Among the different types of technologies employed in quantitative real-time PCR protocols, the use of the fluorescent dye SYBR green allows for the analysis of multiple genes (Giulietti *et al.* 2001). This molecule binds to the minor groove in double-stranded DNA so that the measurement of the increase in fluorescent emission reflects an increase in the amount of dsDNA. In order to discard unspecific dsDNA detection, melting curve analyses were performed and intron-spanning primers were also designed (Ponchel *et al.* 2003). All the factors that are listed below (see 4.1.1.1 and following) were considered while performing the real-time experiments for the present investigation.

The quantitative real-time PCR data for the hippocampus presented in this study were reproducible (each experiment was performed in duplicate). In contrast, varying results obtained from the prefrontal cortex leave some open questions about the study of gene expression in this brain region by means of real-time PCR. Factors such as RNA integrity, reference genes, dissection of the tissue, as well as the interplay between these might have played a preponderant role in the lack of reliability of the data as elaborated below.

#### 4.1.1.1 RNA integrity and sample size

One important factor to consider in gene expression studies by means of quantitative real-time PCR is RNA integrity, since the quality of the cDNA to be generated depends upon the integrity of the template RNA. In the experiments presented here, randomly chosen samples for RNA integrity analysis rendered RNA integrity numbers (RIN) (7 to 10) that indicated high RNA quality and therefore RNA was suitable to be used in downstream applications (Schroeder *et al.* 2006). Accordingly, problems due to RNA degradation level were negligible.

Another important factor that influences results from quantitative real-time PCR and the comparison of multiple samples is the amount of starting material. The samples should be similar in size starting from collection of tissue until the amounts (ng) of total RNA and cDNA used in subsequent reactions (Huggett *et al.* 2005). In the present work, special attention was given to this issue in order to assure comparable populations of total RNA and cDNA molecules in all samples. Therefore, we believe that the inconsistencies in gene expression analysis in the prefrontal cortex are mainly related to factors such as the reference gene of choice as well as the dissection of the tissues, as discussed below.

#### 4.1.1.2 Reference gene expression stability

Several genes like glyceraldehyde-3-phosphate dehydrogenase (Gapd), β-actin, 18S subunit ribosomal RNA (18S rRNA), cyclophilin or the hypoxanthine guanine phosphoribosyl transferase 1 (Hprt1) are traditionally used as reference genes to normalize the data of quantitative real-time PCR analyses in the brain (Qin & Crews 2012, Bonefeld *et al.* 2008, Benekareddy *et al.* 2010, Lee *et al.* 2009). However, an extensive discussion has arisen on the choice of reference gene since normalization assumes constant unaltered expression of

these genes under different metabolic conditions or between treatments. Several studies have demonstrated the instability of expression of the classical housekeeping genes used in real-time PCR quantification (Derks *et al.* 2008, Thellin *et al.* 1999, Tunbridge *et al.* 2010, Vandesompele *et al.* 2002).

This instability was exemplified in a study which analyzed the expression of three common reference genes, GAPDH, 18S and β-actin, in several brain regions after two stress paradigms in male and female rats (Derks *et al.* 2008). The authors reported GAPDH expression variations according to the type of stressor and gender in the prefrontal cortex. Moreover, in the hippocampus, a significant difference in β-actin expression was observed after acute stress (but not after chronic stress) compared to the controls. These results are not unexpected, as different treatments might modulate different cellular processes. However, they highlight the need to carefully choose among a set of commonly used reference genes the one that best fits the requirements of that particular study.

In the present experiments, mRNA quantification of hippocampus gene expression was normalized against cyclophilin, which was previously shown to be the optimal reference gene to study gene expression modulation after chronic social stress in the hippocampus (Alfonso *et al.* 2004) and has also been reported as a gene with stable expression in this region (Bonefeld *et al.* 2008).

In regard to prefrontal cortex gene expression analysis, there are no reports of a reference gene whose expression remains unaltered by the factors analyzed in this study and which could be used for the simultaneous analysis of the effects of chronic social stress, antidepressant treatment with citalopram and hemispheric lateralization in the modulation of gene expression. Therefore, mRNA quantification in the prefrontal cortex was performed using three common reference genes based on other studies of gene expression in the brain. Two genes were reported to be stable in the PFC after chronic variable stress: GAPDH, and β-actin (Derks *et al.* 2008). Cyclophilin was chosen as a third reference gene according to its reported stability in the hippocampus after chronic social stress (Alfonso *et al.* 2004, Bonefeld *et al.* 2008). However, the present comparison of prefrontal cortex results, especially from the left hemisphere in the first chronic social stress experiment (R12-09), revealed inconsistencies in the expression of the studied astrocytic genes according to the reference gene of choice. This strongly suggests instability of reference gene expression and calculation of the ratios ($2^{-CT}$ S/ $2^{-CT}$ C) of reference gene expression (Schmittgen & Livak 2008) further supported the findings. For this reason, three additional genes cited in the

literature were tested as possible reference genes for normalization of the data in prefrontal cortex: ribosomal protein L13A (Rpl13a), tyrosine 3-monooxygenase/tryptophan, 5-monooxygenase activation protein, zeta (Ywhaz) and the succinate dehydrogenase complex, subunit A (SDHa) (Kreth *et al.* 2010, Nelissen *et al.* 2009). All of them appeared to be stably expressed in the right prefrontal cortex; however, none of these genes showed reliably stable expression in the left prefrontal cortex.

As discussed below (section 4.1.1.3), other considerations might account for the inconsistencies observed between two separate experiments (R12-09 and R1-11) and should be taken into account for prefrontal cortex data analysis. Other groups have tried to identify stably expressed reference genes in different brain regions using novel approaches. They have developed software programs such as GeNorm and Normfinder in order to find suitable reference genes from a set of selected genes. GeNorm performs a pair-wise comparison of the candidate genes and ranks them according to their expression stability, while NormFinder estimates intra- and intergroup variability to calculate the stability of expression of a group of potential reference genes (Andersen *et al.* 2004, Vandesompele *et al.* 2002). For the present experiments, the NormFinder was used since it accounts for intergroup variations. According to the analysis, the best gene in both hemispheres of the prefrontal cortex was cyclophilin, which is in agreement with the analysis of the ratios ($2^{-CT}$ S/$2^{-CT}$ C) of reference gene expression stability previously performed. As a second candidate, the program selected Ywhaz for both hemispheres. However, it is important to mention that the NormFinder analysis only provides the best gene from the given set of genes tested. Therefore, the analysis requires a careful pre-selection of such genes and only supplies a relative ranking. Since there is no documented evidence of the stability of the reference genes selected in the prefrontal cortex after chronic social stress, the results of the NormFinder analysis should be handled carefully, especially as the $2^{-CT}$ S/$2^{-CT}$ C analysis showed high instability of all the genes in the left prefrontal cortex.

In summary, the present findings from both analyses of reference gene stability in the prefrontal cortex suggest the use of cyclophilin as a candidate reference gene to normalize gene expression for the right hemisphere after chronic social stress, but none of the genes are reliably suitable for mRNA quantification in the left prefrontal cortex.

#### 4.1.1.3 Dissection of the tissue

Another factor that could have caused alterations in the results of gene expression analysis in the prefrontal cortex was the way in which the tissue was dissected. This was suggested by the analysis of GLAST expression in the left prefrontal cortex or GLT-1 in the right hemisphere in the current study. The results from two separate chronic social stress experiments, R12-09 and R1-11, differed from each other even though the data from three different reference genes (GAPDH, cyclophilin and β-actin) in each experiment were similar. While the R1-11 experiment suggested consistent downregulation of GLAST in the left prefrontal cortex, no effect was observed in experiment R12-09. And the R12-09 suggested an upregulation of GLT-1, which was not found in the R1-11 experiment.

Unlike the hippocampus, whose boundaries are clearly defined and thus easily and accurately dissected from the brain, the prefrontal cortex does not have clear anatomical boundaries. In the present experiments, after dissecting the brain from the skull, we made a vertical cut with a scalpel at the anatomical level approximately 3.2 mm from Bregma (Paxinos and Watson, 1986); we removed the olfactory bulb afterwards. However, depending on the individual brain size, the vertical cut could not always be made exactly at the identical level, meaning that it was sometimes made more anterior, sometimes more posterior. Therefore, the amount of tissue from the different PFC areas and also from the corpus callosum, and possibly the claustrum, might have varied among the samples.

In future experiments, it would be advisable to use other methodologies, such as punching out defined areas or microdissection, in order to reduce the likelihood of introducing bias due to variations in tissue dissection. These approaches would be more advantageous, as they would allow for the specific analysis of distinct areas, such as the PL in the mPFC. However, for a Western blot analysis of protein expression in individual animals, such a technique would probably not provide enough material.

## 4.1.2 Quantitative Western blotting

As mentioned above, the quantification of gene expression through real-time PCR is a first approach to determine changes in the expression of certain genes or groups of genes after different kinds of treatments or in pathology. However, in order to achieve a complete picture, it is also necessary to quantify protein levels given that these molecules are the final product responsible for executing vital and specific functions in the cell. Besides, as shown

in the current results, mRNA levels do not necessarily parallel protein levels (Schedel *et al.* 2004, Gu *et al.* 2006, Wang *et al.* 2009).

Western blotting is a technique by which proteins that have previously been separated by electrophoresis are transferred to a membrane. Once attached to the membrane, the detection of specific proteins can be accomplished through the use of specific antibodies, which provide information about their presence in a given tissue, different forms of that protein and their molecular weights (Towbin *et al.* 1979). Additionally, it is possible to quantify such expression. In the present study, relative quantification of protein expression by means of enhanced chemiluminescence was chosen. The principle is straightforward; luminescense intensity will depend on protein abundance. This procedure enabled us to quantify the expression of specific proteins after chronic stress relative to the expression of the reference protein by measuring the optical density of the protein bands. As previously reported, β-actin was used to normalize protein expression data (Abumaria *et al.* 2006).

Several factors are crucial for reliable and reproducible protein quantification. It is necessary to take into account the amount of total protein loaded, if known, physical and chemical properties of the protein to analyze and also to optimize primary and secondary antibody concentrations and incubation times. The respective experiments were performed to account for all of these considerations and the experiments were systematically conducted. The differences between mRNA and protein levels will be discussed in detail in section 4.1.3.

### 4.1.3 Discrepancies between mRNA and protein expression analyses

Analysis of Ndrg2 gene expression at the mRNA level (real-time PCR quantification) and protein level (quantitative Western blot) in the hippocampus revealed opposite results after chronic social stress. While mRNA expression was downregulated, protein expression was enhanced. On the other hand, GFAP showed no effect at the mRNA level, but a reduction in protein expression after chronic social stress. Similarly, Kir 4.1 only showed a significant reduction at the protein level after chronic restraint stress.

Discrepancies between mRNA and protein levels have been found in other studies as well. For example, chronic restraint stress induced a decrease in vesicle associated membrane protein 2 (VAMP2) protein levels, despite increased mRNA transcripts (Müller *et al.* 2011).

Also, expression of the *p63* mRNA has been reported to be increased in psoriasis, but no alteration has been detected at the protein level (Gu *et al.* 2006). Moreover, in a study that analyzed mRNA and protein expression correlation, changes at the mRNA level in liver in response to treatment reflected only 40% of the variation in protein expression (Tian *et al.* 2004).

While the expression of many genes is controlled at the transcriptional level, the cited studies in combination with our findings emphasize the importance of posttranscriptional regulatory mechanisms. A reduction in mRNA expression compared to protein levels could be related to increased rates of mRNA turnover. In mammalian cells, RNA-binding proteins (RBP) as well as microRNAs are in charge of post-transcriptional regulation of gene expression by means of stabilizing/destabilizing mRNAs and promoting/suppressing translation (for review see Pullmann *et al.* 2007, Lakner *et al.* 2011). On the other hand, changes in protein stability could also be related to the detection of protein alterations despite unaltered mRNA expression. Post-translational modifications such as phosphorylation and methylation of specific amino acids have been related to this process (Accardi *et al.* 2011, Li *et al.* 2002, Cha *et al.* 2011). A detailed description of the mechanisms of mRNA and protein modification and turnover was, however, beyond the scope of this study.

As protein products are the final result of gene expression, along with the compiling evidence supporting the protein quantification results (see sections 4.2.1, 4.2.2, and 4.4.3), we are inclined to believe that protein quantification provides a more realistic picture of the final changes induced by chronic stress in astrocytic gene expression.

### 4.1.4 Physiological changes induced by chronic social and chronic restraint stress

We worked with two different models of chronic stress, immobilization and social defeat, to induce changes at the behavioral and neuroendocrine level similar to the ones observed in depression (McEwen *et al.* 2002).

A reduction in body weight gain as well as the enlargement of the adrenal glands as a sign of hypothalamic-pituitary-adrenal (HPA) axis hyperactivity (Heuser 1998, Weber *et al.* 2000) have been reported as clear indicators of stress effects in rats (Abumaria *et al.* 2007, Czéh *et al.* 2006, Rygula *et al.* 2005). In the present study, both groups of rats (CRS and

CSS) showed significant reductions in body weight gain as well as an increase in adrenal gland weight, suggesting that they were indeed affected by the stress.

However, there was no significant difference in corticosterone levels between control and stress animals following both stress paradigms, only a slight increase. A possible explanation for these results could be an attenuation of the stress response after chronic stress. It has been observed that repeated exposure to the same stressor (e.g. forced swimming, noise, immobilization) causes a gradual reduction in the stress response that is dependent on the type of stressor (for review see Yehuda *et al.* 1991).

A continual HPA axis response to stress, even under chronic stress, might be important for survival, as high glucocorticoid levels guarantee appropriate physiological responses to acute stressors. However, maintenance of HPA axis hyperactivity represents a high metabolic cost and might be detrimental for the organism (reviewed in Dallman 1993). Therefore, attenuation of the stress response after chronic stress likely reflects physiological adaptation of the HPA axis (reviewed in Yehuda *et al.* 1991). The adaptation to chronic stress could be in the form of increased negative feedback sensitivity of the HPA axis at the level of the hippocampus, hypothalamus or pituitary (see Yehuda *et al.* 1991). But also, changes in corticosterone levels could be associated with alterations in glucocorticoid metabolism and the activity of the 11β-hydroxysteroid dehydrogenase (11β-HSD) enzyme, which catalyzes the reversible conversion of glucocorticoids to their inactive form. Accordingly, changes in 11β-HSD activity have been reported after chronic psychosocial stress in tree shrews (Jamieson *et al.* 1997). Similar examples of blunted HPA responses have been reported in individuals subjected to early life stress (Meaney *et al.* 1988, Yee *et al.* 2011). Also, in another study with birds (*Sturnus vulgaris)*, the authors compared whether HPA axis activation after acute stress was different between control and chronically stressed animals, and observed a decrease in basal corticosterone levels with the progression of the experiment as well as a reduced response to acute stressors in the animals subjected to chronic stress (Rich & Romero 2005).

Regarding testosterone concentrations, it has been reported that HPA axis activation in chronic stress leads to a decrease in testosterone levels and to impaired sexual behavior (de Souza *et al.* 2011, Sapolsky *et al.* 2000). The inhibition of hypothalamic-pituitary-gonadal (HPG) axis function both at the hypothalamic and pituitary gland level leads to the suppression of gonadotropin-releasing hormone (GnRH) and gonadotropin release and a subsequent drop in testosterone secretion (Calogero *et al.* 1999, Sapolsky *et al.* 2000). The

current experiments showed a trend to lower testosterone concentration after chronic social stress in the stressed animals, which provides supporting evidence of ongoing physiological stress responses. On the other hand, no significant effects on testosterone were observed after chronic restraint stress. Conflicting results are found in the literature, where some authors report no differences after three weeks of chronic restraint stress (Retana-Marquez *et al.* 2003), while others report significant differences after a longer restraint stress period (6 weeks/2 hours per day) (de Souza *et al.* 2011).

The current results are not unexpected as in the chronic social stress model, subordination to the dominant male might have a strong impact in gonadal function in comparison to chronic restraint stress, where such social signals are missing. Therefore, each model apparently has differential effects on specific physiological parameters. These results further highlight the importance of the careful selection of a model that best approaches the problem(s) under investigation.

### 4.1.5 Cell culture experiments

Cell culture is a widely used method in which cells from specific tissues are disaggregated, collected and seeded in a favorable artificial environment. Accordingly, several protocols (Saura 2007) that stem from the original methods (Booher & Sensenbrenner 1972, McCarthy & de Vellis 1980) have been developed to prepare astroglial-enriched cultures from CNS tissue. Astroglial-enriched cultures have become a valuable tool in molecular biology since the method represents a simplified manner of performing a wide range of studies aimed at gaining a better understanding of cell physiology and biochemistry both in normal conditions and under the influence of different factors (Saura 2007). The fact that cells grow in a medium rich in essential nutrients, growth factors and hormones, under controlled pH, temperature and gas exchange conditions should, in principle, allow obtainment of consistent and reproducible results. However, this might not necessarily be the case (Brunner *et al.* 2010, Duell *et al.* 2011), as discussed below (see section 4.6).

Therefore, in the final phase of the present study, astrocyte cultures were transduced with the Ndrg2 gene in order to gather information that could help shed light on Ndrg2's role in the brain, as well as the physiological meaning of its regulation after stress. The method of choice to introduce and over-express Ndrg2 was the utilization of vectors based on the adeno-associated virus type 6 (AAV-6). AAV is a parvovirus with a small single-stranded

DNA genome, which is not known to cause disease. Its name derives from the fact that it needs the helper functions of an adenovirus for efficient replication and transcription. Several vector serotypes have been identified. They show different properties conferred by their capsid composition, such as tissue specificity and efficiency of transduction (Halbert *et al.* 2007, Halbert *et al.* 1997, Markakis *et al.* 2009, Shevtsova *et al.* 2005). The ability of AAV-6 to transduce neural cells, specifically glia, has been previously proven (Howard *et al.* 2008). The selected DNA transfer system allowed efficient transduction of cells due to low immunogenicity and high specificity of expression owed to the astrocyte-specific promoter. Also it represented a low risk for the experimenter since it only required S1 laboratory safety conditions. In the current experiments AAV transduction of astrocyte cultures with Ndrg2S, Ndrg2L and EGFP resulted in increased protein expression of NDRG2 or EGFP in the astrocytes.

## 4.2 Chronic social stress modulation of gene expression in the hippocampus

### 4.2.1 Ndrg2 and stress

The proteins belonging to the NDRG family have been shown to be involved in responses to cellular stress. For instance, N-myc downregulated gene 1 (Ndrg1) was induced in response to DNA damaging agents in a p53-dependent fashion and remained unaltered in the T47D cell line, which contains a mutated p53, regardless of treatment with mitomycin C or actinomycin D (Kurdistani *et al.* 1998). The same authors also reported changes in the subcellular location of the protein, as more NDRG1 was found in the nucleus after DNA damage (Kurdistani *et al.* 1998). Another study indicated involvement of the Ndrg1 gene in the apoptotic processes after p53-induced caspase activation (Stein *et al.* 2004). Also, NDRG1 expression was upregulated by hypoxia agents in a HIF-1-dependent manner (Cangul 2004).

Similar to Ndrg1, Ndrg2 expression has also been associated with cell stress. Ndrg2 mRNA and protein expression were upregulated in A549 cells (human alveolar adenocarcinoma cell line) exposed to hypoxia or hypoxia mimetic compounds ($NiCl_2$, $CoCl_2$). Moreover, the gene appeared to be a target for the transcription factor HIF-1 and essential for hypoxia-induced apoptosis (Wang *et al.* 2008).

Furthermore, Ndrg2 can be phosphorylated by serum- and glucocorticoid-induced kinase 1 (Murray *et al.* 2004). Also, a recent study using primary rat astrocytes showed that Ndrg2 expression was indirectly induced by the synthetic glucocorticoid dexamethasone at the DNA level. The mechanism likely involved binding of the transcription factors NFκB and Pax5, but not the glucocorticoid response element (GRE) half-site, as there was a delay in the response which is not characteristic of primary glucocorticoid response and GRE activation (Takahashi *et al.* 2011).

Previous studies in our group detected upregulation of Ndrg2 transcripts in the dorsal raphe nucleus of male rats after chronic social stress (Abumaria *et al.* 2006). In the current study, chronic social stress resulted in NDRG2 protein expression upregulation in the hippocampal formation. In order to rule out an increase in the number of NDRG2-positive cells as the cause of the observed increased in protein, we counted NDRG2-immunoreactive cells in two areas of the hippocampus: the stratum radiatum and stratum oriens. We observed no significant chronic stress-induced changes in the number of NDRG2-immunoreactive cells. Therefore, we concluded that the increased expression detected by protein analysis reflected enhanced protein expression in the individual cells.

In agreement with the results mentioned above, Ndrg2 mRNA has been shown to be a target of glucocorticoids, which are elevated in the plasma of stressed animals (Nichols & Finch 1994, Takahashi *et al.* 2011). Ndrg2 expression was also upregulated at the mRNA level after corticosterone administration in the adult rat heart, cerebral cortex, as well as in cultured astrocytes (Nichols 2003). These findings, together with a high concentration of glucocorticoid receptors in the hippocampus, are consistent with enhanced NDRG2 expression in this brain region after stress. However, the exact mechanisms and molecular pathways mediating NDRG2 regulation by a diverse group of stress factors are unknown, as are the physiological implications of stress-induced changes in expression.

Several functional roles have been proposed for Ndrg2. According to Nichols, the increase in Ndrg2 expression after glucocorticoid administration in adrenolectomized rats, together with the predominant expression of NDRG2 protein in the neurogenic zone of the dentate gyrus, could indicate a role of the gene in inhibition of cell proliferation or differentiation (Liu *et al.* 2011a, Nichols 2003). It has been reported that astroglia play a role in the control of local environment and prompt the origin of new neurons, either by regulation of fate specification of adult neural stem cells (Song *et al.* 2002) or by division of cells with astrocyte characteristics in the subgranular zone (Seri *et al.* 2001). However, in spite of a

study showing chronic stress-induced reduction in neurogenesis in the dentate gyrus (proliferative activity and survival of newborn cells) (Czéh *et al.* 2007), there is no direct relation between these processes and Ndrg2 expression.

*In vitro* cell culture studies relate Ndrg2 expression to processes of cell proliferation and differentiation. For example, the analysis of human monocyte-derived dendritic cells (DCs) reported downregulation of Ndrg2 after dexamethasone-evoked inhibition of differentiation, while the differentiation of a myelomonocytic leukemia cell line into DCs induced Ndrg2 gene expression (Choi *et al.* 2003). On the other hand, tumorigenesis studies report a positive correlation between Ndrg2 and tumor differentiation, as NDRG2 showed conspicuous expression in well-differentiated colon carcinomas in contrast to poorly differentiated tumor tissues (Kim *et al.* 2009b).

Alternative ideas of Ndrg2's roles in brain function could be inferred from a study in epithelial cells reporting the interaction with a subunit of the Na+/K+-ATPase (Li *et al.* 2011). This ATPase has been linked to numerous biological processes, including ion transport and reabsorption, and in the particular case of astrocytes, it is activated after synaptic activity to restore the ion gradient necessary to drive glutamate transport (Haydon & Carmignoto 2006, Pellerin & Magistretti 1997). Astrocytic uptake of glutamate from the synaptic cleft is an essential regulatory mechanism in synaptic transmission (Araque *et al.* 1999, Piet *et al.* 2004). Accordingly, mRNA expression for the astroglial glutamate transporter 1 was shown to be increased after chronic restraint stress (Reagan *et al.* 2004).

Altogether, the interpretation and integration of the data into convergent mechanisms to elucidate Ndrg2 function seems hard to achieve. Part of the problem may be an ambiguous use of the terms 'proliferation' and 'differentiation'. This could be related to technical limitations of the assays performed to assess these processes, which might disallow establishing a clear-cut distinction between them and an appropriate association of Ndrg2 with either proliferation or differentiation. Finally, the gene could also play a different, so far unknown, role according to the tissue where it is expressed.

## 4.2.2 GFAP and stress

As an integral component of the cytoskeleton, the intermediate filament protein GFAP is involved in astrocytic differentiation, e.g., the formation of cell processes. Accordingly, expression of this protein has become a prototypical marker in immunohistochemical studies to identify and characterize astrocytes in healthy and pathological tissue (Sofroniew 2009). However, in the healthy CNS, many mature astrocytes do not express detectable levels of GFAP. Besides, the protein is only present in about 15% of the total volume of astrocytes (main stem branches), and fine perisynaptic astrocytic processes do not contain GFAP (Bushong *et al.* 2002, Lavialle *et al.* 2011). Several studies have shown modulation of GFAP expression by stress. Increased GFAP immunoreactivity was reported after acute systemic heat stress (38 ºC for 4 h) in different brain regions (Sharma *et al.* 1992) and following running wheel activity in the hippocampus (Lambert *et al.* 2000). Contrasting effects have been observed in chronic social stress studies, which reported a decline in GFAP immunoreactive cells. In male tree shrews subjected to chronic social defeat, stressed animals showed a reduction in the number of GFAP-immunoreactive astrocytes in the hippocampus (Czéh *et al.* 2006), while juvenile stress by separation from the family reduced the density of GFAP-immunoreactivity in the medial prefrontal cortex of degus (Braun *et al.* 2009). In agreement with these chronic stress experiments, the present findings also showed downregulated GFAP expression in the hippocampus of male rats, which might be related to the stress-induced elevation of glucocorticoids, since it was shown that corticosterone reduced GFAP levels in the rat brain (Nichols *et al.* 1990, O'Callaghan *et al.* 1991). These findings indicate differential effects on astrocyte GFAP expression according to the characteristics (i.e. duration) of the stressors. The induction of the intermediate filament GFAP after acute stress could reflect activation of astrocytes, as strong GFAP-immunoreactive intermediate filaments are a common hallmark of reactive astrocytes (Bushong *et al.* 2002). Consequently, the downregulation of GFAP expression observed after chronic stress could suggest the presence of non-reactive astroglia.

## 4.2.3 Stress-induced changes in glia

Astrocytes are dynamic regulators of synaptogenesis and synaptic strength and also control neurogenesis in the adult dentate gyrus (Araque *et al.* 1999; Goldman 2003). The stress-induced changes in NDRG2 and GFAP protein expression in glia reported in this study may

reflect a strong change in the metabolic activity of the astrocytes. It is likely that altered metabolism correlates with alterations in neuronal network function as well as with changes in the astrocytic capacity of supplying neurotrophic factors to the neuropil (Reuss & Unsicker 2005).

Some authors interpreted stress-induced reduction in GFAP immunoreactivity as glial atrophy (e.g. Liu *et al.* 2011b). However, this seems unlikely, as data from the hippocampal formation reveal no experimental evidence for atrophy processes, including apoptosis. Apoptosis in the hippocampus is a rather rare event and chronic social stress was shown to increase apoptosis only in the hilus, but reduced the number of apoptotic cells in other hippocampal subfields (Lucassen *et al.* 2001).

Although astroglial activation represents an important cellular defense mechanism in early phases of brain injury, chronic activation could cause further damaging effects on the neuronal network (Sofroniew 2009). Chronic stress-induced downregulation of GFAP expression might be part of an adaptive response induced by long term exposure to harmful stimuli in order to protect the system from overshooting. However, this could also compromise normal astrocyte function and may have negative effects on neuronal functioning and neurogenesis, e.g., in the subgranular zone of the hippocampal formation.

### 4.2.4 Citalopram administration

Chronic citalopram was administered orally via the drinking water, as described previously (Abumaria *et al.* 2007, Rygula *et al.* 2005). At the end of the treatment period, the concentrations of the antidepressant and its metabolites in plasma were in the range of those found in earlier studies. Besides that, the drug effectively reached the brain, as shown by the high concentrations found in the cerebral cortex. Antidepressant administration also had an effect on certain measured physiological parameters that are consistent with previous studies. For example, the SSRI decreased body weight gain, which is in accordance with previous observations (D'Souza *et al.* 2004, Landry *et al.* 2005), but did not change adrenal weight, as also described for other SSRIs (Abumaria *et al.* 2007, Czéh *et al.* 2006, D'Souza *et al.* 2004, Landry *et al.* 2005, Schulte-Herbruggen *et al.* 2009).

The current findings showed that citalopram administration did not prevent or reverse chronic stress effects on the glial genes NDRG2 and GFAP in the hippocampus. However, the stress-induced upregulation of the neuronal proteins SNAP-25 and syntaxin-1A was

prevented by citalopram, suggesting that antidepressant therapy had a cell type-dependent effect on gene expression.

Both synaptic proteins are involved in synaptic vesicle exocytosis. Synaptic plasticity in different brain regions has been consistently shown to be modulated both by stress and antidepressant treatment (Abumaria *et al.* 2007, Müller *et al.* 2011). However, only a few studies have shown an effect of stress and antidepressant treatment (non-SSRIs) on glial gene expression in the hippocampus. For example, chronic restraint stress-induced changes in GLT-1 expression were inhibited by tianeptine (Reagan *et al.* 2004, Wood *et al.* 2004). In addition, GFAP was downregulated by chronic unpredictable stress in the hippocampus and reversed by treatment with the tricyclic antidepressant clomipramine (Liu *et al.* 2009). Besides usage of a different drug, the difference between outcomes in the latter study and our present results might be related to the specific stress paradigms. One may expect that the consequences of chronic unpredictable stress are more easily reversible than consequences of daily social stress, since the latter is regarded as a severe, traumatic experience for males in several species (Koolhaas *et al.* 2011).

Regarding chronic social stress-induced changes in astroglia and antidepressant therapy, previous studies have shown that treatment with the SSRI fluoxetine offered only a partial protection against astroglia changes during 5 weeks of social defeat in tree shrews. While fluoxetine could counteract the reductions in the number of GFAP-immunoreactive cells, it could not reverse astrocyte volume alterations in the hippocampus (Czéh *et al.* 2006). These findings are in contrast with observations in the dorsal raphe nucleus of rats experiencing chronic social stress, in which citalopram normalized Ndrg2 mRNA expression (Abumaria *et al.* 2007).

Antidepressant drugs are used as the first-line treatment in depression, but patients' responses are known to be highly heterogeneous (Koenig & Thase 2009). One may speculate that citalopram is more effective in regulating astrocytic gene expression in the dorsal raphe nucleus, as it represents a large serotonergic nucleus which contains around 30% of all brain serotonergic neurons. However, it has also been proposed that SSRIs modulate astroglial gene expression via mechanisms that do not necessarily involve serotonin, as shown for the effects of fluoxetine on S100ß (Tramontina *et al.* 2008). Serotonergic projections from the midbrain modulate hippocampal activity (Vertes 1991). Changes in corticosteroid concentrations (e.g. in stress) caused alterations in the raphe nucleus that were reflected by alterations in hippocampal function as well (Meijer & de

Kloet 1998). However, it is probable that antidepressant efficacy in different brain regions depends on the neurochemical milieu of the regional neuropil, as determined by different cellular composition in the dorsal raphe nucleus and hippocampus. Also, regional differences in the properties of astrocytes might play a role, as these cells do not represent a homogeneous cell population, and evidence from studies in mice suggest that at least two subpopulations of astrocytes exist in the hippocampus (Himeda *et al.* 2006, Jinno 2011, Kettenmann & Verkhratsky 2008, Wallraff *et al.* 2004, Walz & Lang 1998). Furthermore, we cannot exclude the possibility that a longer treatment with citalopram (> 4 weeks) would have normalized the expression of the glial proteins studied here.

Finally, the current study showed that citalopram treatment upregulated NDRG2 and SNAP-25, downregulated GFAP and had no effect on syntaxin 1A in nonstressed rats. These observations are concordant with previous findings that antidepressants have different effects on gene expression in subjects experiencing a depressive-like state compared to healthy individuals (Takahashi *et al.* 2005b, Abumaria *et al.* 2007).

In summary, the current findings in conjunction with other studies indicate that the effects of chronic antidepressant treatment in animal models of stress depend on the regional environment in the CNS, the type of target cell and the experimental stress paradigm. Generally, the present findings agree with the hypothesis that a long-term antidepressive drug treatment stimulates the plasticity of brain cells (Sairanen *et al.* 2007); however, glial changes may show a different time course compared to neuronal changes.

## 4.3 Chronic social stress modulation of gene expression in the prefrontal cortex

Taking into consideration the effects of altered reference gene expression as well as differences in brain dissection in the prefrontal cortex, it is not possible to draw clear conclusions about stress-induced changes in astroglia gene expression in this brain region.

Regardless of reference gene expression stability in the right prefrontal cortex, GLT-1 expression was not modulated in the right prefrontal cortex in the R1-11 experiment, while the previous R12-09 experiment showed increased expression when normalized against three reference genes (GADPH, β-actin and cyclophilin). Inconsistencies could be related to

differences in the dissection that might alter the local effects of stress. New studies need to be performed to elucidate this issue.

## 4.4 Modulation of gene expression in the hippocampus by chronic restraint stress

### 4.4.1 Chronic restraint stress upregulated GLT-1 mRNA expression

Glutamate is the principal excitatory neurotransmitter in the CNS. It shows marked concentration within the cells and it has been reported that acute stress and glucocorticoids increase glutamate release in the hippocampus and prefrontal cortex (Moghaddam 1993, Lowy *et al.* 1993, Moghaddam *et al.* 1994, Musazzi *et al.* 2010). Less is known about chronic social stress-induced alterations in glutamate release (Popoli *et al.* 2012). However, chronic immobilization stress increased glutamate levels in the hippocampus of rodents (Satoh *et al.* 2011, Fontella *et al.* 2004). Also changes in glutamatergic neurotransmission might be related to alterations in structural plasticity and reduced long-term potentiation in CA3, as reported after restraint stress (Pavlides *et al.* 2002). High extracellular glutamate concentrations might interfere with neuronal activity as well as cause neurotoxic effects. Therefore, glutamatergic neurotransmission takes place in tripartite synapses, where astrocytes tightly control glutamate levels by GLT-1-mediated uptake (for a detailed review see Popoli *et al.* 2011).

Our results showed an increase in GLT-1 transcripts in the hippocampus after chronic restraint stress. GLT-1 was reported to be a target of glucocorticoids (Zschocke *et al.* 2005) and chronic restraint stress in the hippocampus (Reagan *et al.* 2004). Immobilization stress (3weeks, 6h/day) increased GLT-1 mRNA expression in the CA3 subfield, which is distinguished for marked dendritic remodeling (Reagan *et al.* 2004). Furthermore, the stress-induced changes in dendritic arborization as well as GLT-1 increased expression after restraint stress were prevented by lithium administration (Wood *et al.* 2004).

Therefore, our findings of enhanced GLT-1 mRNA expression in the hippocampus parallel previous results and suggest altered glutamatergic neurotransmission induced by chronic stress. Upregulation of the glutamate transporter GLT-1 in astrocytes as well as structural

changes in plasticity have been suggested to represent compensatory mechanisms to counteract glutamate excitotoxicity in the CNS after chronic stress (Wood *et al.* 2004).

### 4.4.2 Chronic restraint stress modulation of Kir 4.1 expression

Kir4.1 is a glia-specific inwardly rectifying $K^+$ channel involved in the spatial buffering of extracellular $K^+$ (Neusch *et al.* 2006). Since any increase in extracellular $K^+$ could compromise neuronal firing and normal network function, it is important to effectively regulate $K^+$ clearance. Furthermore, Kir4.1 is essential for effective glutamate homeostasis. Alterations in $K^+$ clearance by means of Kir4.1 could alter the electrochemical gradient and compromise glutamate uptake by astrocytes (reviewed in Olsen & Sontheimer 2008). Accordingly, the suppression of Kir4.1 channels by siRNA in cultured astrocytes reduced GLT-1-mediated glutamate uptake (Kucheryavykh *et al.* 2007).

We cannot clearly state the exact consequences of Kir4.1 downregulation in the hippocampus. Nonetheless, in the context of the current findings and data from the literature, one could speculate that reduced Kir4.1 expression could cause alterations in extracellular $K^+$ concentrations, which would also alter neuronal activity. Unfortunately, we did not measure extracellular $K^+$ concentration in the hippocampus after chronic restraint stress. However, in a recent collaborative study, chronic restraint stressed rats showed increased hypoxia-induced interstitial $K^+$ accumulation in the hippocampus. In spite of reduced Kir4.1 protein expression and an observed accumulation of $K^+$ ions in the extracellular space, it is not currently known if those alterations can be related to an impaired glia-mediated buffering, since astrocyte electrophysiological properties in stressed animals were not different from controls (Schnell *et al.* 2012).

## 4.5 Other glial genes were not modulated by chronic stress

Chronic social stress as well as chronic restraint stress caused certain alterations in astroglial gene expression that might be reflected by changes in neural network function. However, other glial genes remained unaltered. Furthermore, the pattern of alterations in gene expression differed according to the chronic stress model followed. After 5 weeks of chronic social stress, GLT-1, GLAST and AQP4 showed no stress-induced changes in

mRNA expression in the hippocampus. Yet three weeks of chronic restraint stress (6h/day) did not change gene expression at the mRNA transcript level of GLAST and GFAP as well as AQP4 and Ndrg2 at the mRNA and protein level.

Certainly, AQP4 alterations could have a strong impact on brain function. One may speculate that alterations in the expression of the main water channel in the CNS could have an effect on fluid balance in the brain, which might give insights into the mechanisms behind the reported volume reductions in the hippocampus observed after stress. To our knowledge, there are no reports of altered AQP4 expression in the hippocampus after chronic stress. Our results suggest stable expression of AQP4 in the hippocampus following chronic stress and seem to exclude the possibility of changes in water balance in the brain after chronic stress due to alterations in AQP4 expression.

Similarly, besides reports of GLT-1 modulation by chronic restraint stress (Reagan *et al.* 2004, Wood *et al.* 2004) and by glucocorticoids (Zschocke *et al.* 2005), the other glutamate transporter in astrocytes, GLAST, was shown to remain unaltered in astrocyte cultures treated with the synthetic glucocorticoid dexamethasone (Zschocke *et al.* 2005). There are no other reports showing alterations of GLAST expression after chronic stress in the brain.

In regard to GLT-1 expression in the hippocampus, there are studies showing increased GLT-1 expression after immobilization stress with possible implications for changes in structural synaptic plasticity (Magarinos *et al.* 1997). However, we did not observe any changes at the mRNA level of the glutamate transporter GLT-1 in the hippocampus of chronic social stressed rats. It is important to consider that we performed total RNA extraction of the whole hippocampi, which could prevent the detection of local alterations in GLT-1 mRNA expression (Reagan *et al.* 2004). Moreover, protein quantification was not assessed due to reduced amount of protein extraction material. We cannot exclude an effect at the protein level, especially considering that other glial genes (Ndrg2, GFAP and Kir4.1) seemed to be differentially regulated by posttranscriptional mechanisms, which resulted in discrepancies between mRNA and protein quantification.

Our data on GFAP mRNA and protein expression in the hippocampus revealed no alterations in GFAP expression after chronic restraint stress at both levels. In contrast, the number of GFAP immunoreactive cells were shown to be increased specifically in the CA1 subregion of the hippocampus after chronic immobilization stress (Schnell *et al.* 2012). As

previously discussed, local alterations in gene expression in the hippocampus might have been overlooked due to the use of whole hippocampi for analyses.

The current findings in the hippocampus after chronic restraint stress showed no significant changes at the mRNA and protein levels of NDRG2, though a trend for reduction of mRNA expression was observed. These data further support the important role played by the type of stressor in the modulatory effects of stress on specific physiological processes.

## 4.6 Cell culture experiments

In order to examine the possible implications of NDRG2 upregulation by chronic social stress, astrocyte-enriched cultures were transduced with three AAV vectors that expressed either the long or the short forms of the NDRG2 protein or EGFP. Ndrg2 and EGFP expression in this system were under the regulation of a small GFAP promoter that ensured astrocyte-specific expression. As shown by the immunohistochemistry analysis in the current study, AAV vectors were able to transduce astrocytes and direct the expression of Ndrg2L, Ndrg2S and EGFP in the cells. However, it is noteworthy to point out that there were also a number of cells that were obviously not transduced, as observed by the comparison to astrocytes that clearly expressed high amounts of NDRG2 (red immunofluorescence) or the lack of green florescence in some cells in the EGFP-transduced cultures. As a result, we did not detect a significant increase in NDRG2 protein by means of quantitative Western blot, even when the immunohistochemistry experiments showed increased NDRG2 expression in the astrocyte cultures. High variability in transduction efficiency among cultures seemed to contribute to the lack of significant statistical differences. The high variance suggests that changes in the particular environment of the cultures over the relative long periods of incubation might have contributed to the high variability in transduction observed between culture plates, regardless of parallel processing of the samples during preparation of the primary cultures, passaging and transduction. We consider that factors such as alterations in pH, glucocorticoid content in the media (fetal bovine serum) and changes in temperature could have played a role in the observed variability, and also had an effect on protein quantification experiments (Duell *et al.* 2011). A general practice in cell culture experiments is the supplementation of cell culture media with FBS. On one hand, the use of this serum has advantages as it provides the cells with essential nutrients necessary for attachment, growth and proliferation. On the other hand, the

complexity of serum composition, which includes different proteins, hormones (e.g. glucocorticoids), fatty acids, vitamins, growth factors and carbohydrates, might have an effect on the outcome of the experiment in terms of variability and reproducibility (Brunner *et al.* 2010).

With regard to the cell proliferation experiments, the present results showed reduced proliferation in the Ndrg2-transduced cultures in comparison to the PBS control cultures, but not compared to the EGFP-transduced cultures, which also showed significant differences compared to PBS. EGFP served as a control of transduction aimed at assessing the possible effects of transduction with AAV6 on the cells. The fact that EGFP cultures showed differences compared to PBS suggests that changes were induced by the transduction procedure or by EGFP expression itself. In one study utilizing primary cortical cell cultures, the authors investigated the toxicity associated with several viral vectors, AAV-6 among them, and found a toxic effect of all AAV serotypes (except for serotypes 2 and 9) that was dependent on the amount of viral genomes used in the transduction (Howard *et al.* 2008). However, the same authors also showed that the toxic effect was only partially induced by the AAVs *per se,* as a frameshift mutation in the EGFP gene reduced the overall toxicity except for serotypes 7 and 8. Other studies further support EGFP mediated toxicity in the cells. Consequently, transduction of neurons with EGFP had toxic effects on them (Klein *et al.* 2006, Detrait *et al.* 2002), and EGFP also induced cellular stress in mature oligodendrocytes (Millet *et al.* 2011).

Therefore, given that EGFP transduction had an effect compared to PBS control results, we cannot draw clear conclusions from the current findings. Even when they might be interpreted as a lack of effect of Ndrg2 transduction on cell proliferation, one cannot discard the opposite case. Previous experiments have shown reduced BrdU labelled cells in cultures that overexpress NDRG2 (Takeichi *et al.* 2011).

Concerning the morphological analysis of astrocytes transduced with Ndrg2S, Ndrg2L and EGFP, our results showed no significant alteration in the morphological parameters measured. In these experiments, only the astrocytes that appeared with an intense NDRG2 or EGFP immunoreactivity were taken into account. However, there was a trend for a reduction in the area (surface, included within the cell membrane, occupied by an astrocyte) of astrocytes transduced with Ndrg2L. Accordingly, these cells exhibited the smallest perimeters as well as a rounded shape.

We were also interested to test if increased NDRG2 expression in the astrocyte cultures could mimic effects induced in GFAP protein expression in the hippocampus by chronic social stress. Therefore, GFAP expression was measured in a group of cultures transduced with Ndrg2S, Ndrg2L or EGFP and compared against the PBS control cultures. Similar to NDRG2 quantification of protein expression, GFAP quantification also revealed high variability among cultures, and there were no significant changes in expression compared to PBS cultures. However, the Ndrg2L cultures showed the lowest GFAP expression. It remains to be clarified whether this finding is related to the morphological findings of smaller cells in those cultures (Ndrg2L).

Altogether, these findings suggest high sensitivity of the cells to the culture conditions. Also, the manipulations performed in astroglia cultures will probably not parallel the stress-induced changes in astroglia in rats. It is clear that the relationship between Ndrg2 and chronic stress in the whole organism is much more complex than the artificial one that can be achieved by over-expressing NDRG2 in astrocyte-enriched cultures. Furthermore, physiological changes induced by chronic stress cannot be reduced to a single gene effect.

## 4.7 Final conclusions

In conclusion, the current dissertation presented the results of analysis of astroglial-specific gene expression in rats subjected to chronic restraint stress and chronic social stress. The main results in the hippocampus suggest that chronic stress caused alterations in astroglial-gene expression according to the specific stress model. Chronic restraint stress seemed to modulate astrocyte-specific genes related to neurotransmission (GLT-1 and Kir 4.1), while chronic social stress altered Ndrg2 and GFAP expression, suggesting major metabolic alterations. Furthermore, after chronic social stress, citalopram administration did not restore normal glial function. Factors such as the regional environment in the brain and the target cells might play a role in antidepressant therapy efficiency.

The cell culture experiments did not shed light on the physiological role of Ndrg2 in astrocytes. Transduction with Ndrg2 but also EGFP (transduction control) had an effect on cell proliferation and morphology. Therefore, it was not possible to conclude whether the changes observed were due to Ndrg2 expression or to an effect of viral transduction. Also, these findings suggest high sensitivity of the cells to the culture conditions.

These changes in astroglial gene expression after chronic stress exposure suggest that alterations in glia are involved in and may contribute to the pathophysiology of depression.

# References

Abumaria, N., Rygula, R., Havemann-Reinecke, U., Ruther, E., Bodemer, W., Roos, C. and Flügge, G. (2006) Identification of genes regulated by chronic social stress in the rat dorsal raphe nucleus. *Cell Mol Neurobiol,* **26,** 145-162.

Abumaria, N., Rygula, R., Hiemke, C., Fuchs, E., Havemann-Reinecke, U., Rüther, E. and Flügge, G. (2007) Effect of chronic citalopram on serotonin-related and stress-regulated genes in the dorsal raphe nucleus of the rat. *Eur Neuropsychopharmacol,* **17,** 417-429.

Accardi, R., Scalise, M., Gheit, T. *et al.* (2011) IkappaB kinase beta promotes cell survival by antagonizing p53 functions through DeltaNp73alpha phosphorylation and stabilization. *Mol Cell Biol,* **31,** 2210-2226.

Akopian, G., Kuprijanova, E., Kressin, K. and Steinhuser, C. (1997) Analysis of ion channel expression by astrocytes in red nucleus brain stem slices of the rat. *Glia,* **19,** 234-246.

Alfonso, J., Pollevick, G. D., Van Der Hart, M. G., Flügge, G., Fuchs, E. and Frasch, A. C. (2004) Identification of genes regulated by chronic psychosocial stress and antidepressant treatment in the hippocampus. *Eur J Neurosci,* **19,** 659-666.

Allaman, I., Belanger, M. and Magistretti, P. J. (2011) Astrocyte-neuron metabolic relationships: for better and for worse. *Trends Neurosci,* **34,** 76-87.

Andersen, C. L., Jensen, J. L. and Orntoft, T. F. (2004) Normalization of real-time quantitative reverse transcription-PCR data: a model-based variance estimation approach to identify genes suited for normalization, applied to bladder and colon cancer data sets. *Cancer Res,* **64,** 5245-5250.

Andrew, R. D., Labron, M. W., Boehnke, S. E., Carnduff, L. and Kirov, S. A. (2007) Physiological evidence that pyramidal neurons lack functional water channels. *Cereb Cortex,* **17,** 787-802.

Araque, A., Parpura, V., Sanzgiri, R. P. and Haydon, P. G. (1999) Tripartite synapses: glia, the unacknowledged partner. *Trends Neurosci,* **22,** 208-215.

Arcangeli, A., Becchetti, A., Mannini, A. *et al.* (1993) Integrin-mediated neurite outgrowth in neuroblastoma cells depends on the activation of potassium channels. *J Cell Biol,* **122,** 1131-1143.

Badaut, J., Lasbennes, F., Magistretti, P. J. and Regli, L. (2002) Aquaporins in brain: distribution, physiology, and pathophysiology. *J Cereb Blood Flow Metab,* **22,** 367-378.

Banasr, M., Chowdhury, G. M., Terwilliger, R., Newton, S. S., Duman, R. S., Behar, K. L. and Sanacora, G. (2010) Glial pathology in an animal model of depression: reversal

of stress-induced cellular, metabolic and behavioral deficits by the glutamate-modulating drug riluzole. *Mol Psychiatry,* **15,** 501-511.

Banasr, M., Valentine, G. W., Li, X. Y., Gourley, S. L., Taylor, J. R. and Duman, R. S. (2007) Chronic unpredictable stress decreases cell proliferation in the cerebral cortex of the adult rat. *Biol Psychiatry,* **62,** 496-504.

Bass, N. H., Hess, H. H., Pope, A. and Thalheimer, C. (1971) Quantitative cytoarchitectonic distribution of neurons, glia, and DNa in rat cerebral cortex. *J Comp Neurol,* **143,** 481-490.

Benekareddy, M., Goodfellow, N. M., Lambe, E. K. and Vaidya, V. A. (2010) Enhanced function of prefrontal serotonin 5-HT(2) receptors in a rat model of psychiatric vulnerability. *J Neurosci,* **30,** 12138-12150.

Blanchard, R. J., McKittrick, C. R. and Blanchard, D. C. (2001) Animal models of social stress: effects on behavior and brain neurochemical systems. *Physiol Behav,* **73,** 261-271.

Bonefeld, B. E., Elfving, B. and Wegener, G. (2008) Reference genes for normalization: a study of rat brain tissue. *Synapse,* **62,** 302-309.

Booher, J. and Sensenbrenner, M. (1972) Growth and cultivation of dissociated neurons and glial cells from embryonic chick, rat and human brain in flask cultures. *Neurobiology,* **2,** 97-105.

Botteron, K. N., Raichle, M. E., Drevets, W. C., Heath, A. C. and Todd, R. D. (2002) Volumetric reduction in left subgenual prefrontal cortex in early onset depression. *Biol Psychiatry,* **51,** 342-344.

Boulkroun, S., Fay, M., Zennaro, M. C., Escoubet, B., Jaisser, F., Blot-Chabaud, M., Farman, N. and Courtois-Coutry, N. (2002) Characterization of rat NDRG2 (N-Myc downstream regulated gene 2), a novel early mineralocorticoid-specific induced gene. *J Biol Chem,* **277,** 31506-31515.

Braun, K., Antemano, R., Helmeke, C., Buchner, M. and Poeggel, G. (2009) Juvenile separation stress induces rapid region- and layer-specific changes in S100ss- and glial fibrillary acidic protein-immunoreactivity in astrocytes of the rodent medial prefrontal cortex. *Neuroscience,* **160,** 629-638.

Brunner, D., Frank, J., Appl, H., Schoffl, H., Pfaller, W. and Gstraunthaler, G. (2010) Serum-free cell culture: the serum-free media interactive online database. *ALTEX,* **27,** 53-62.

Bushong, E. A., Martone, M. E., Jones, Y. Z. and Ellisman, M. H. (2002) Protoplasmic astrocytes in CA1 stratum radiatum occupy separate anatomical domains. *J Neurosci,* **22,** 183-192.

Calogero, A. E., Burrello, N., Bosboom, A. M., Garofalo, M. R., Weber, R. F. and D'Agata, R. (1999) Glucocorticoids inhibit gonadotropin-releasing hormone by acting directly at the hypothalamic level. *J Endocrinol Invest,* **22,** 666-670.

Cangul, H. (2004) Hypoxia upregulates the expression of the NDRG1 gene leading to its overexpression in various human cancers. *BMC Genet,* **5,** 27.

Cannon, W. B. (1932) *The Wisdom of the Body*. pp. xv. 312. Kegan Paul & Co.: London; printed in U.S.A.

Castren, E. and Rantamaki, T. (2010) The role of BDNF and its receptors in depression and antidepressant drug action: Reactivation of developmental plasticity. *Dev Neurobiol,* **70,** 289-297.

Cerqueira, J. J., Almeida, O. F. and Sousa, N. (2008) The stressed prefrontal cortex. Left? Right! *Brain Behav Immun,* **22,** 630-638.

Cha, B., Kim, W., Kim, Y. K. *et al.* (2011) Methylation by protein arginine methyltransferase 1 increases stability of Axin, a negative regulator of Wnt signaling. *Oncogene,* **30,** 2379-2389.

Chen, K. C. and Nicholson, C. (2000) Spatial buffering of potassium ions in brain extracellular space. *Biophys J,* **78,** 2776-2797.

Choi, S. C., Kim, K. D., Kim, J. T., Kim, J. W., Yoon, D. Y., Choe, Y. K., Chang, Y. S., Paik, S. G. and Lim, J. S. (2003) Expression and regulation of NDRG2 (N-myc downstream regulated gene 2) during the differentiation of dendritic cells. *FEBS Lett,* **553,** 413-418.

Chomczynski, P. (1993) A reagent for the single-step simultaneous isolation of RNA, DNA and proteins from cell and tissue samples. *Biotechniques,* **15,** 532-534, 536-537.

Chomczynski, P. and Sacchi, N. (1987) Single-step method of RNA isolation by acid guanidinium thiocyanate-phenol-chloroform extraction. *Anal Biochem,* **162,** 156-159.

Czéh, B. and Lucassen, P. J. (2007) What causes the hippocampal volume decrease in depression? Are neurogenesis, glial changes and apoptosis implicated? *Eur Arch Psychiatry Clin Neurosci,* **257,** 250-260.

Czéh, B., Michaelis, T., Watanabe, T., Frahm, J., de Biurrun, G., van Kampen, M., Bartolomucci, A. and Fuchs, E. (2001) Stress-induced changes in cerebral metabolites, hippocampal volume, and cell proliferation are prevented by antidepressant treatment with tianeptine. *Proc Natl Acad Sci U S A,* **98,** 12796-12801.

Czéh, B., Muller-Keuker, J. I., Rygula, R., Abumaria, N., Hiemke, C., Domenici, E. and Fuchs, E. (2007) Chronic social stress inhibits cell proliferation in the adult medial prefrontal cortex: hemispheric asymmetry and reversal by fluoxetine treatment. *Neuropsychopharmacology,* **32,** 1490-1503.

Czéh, B., Pérez-Cruz, C., Fuchs, E. and Flügge, G. (2008) Chronic stress-induced cellular changes in the medial prefrontal cortex and their potential clinical implications: does hemisphere location matter? *Behav Brain Res,* **190,** 1-13.

Czéh, B., Simon, M., Schmelting, B., Hiemke, C. and Fuchs, E. (2006) Astroglial plasticity in the hippocampus is affected by chronic psychosocial stress and concomitant fluoxetine treatment. *Neuropsychopharmacology,* **31,** 1616-1626.

D'Ambrosio, R., Maris, D. O., Grady, M. S., Winn, H. R. and Janigro, D. (1999) Impaired K(+) homeostasis and altered electrophysiological properties of post-traumatic hippocampal glia. *J Neurosci,* **19,** 8152-8162.

D'Aquila, P. S., Peana, A. T., Carboni, V. and Serra, G. (2000) Exploratory behaviour and grooming after repeated restraint and chronic mild stress: effect of desipramine. *Eur J Pharmacol,* **399,** 43-47.

D'Souza, D. N., Zhang, Y., Garcia, F., Battaglia, G. and Van de Kar, L. D. (2004) Fluoxetine-induced changes in body weight and 5-HT1A receptor-mediated

hormone secretion in rats on a tryptophan-deficient diet. *Am J Physiol Regul Integr Comp Physiol,* **286,** R390-397.

Dallman, M. F. (1993) Stress update Adaptation of the hypothalamic-pituitary-adrenal axis to chronic stress. *Trends Endocrinol Metab,* **4,** 62-69.

Dallman, M. F., Jones, M. T., Vernikos-Danellis, J. and Ganong, W. F. (1972) Corticosteroid feedback control of ACTH secretion: rapid effects of bilateral adrenalectomy on plasma ACTH in the rat. *Endocrinology,* **91,** 961-968.

De Kloet, E. R., Vreugdenhil, E., Oitzl, M. S. and Joels, M. (1998) Brain corticosteroid receptor balance in health and disease. *Endocr Rev,* **19,** 269-301.

de Souza, D. B., Silva, D., Cortez, C. M., Costa, W. S. and Sampaio, F. J. (2011) Effects of Chronic Stress on Penile Corpus Cavernosum of Rats. *J Androl*.

Deng, Y., Yao, L., Chau, L. *et al.* (2003) N-Myc downstream-regulated gene 2 (NDRG2) inhibits glioblastoma cell proliferation. *Int J Cancer,* **106,** 342-347.

Derks, N. M., Muller, M., Gaszner, B., Tilburg-Ouwens, D. T., Roubos, E. W. and Kozicz, L. T. (2008) Housekeeping genes revisited: different expressions depending on gender, brain area and stressor. *Neuroscience,* **156,** 305-309.

Detrait, E. R., Bowers, W. J., Halterman, M. W., Giuliano, R. E., Bennice, L., Federoff, H. J. and Richfield, E. K. (2002) Reporter gene transfer induces apoptosis in primary cortical neurons. *Mol Ther,* **5,** 723-730.

Ding, J. H., Sha, L. L., Chang, J., Zhou, X. Q., Fan, Y. and Hu, G. (2007) Alterations of striatal neurotransmitter release in aquaporin-4 deficient mice: An in vivo microdialysis study. *Neurosci Lett,* **422,** 175-180.

Diorio, D., Viau, V. and Meaney, M. J. (1993) The role of the medial prefrontal cortex (cingulate gyrus) in the regulation of hypothalamic-pituitary-adrenal responses to stress. *J Neurosci,* **13,** 3839-3847.

Djukic, B., Casper, K. B., Philpot, B. D., Chin, L. S. and McCarthy, K. D. (2007) Conditional knock-out of Kir4.1 leads to glial membrane depolarization, inhibition of potassium and glutamate uptake, and enhanced short-term synaptic potentiation. *J Neurosci,* **27,** 11354-11365.

Drevets, W. C., Price, J. L., Bardgett, M. E., Reich, T., Todd, R. D. and Raichle, M. E. (2002) Glucose metabolism in the amygdala in depression: relationship to diagnostic subtype and plasma cortisol levels. *Pharmacol Biochem Behav,* **71,** 431-447.

Drevets, W. C., Price, J. L. and Furey, M. L. (2008) Brain structural and functional abnormalities in mood disorders: implications for neurocircuitry models of depression. *Brain Struct Funct,* **213,** 93-118.

Drevets, W. C., Price, J. L., Simpson, J. R., Jr., Todd, R. D., Reich, T., Vannier, M. and Raichle, M. E. (1997) Subgenual prefrontal cortex abnormalities in mood disorders. *Nature,* **386,** 824-827.

Drevets, W. C., Videen, T. O., Price, J. L., Preskorn, S. H., Carmichael, S. T. and Raichle, M. E. (1992) A functional anatomical study of unipolar depression. *J Neurosci,* **12,** 3628-3641.

DSM-IV (1994) *Diagnostic and statistical manual of mental disorders : DSM-IV*. American Psychiatric Association, Washington, D.C.

Duell, B. L., Cripps, A. W., Schembri, M. A. and Ulett, G. C. (2011) Epithelial cell coculture models for studying infectious diseases: benefits and limitations. *J Biomed Biotechnol,* **2011,** 852419.

Duman, R. S. (2002) Pathophysiology of depression: the concept of synaptic plasticity. *Eur Psychiatry,* **17 Suppl 3,** 306-310.

Eng, L. F. and Ghirnikar, R. S. (1994) GFAP and astrogliosis. *Brain Pathol,* **4,** 229-237.

Fellin, T. and Carmignoto, G. (2004) Neurone-to-astrocyte signalling in the brain represents a distinct multifunctional unit. *J Physiol,* **559,** 3-15.

Foletta, V. C., Prior, M. J., Stupka, N. *et al.* (2009) NDRG2, a novel regulator of myoblast proliferation, is regulated by anabolic and catabolic factors. *J Physiol,* **587,** 1619-1634.

Fontella, F. U., Vendite, D. A., Tabajara, A. S. *et al.* (2004) Repeated restraint stress alters hippocampal glutamate uptake and release in the rat. *Neurochem Res,* **29,** 1703-1709.

Fuchs, E. and Flügge, G. (2002) Social stress in tree shrews: effects on physiology, brain function, and behavior of subordinate individuals. *Pharmacol Biochem Behav,* **73,** 247-258.

Fuchs, E. and Flügge, G. (2003) Chronic social stress: effects on limbic brain structures. *Physiol Behav,* **79,** 417-427.

Fuchs, E., Flügge, G. and Czéh, B. (2006) Remodeling of neuronal networks by stress. *Front Biosci,* **11,** 2746-2758.

Furman, C. S., Gorelick-Feldman, D. A., Davidson, K. G., Yasumura, T., Neely, J. D., Agre, P. and Rash, J. E. (2003) Aquaporin-4 square array assembly: opposing actions of M1 and M23 isoforms. *Proc Natl Acad Sci U S A,* **100,** 13609-13614.

Giulietti, A., Overbergh, L., Valckx, D., Decallonne, B., Bouillon, R. and Mathieu, C. (2001) An overview of real-time quantitative PCR: applications to quantify cytokine gene expression. *Methods,* **25,** 386-401.

Gu, X., Lundqvist, E. N., Coates, P. J., Thurfjell, N., Wettersand, E. and Nylander, K. (2006) Dysregulation of TAp63 mRNA and protein levels in psoriasis. *J Invest Dermatol,* **126,** 137-141.

Halbert, C. L., Lam, S. L. and Miller, A. D. (2007) High-efficiency promoter-dependent transduction by adeno-associated virus type 6 vectors in mouse lung. *Hum Gene Ther,* **18,** 344-354.

Halbert, C. L., Standaert, T. A., Aitken, M. L., Alexander, I. E., Russell, D. W. and Miller, A. D. (1997) Transduction by adeno-associated virus vectors in the rabbit airway: efficiency, persistence, and readministration. *J Virol,* **71,** 5932-5941.

Haydon, P. G. and Carmignoto, G. (2006) Astrocyte control of synaptic transmission and neurovascular coupling. *Physiol Rev,* **86,** 1009-1031.

Heidbreder, C. A. and Groenewegen, H. J. (2003) The medial prefrontal cortex in the rat: evidence for a dorso-ventral distinction based upon functional and anatomical characteristics. *Neurosci Biobehav Rev,* **27,** 555-579.

Heni, M., Hennige, A. M., Peter, A. *et al.* (2011) Insulin promotes glycogen storage and cell proliferation in primary human astrocytes. *PLoS One,* **6,** e21594.

Heuser, I. (1998) Anna-Monika-Prize paper. The hypothalamic-pituitary-adrenal system in depression. *Pharmacopsychiatry,* **31,** 10-13.

Himeda, T., Watanabe, Y., Tounai, H., Hayakawa, N., Kato, H. and Araki, T. (2006) Time dependent alterations of co-localization of S100beta and GFAP in the MPTP-treated mice. *J Neural Transm,* **113,** 1887-1894.

Howard, D. B., Powers, K., Wang, Y. and Harvey, B. K. (2008) Tropism and toxicity of adeno-associated viral vector serotypes 1, 2, 5, 6, 7, 8, and 9 in rat neurons and glia *in vitro*. *Virology,* **372,** 24-34.

Hu, X. L., Yao, L. B., Zhang, Y. Q., Deng, Y. C. and Liu, X. P. (2006) [Distribution characteristic of NDRG2 expression in human fetal tissues.]. *Sheng Li Xue Bao,* **58,** 331-336.

Huggett, J., Dheda, K., Bustin, S. and Zumla, A. (2005) Real-time RT-PCR normalisation; strategies and considerations. *Genes Immun,* **6,** 279-284.

Jamieson, P. M., Fuchs, E., Flügge, G. and Seckl, J. R. (1997) Attenuation of Hippocampal 11beta-Hydroxysteroid Dehydrogenase Type 1 by Chronic Psychosocial Stress in the Tree Shrew. *Stress,* **2,** 123-132.

Jing, R., Wilhelmsson, U., Goodwill, W., Li, L., Pan, Y., Pekny, M. and Skalli, O. (2007) Synemin is expressed in reactive astrocytes in neurotrauma and interacts differentially with vimentin and GFAP intermediate filament networks. *J Cell Sci,* **120,** 1267-1277.

Jinno, S. (2011) Regional and laminar differences in antigen profiles and spatial distributions of astrocytes in the mouse hippocampus, with reference to aging. *Neuroscience,* **180,** 41-52.

Joels, M. and Baram, T. Z. (2009) The neuro-symphony of stress. *Nat Rev Neurosci,* **10,** 459-466.

Jung, J. S., Bhat, R. V., Preston, G. M., Guggino, W. B., Baraban, J. M. and Agre, P. (1994) Molecular characterization of an aquaporin cDNA from brain: candidate osmoreceptor and regulator of water balance. *Proc Natl Acad Sci U S A,* **91,** 13052-13056.

Kempermann, G. and Kronenberg, G. (2003) Depressed new neurons--adult hippocampal neurogenesis and a cellular plasticity hypothesis of major depression. *Biol Psychiatry,* **54,** 499-503.

Kendler, K. S., Karkowski, L. M. and Prescott, C. A. (1999) Causal relationship between stressful life events and the onset of major depression. *Am J Psychiatry,* **156,** 837-841.

Kettenmann, H. and Ransom, B. R. (2005) *Neuroglia*. Oxford University Press, Oxford.

Kettenmann, H. and Verkhratsky, A. (2008) Neuroglia: the 150 years after. *Trends Neurosci,* **31,** 653-659.

Kim, Y. J., Yoon, S. Y., Kim, J. T. *et al.* (2009a) NDRG2 suppresses cell proliferation through down-regulation of AP-1 activity in human colon carcinoma cells. *Int J Cancer,* **124,** 7-15.

Kim, Y. J., Yoon, S. Y., Kim, J. T. *et al.* (2009b) NDRG2 expression decreases with tumor stages and regulates TCF/beta-catenin signaling in human colon carcinoma. *Carcinogenesis,* **30,** 598-605.

Klein, R. L., Dayton, R. D., Leidenheimer, N. J., Jansen, K., Golde, T. E. and Zweig, R. M. (2006) Efficient neuronal gene transfer with AAV8 leads to neurotoxic levels of tau or green fluorescent proteins. *Mol Ther,* **13,** 517-527.

Koenig, A. M. and Thase, M. E. (2009) First-line pharmacotherapies for depression - what is the best choice? *Pol Arch Med Wewn,* **119,** 478-486.

Kofuji, P., Biedermann, B., Siddharthan, V. *et al.* (2002) Kir potassium channel subunit expression in retinal glial cells: implications for spatial potassium buffering. *Glia,* **39,** 292-303.

Kofuji, P., Ceelen, P., Zahs, K. R., Surbeck, L. W., Lester, H. A. and Newman, E. A. (2000) Genetic inactivation of an inwardly rectifying potassium channel (Kir4.1 subunit) in mice: phenotypic impact in retina. *J Neurosci,* **20,** 5733-5740.

Kong, H., Fan, Y., Xie, J., Ding, J., Sha, L., Shi, X., Sun, X. and Hu, G. (2008) AQP4 knockout impairs proliferation, migration and neuronal differentiation of adult neural stem cells. *J Cell Sci,* **121,** 4029-4036.

Koolhaas, J. M., Bartolomucci, A., Buwalda, B. *et al.* (2011) Stress revisited: a critical evaluation of the stress concept. *Neurosci Biobehav Rev,* **35,** 1291-1301.

Kreth, S., Heyn, J., Grau, S., Kretzschmar, H. A., Egensperger, R. and Kreth, F. W. (2010) Identification of valid endogenous control genes for determining gene expression in human glioma. *Neuro Oncol,* **12,** 570-579.

Krettek, J. E. and Price, J. L. (1977) The cortical projections of the mediodorsal nucleus and adjacent thalamic nuclei in the rat. *J Comp Neurol,* **171,** 157-191.

Kubista, M., Andrade, J. M., Bengtsson, M. *et al.* (2006) The real-time polymerase chain reaction. *Mol Aspects Med,* **27,** 95-125.

Kucheryavykh, Y. V., Kucheryavykh, L. Y., Nichols, C. G., Maldonado, H. M., Baksi, K., Reichenbach, A., Skatchkov, S. N. and Eaton, M. J. (2007) Downregulation of Kir4.1 inward rectifying potassium channel subunits by RNAi impairs potassium transfer and glutamate uptake by cultured cortical astrocytes. *Glia,* **55,** 274-281.

Kuffler, S. W., Nicholls, J. G. and Orkand, R. K. (1966) Physiological properties of glial cells in the central nervous system of amphibia. *J Neurophysiol,* **29,** 768-787.

Kurdistani, S. K., Arizti, P., Reimer, C. L., Sugrue, M. M., Aaronson, S. A. and Lee, S. W. (1998) Inhibition of tumor cell growth by RTP/rit42 and its responsiveness to p53 and DNA damage. *Cancer Res,* **58,** 4439-4444.

Lakner, A. M., Bonkovsky, H. L. and Schrum, L. W. (2011) microRNAs: fad or future of liver disease. *World J Gastroenterol,* **17,** 2536-2542.

Lambert, K. G., Gerecke, K. M., Quadros, P. S., Doudera, E., Jasnow, A. M. and Kinsley, C. H. (2000) Activity-stress increases density of GFAP-immunoreactive astrocytes in the rat hippocampus. *Stress,* **3,** 275-284.

Landry, M., Frasier, M., Chen, Z., Van De Kar, L. D., Zhang, Y., Garcia, F. and Battaglia, G. (2005) Fluoxetine treatment of prepubescent rats produces a selective functional reduction in the 5-HT2A receptor-mediated stimulation of oxytocin. *Synapse,* **58,** 102-109.

Larkin, M. A., Blackshields, G., Brown, N. P. *et al.* (2007) Clustal W and Clustal X version 2.0. *Bioinformatics,* **23,** 2947-2948.

Lavialle, M., Aumann, G., Anlauf, E., Prols, F., Arpin, M. and Derouiche, A. (2011) Structural plasticity of perisynaptic astrocyte processes involves ezrin and metabotropic glutamate receptors. *Proc Natl Acad Sci U S A,* **108,** 12915-12919.

Lee, K. S., Alvarenga, T. A., Guindalini, C., Andersen, M. L., Castro, R. M. and Tufik, S. (2009) Validation of commonly used reference genes for sleep-related gene expression studies. *BMC Mol Biol,* **10,** 45.

Lee, S., Jeong, J., Kwak, Y. and Park, S. K. (2010) Depression research: where are we now? *Mol Brain,* **3,** 8.

Lehre, K. P., Levy, L. M., Ottersen, O. P., Storm-Mathisen, J. and Danbolt, N. C. (1995) Differential expression of two glial glutamate transporters in the rat brain: quantitative and immunocytochemical observations. *J Neurosci,* **15,** 1835-1853.

Lepekhin, E. A., Eliasson, C., Berthold, C. H., Berezin, V., Bock, E. and Pekny, M. (2001) Intermediate filaments regulate astrocyte motility. *J Neurochem,* **79,** 617-625.

Li, Y., Dowbenko, D. and Lasky, L. A. (2002) AKT/PKB phosphorylation of p21Cip/WAF1 enhances protein stability of p21Cip/WAF1 and promotes cell survival. *J Biol Chem,* **277,** 11352-11361.

Li, Y., Yang, J., Li, S. *et al.* (2011) N-myc Downstream-regulated Gene 2, a Novel Estrogen-targeted Gene, Is Involved in the Regulation of Na+/K+-ATPase. *J Biol Chem,* **286,** 32289-32299.

Liu, L., Shi, M., Wang, L., Hou, S., Wu, Z., Zhao, G. and Deng, Y. (2011a) Ndrg2 expression in neurogenic germinal zones of embryonic and postnatal mouse brain. *J Mol Histol,* **43,** 27-35.

Liu, N., Wang, L., Li, X. *et al.* (2008) N-Myc downstream-regulated gene 2 is involved in p53-mediated apoptosis. *Nucleic Acids Res,* **36,** 5335-5349.

Liu, Q., Li, B., Zhu, H. Y., Wang, Y. Q., Yu, J. and Wu, G. C. (2009) Clomipramine treatment reversed the glial pathology in a chronic unpredictable stress-induced rat model of depression. *Eur Neuropsychopharmacol,* **19,** 796-805.

Liu, Q., Li, B., Zhu, H. Y., Wang, Y. Q., Yu, J. and Wu, G. C. (2011b) Glia atrophy in the hippocampus of chronic unpredictable stress-induced depression model rats is reversed by electroacupuncture treatment. *J Affect Disord,* **128,** 309-313.

Lowy, M. T., Gault, L. and Yamamoto, B. K. (1993) Adrenalectomy attenuates stress-induced elevations in extracellular glutamate concentrations in the hippocampus. *J Neurochem,* **61,** 1957-1960.

Lucas, D. R. and Newhouse, J. P. (1957) The toxic effect of sodium L-glutamate on the inner layers of the retina. *AMA Arch Ophthalmol,* **58,** 193-201.

Lucassen, P. J., Muller, M. B., Holsboer, F., Bauer, J., Holtrop, A., Wouda, J., Hoogendijk, W. J., De Kloet, E. R. and Swaab, D. F. (2001) Hippocampal apoptosis in major depression is a minor event and absent from subareas at risk for glucocorticoid overexposure. *Am J Pathol,* **158,** 453-468.

Luine,V., Villegas, M., Martínez C. and McEwen, B. S. (1994) Repeated stress causes reversible impairments of spatial memory performance. *Brain Res,* **639,** 167-170.

Magarinos, A. M., McEwen, B. S., Flügge, G. and Fuchs, E. (1996) Chronic psychosocial stress causes apical dendritic atrophy of hippocampal CA3 pyramidal neurons in subordinate tree shrews. *J Neurosci,* **16,** 3534-3540.

Magarinos, A. M., Verdugo, J. M. and McEwen, B. S. (1997) Chronic stress alters synaptic terminal structure in hippocampus. *Proc Natl Acad Sci U S A,* **94,** 14002-14008.

Markakis, E. A., Vives, K. P., Bober, J. *et al.* (2009) Comparative transduction efficiency of AAV vector serotypes 1-6 in the substantia nigra and striatum of the primate brain. *Mol Ther,* **18,** 588-593.

Mason, J. W. (1968) A review of psychoendocrine research on the pituitary-adrenal cortical system. *Psychosom Med,* **30,** Suppl:576-607.

McCarthy, K. D. and de Vellis, J. (1980) Preparation of separate astroglial and oligodendroglial cell cultures from rat cerebral tissue. *J Cell Biol,* **85,** 890-902.

McEwen, B. S., Chattarji, S., Diamond, D. M., Jay, T. M., Reagan, L. P., Svenningsson, P. and Fuchs, E. (2009) The neurobiological properties of tianeptine (Stablon): from monoamine hypothesis to glutamatergic modulation. *Mol Psychiatry,* **15,** 237-249.

McEwen, B. S., Magarinos, A. M. and Reagan, L. P. (2002) Studies of hormone action in the hippocampal formation: possible relevance to depression and diabetes. *J Psychosom Res,* **53,** 883-890.

McLaughlin, K. J., Gomez, J. L., Baran, S. E. and Conrad, C. D. (2007) The effects of chronic stress on hippocampal morphology and function: an evaluation of chronic restraint paradigms. *Brain Res,* **1161,** 56-64.

Meaney, M. J., Aitken, D. H., van Berkel, C., Bhatnagar, S. and Sapolsky, R. M. (1988) Effect of neonatal handling on age-related impairments associated with the hippocampus. *Science,* **239,** 766-768.

Meijer, O. C. and de Kloet, E. R. (1998) Corticosterone and serotonergic neurotransmission in the hippocampus: functional implications of central corticosteroid receptor diversity. *Crit Rev Neurobiol,* **12,** 1-20.

Meyer, U., van Kampen, M., Isovich, E., Flügge, G. and Fuchs, E. (2001) Chronic psychosocial stress regulates the expression of both GR and MR mRNA in the hippocampal formation of tree shrews. *Hippocampus,* **11,** 329-336.

Miguel-Hidalgo, J. J., Waltzer, R., Whittom, A. A., Austin, M. C., Rajkowska, G. and Stockmeier, C. A. (2010) Glial and glutamatergic markers in depression, alcoholism, and their comorbidity. *J Affect Disord,* **127,** 230-240.

Millet, V., Marder, M. and Pasquini, L. A. (2011) Adult CNP::EGFP transgenic mouse shows pronounced hypomyelination and an increased vulnerability to cuprizone-induced demyelination. *Exp Neurol,* **233,** 490-504.

Mitchelmore, C., Buchmann-Moller, S., Rask, L., West, M. J., Troncoso, J. C. and Jensen, N. A. (2004) NDRG2: a novel Alzheimer's disease associated protein. *Neurobiol Dis,* **16,** 48-58.

Moghaddam, B. (1993) Stress preferentially increases extraneuronal levels of excitatory amino acids in the prefrontal cortex: comparison to hippocampus and basal ganglia. *J Neurochem,* **60,** 1650-1657.

Moghaddam, B., Bolinao, M. L., Stein-Behrens, B. and Sapolsky, R. (1994) Glucocorticoids mediate the stress-induced extracellular accumulation of glutamate. *Brain Res,* **655,** 251-254.

Muller, H. K., Wegener, G., Popoli, M. and Elfving, B. (2011) Differential expression of synaptic proteins after chronic restraint stress in rat prefrontal cortex and hippocampus. *Brain Res,* **1385,** 26-37.

Muller, M. B., Lucassen, P. J., Yassouridis, A., Hoogendijk, W. J., Holsboer, F. and Swaab, D. F. (2001) Neither major depression nor glucocorticoid treatment affects the cellular integrity of the human hippocampus. *Eur J Neurosci,* **14,** 1603-1612.

Murray, J. T., Campbell, D. G., Morrice, N. *et al.* (2004) Exploitation of KESTREL to identify NDRG family members as physiological substrates for SGK1 and GSK3. *Biochem J,* **384,** 477-488.

Musazzi, L., Milanese, M., Farisello, P. *et al.* (2010) Acute stress increases depolarization-evoked glutamate release in the rat prefrontal/frontal cortex: the dampening action of antidepressants. *PLoS One,* **5,** e8566.

Naert, G., Ixart, G., Maurice, T., Tapia-Arancibia, L. and Givalois, L. (2010) Brain-derived neurotrophic factor and hypothalamic-pituitary-adrenal axis adaptation processes in a depressive-like state induced by chronic restraint stress. *Mol Cell Neurosci,* **46,** 55-66.

Nedergaard, M., Ransom, B. and Goldman, S. A. (2003) New roles for astrocytes: redefining the functional architecture of the brain. *Trends Neurosci,* **26,** 523-530.

Nelissen, K., Smeets, K., Mulder, M., Hendriks, J. J. and Ameloot, M. (2009) Selection of reference genes for gene expression studies in rat oligodendrocytes using quantitative real time PCR. *J Neurosci Methods,* **187,** 78-83.

Neusch, C., Papadopoulos, N., Muller, M. *et al.* (2006) Lack of the Kir4.1 channel subunit abolishes K+ buffering properties of astrocytes in the ventral respiratory group: impact on extracellular K+ regulation. *J Neurophysiol,* **95,** 1843-1852.

Newman, E. A. (1993) Inward-rectifying potassium channels in retinal glial (Muller) cells. *J Neurosci,* **13,** 3333-3345.

Nicholls, D. G. and Budd, S. L. (1998) Neuronal excitotoxicity: the role of mitochondria. *Biofactors,* **8,** 287-299.

Nichols, N. R. (2003) Ndrg2, a novel gene regulated by adrenal steroids and antidepressants, is highly expressed in astrocytes. *Ann N Y Acad Sci,* **1007,** 349-356.

Nichols, N. R., Agolley, D., Zieba, M. and Bye, N. (2005) Glucocorticoid regulation of glial responses during hippocampal neurodegeneration and regeneration. *Brain Res Brain Res Rev,* **48,** 287-301.

Nichols, N. R. and Finch, C. E. (1994) Gene products of corticosteroid action in hippocampus. *Ann N Y Acad Sci,* **746,** 145-154; discussion 154-146.

Nichols, N. R., Osterburg, H. H., Masters, J. N., Millar, S. L. and Finch, C. E. (1990) Messenger RNA for glial fibrillary acidic protein is decreased in rat brain following acute and chronic corticosterone treatment. *Brain Res Mol Brain Res,* **7,** 1-7.

O'Callaghan, J. P., Brinton, R. E. and McEwen, B. S. (1991) Glucocorticoids regulate the synthesis of glial fibrillary acidic protein in intact and adrenalectomized rats but do not affect its expression following brain injury. *J Neurochem,* **57,** 860-869.

Okuda, T., Kokame, K. and Miyata, T. (2008) Differential expression patterns of NDRG family proteins in the central nervous system. *J Histochem Cytochem,* **56,** 175-182.

Okuda, T. and Kondoh, H. (1999) Identification of new genes ndr2 and ndr3 which are related to Ndr1/RTP/Drg1 but show distinct tissue specificity and response to N-myc. *Biochem Biophys Res Commun,* **266,** 208-215.

Olsen, M. L. and Sontheimer, H. (2008) Functional implications for Kir4.1 channels in glial biology: from K+ buffering to cell differentiation. *J Neurochem,* **107,** 589-601.

Ongur, D., Drevets, W. C. and Price, J. L. (1998) Glial reduction in the subgenual prefrontal cortex in mood disorders. *Proc Natl Acad Sci U S A,* **95,** 13290-13295.

Ongur, D. and Price, J. L. (2000) The organization of networks within the orbital and medial prefrontal cortex of rats, monkeys and humans. *Cereb Cortex,* **10,** 206-219.

Ostby, I., Oyehaug, L., Einevoll, G. T., Nagelhus, E. A., Plahte, E., Zeuthen, T., Lloyd, C. M., Ottersen, O. P. and Omholt, S. W. (2009) Astrocytic mechanisms explaining neural-activity-induced shrinkage of extraneuronal space. *PLoS Comput Biol,* **5,** e1000272.

Pavlides, C., Nivon, L. G. and McEwen, B. S. (2002) Effects of chronic stress on hippocampal long-term potentiation. *Hippocampus,* **12,** 245-257.

Paxinos, G. and Watson, C. (1986) *The rat brain in stereotaxic coordinates*. Academic Press, San Diego, Calif.

Pellerin, L. and Magistretti, P. J. (1997) Glutamate uptake stimulates Na+,K+-ATPase activity in astrocytes via activation of a distinct subunit highly sensitive to ouabain. *J Neurochem,* **69,** 2132-2137.

Pellerin, L. and Magistretti, P. J. (2005) The central role of astrocytes in neuroenergetics. In: *Neuroglia,* (H. Kettenmann and B. R. Ransom eds.), pp. 367-376. Oxford University Press, Oxford.

Perea, G. and Araque, A. (2005) Properties of synaptically evoked astrocyte calcium signal reveal synaptic information processing by astrocytes. *J Neurosci,* **25,** 2192-2203.

Perea, G., Navarrete, M. and Araque, A. (2009) Tripartite synapses: astrocytes process and control synaptic information. *Trends Neurosci,* **32,** 421-431.

Pérez-Cruz, C., Muller-Keuker, J. I., Heilbronner, U., Fuchs, E. and Flügge, G. (2007) Morphology of pyramidal neurons in the rat prefrontal cortex: lateralized dendritic remodeling by chronic stress. *Neural Plast,* **2007,** 46276.

Pérez-Cruz, C., Simon, M., Czéh, B., Flügge, G. and Fuchs, E. (2009) Hemispheric differences in basilar dendrites and spines of pyramidal neurons in the rat prelimbic cortex: activity- and stress-induced changes. *Eur J Neurosci,* **29,** 738-747.

Piet, R., Vargova, L., Sykova, E., Poulain, D. A. and Oliet, S. H. (2004) Physiological contribution of the astrocytic environment of neurons to intersynaptic crosstalk. *Proc Natl Acad Sci U S A,* **101,** 2151-2155.

Pines, G., Danbolt, N. C., Bjoras, M. *et al.* (1992) Cloning and expression of a rat brain L-glutamate transporter. *Nature,* **360,** 464-467.

Pirttimaki, T. M., Hall, S. D. and Parri, H. R. (2011) Sustained neuronal activity generated by glial plasticity. *J Neurosci,* **31,** 7637-7647.

Ponchel, F., Toomes, C., Bransfield, K. *et al.* (2003) Real-time PCR based on SYBR-Green I fluorescence: an alternative to the TaqMan assay for a relative quantification of gene rearrangements, gene amplifications and micro gene deletions. *BMC Biotechnol,* **3,** 18.

Popoli, M., Yan, Z., McEwen, B. S. and Sanacora, G. (2011) The stressed synapse: the impact of stress and glucocorticoids on glutamate transmission. *Nat Rev Neurosci,* **13,** 22-37.

Popoli, M., Yan, Z., McEwen, B. S. and Sanacora, G. (2012) The stressed synapse: the impact of stress and glucocorticoids on glutamate transmission. *Nat Rev Neurosci,* **13,** 22-37.

Porsolt, R. D., Bertin, A. and Jalfre, M. (1977) Behavioral despair in mice: a primary screening test for antidepressants. *Arch Int Pharmacodyn Ther,* **229,** 327-336.

Pullmann, R., Jr., Kim, H. H., Abdelmohsen, K., Lal, A., Martindale, J. L., Yang, X. and Gorospe, M. (2007) Analysis of turnover and translation regulatory RNA-binding protein expression through binding to cognate mRNAs. *Mol Cell Biol,* **27,** 6265-6278.

Qin, L. and Crews, F. T. (2012) NADPH oxidase and reactive oxygen species contribute to alcohol-induced microglial activation and neurodegeneration. *J Neuroinflammation,* **9,** 5.

Rajkowska, G. (2000) Postmortem studies in mood disorders indicate altered numbers of neurons and glial cells. *Biol Psychiatry,* **48,** 766-777.

Rajkowska, G. and Miguel-Hidalgo, J. J. (2007) Gliogenesis and glial pathology in depression. *CNS Neurol Disord Drug Targets,* **6,** 219-233.

Reagan, L. P., Rosell, D. R., Wood, G. E., Spedding, M., Munoz, C., Rothstein, J. and McEwen, B. S. (2004) Chronic restraint stress up-regulates GLT-1 mRNA and protein expression in the rat hippocampus: reversal by tianeptine. *Proc Natl Acad Sci U S A,* **101,** 2179-2184.

Reichenbach, A. and Wolburg, H. (2005) Astrocytes and ependymal glia. In: *Neuroglia,* (H. Kettenmann and B. R. Ransom eds.), pp. 19-35. Oxford University Press, Oxford.

Retana-Marquez, S., Bonilla-Jaime, H., Vazquez-Palacios, G., Martinez-Garcia, R. and Velazquez-Moctezuma, J. (2003) Changes in masculine sexual behavior, corticosterone and testosterone in response to acute and chronic stress in male rats. *Horm Behav,* **44,** 327-337.

Reul, J. M. and de Kloet, E. R. (1985) Two receptor systems for corticosterone in rat brain: microdistribution and differential occupation. *Endocrinology,* **117,** 2505-2511.

Reuss, B. and Unsicker, K. (2005) Growth factors for neurons provided by macroglial cells. In: *Neuroglia*, (H. Kettenmann and B. R. Ransom eds.), pp. xix, 601 p. Oxford University Press, Oxford.

Rich, E. L. and Romero, L. M. (2005) Exposure to chronic stress downregulates corticosterone responses to acute stressors. *Am J Physiol Regul Integr Comp Physiol,* **288,** R1628-1636.

Ririe, K. M., Rasmussen, R. P. and Wittwer, C. T. (1997) Product differentiation by analysis of DNA melting curves during the polymerase chain reaction. *Anal Biochem,* **245,** 154-160.

Rozen, S. and Skaletsky, H. (2000) Primer3 on the WWW for general users and for biologist programmers. *Methods Mol Biol,* **132,** 365-386.

Ruhe, H. G., Mason, N. S. and Schene, A. H. (2007) Mood is indirectly related to serotonin, norepinephrine and dopamine levels in humans: a meta-analysis of monoamine depletion studies. *Mol Psychiatry,* **12,** 331-359.

Rygula, R., Abumaria, N., Flügge, G., Fuchs, E., Ruther, E. and Havemann-Reinecke, U. (2005) Anhedonia and motivational deficits in rats: impact of chronic social stress. *Behav Brain Res,* **162,** 127-134.

Rygula, R., Abumaria, N., Flügge, G., Hiemke, C., Fuchs, E., Ruther, E. and Havemann-Reinecke, U. (2006) Citalopram counteracts depressive-like symptoms evoked by chronic social stress in rats. *Behav Pharmacol,* **17,** 19-29.

Saadoun, S., Papadopoulos, M. C., Watanabe, H., Yan, D., Manley, G. T. and Verkman, A. S. (2005) Involvement of aquaporin-4 in astroglial cell migration and glial scar formation. *J Cell Sci,* **118,** 5691-5698.

Sairanen, M., O'Leary, O. F., Knuuttila, J. E. and Castren, E. (2007) Chronic antidepressant treatment selectively increases expression of plasticity-related proteins in the hippocampus and medial prefrontal cortex of the rat. *Neuroscience,* **144,** 368-374.

Saleem, K. S., Kondo, H. and Price, J. L. (2008) Complementary circuits connecting the orbital and medial prefrontal networks with the temporal, insular, and opercular cortex in the macaque monkey. *J Comp Neurol,* **506,** 659-693.

Sapolsky, R. M., Romero, L. M. and Munck, A. U. (2000) How do glucocorticoids influence stress responses? Integrating permissive, suppressive, stimulatory, and preparative actions. *Endocr Rev,* **21,** 55-89.

Satoh, E., Tada, Y. and Matsuhisa, F. (2011) Chronic stress enhances calcium mobilization and glutamate exocytosis in cerebrocortical synaptosomes from mice. *Neurol Res,* **33,** 899-907.

Saura, J. (2007) Microglial cells in astroglial cultures: a cautionary note. *J Neuroinflammation,* **4,** 26.

Schedel, J., Distler, O., Woenckhaus, M., Gay, R. E., Simmen, B., Michel, B. A., Muller-Ladner, U. and Gay, S. (2004) Discrepancy between mRNA and protein expression of tumour suppressor maspin in synovial tissue may contribute to synovial hyperplasia in rheumatoid arthritis. *Ann Rheum Dis,* **63,** 1205-1211.

Schildkraut, J. J. (1965) The catecholamine hypothesis of affective disorders: a review of supporting evidence. *Am J Psychiatry,* **122,** 509-522.

Schmittgen, T. D. and Livak, K. J. (2008) Analyzing real-time PCR data by the comparative C(T) method. *Nat Protoc,* **3,** 1101-1108.

Schnell, C., Janc, O., Kempkes, B., Araya-Callís, C., Flügge, G., Hülsmann, S. and Müller, M. (2012). Restraint stress intensifies interstitial $K^+$ accumulation during severe hypoxia. *Front Neuropharmacol,* **3**: 53.

Schroder, W., Seifert, G., Huttmann, K., Hinterkeuser, S. and Steinhauser, C. (2002) AMPA receptor-mediated modulation of inward rectifier K+ channels in astrocytes of mouse hippocampus. *Mol Cell Neurosci,* **19,** 447-458.

Schroeder, A., Mueller, O., Stocker, S. *et al.* (2006) The RIN: an RNA integrity number for assigning integrity values to RNA measurements. *BMC Mol Biol,* **7,** 3.

Schulte-Herbrüggen, O., Fuchs, E., Abumaria, N., Ziegler, A., Danker-Hopfe, H., Hiemke, C. and Hellweg, R. (2009) Effects of escitalopram on the regulation of brain-derived

neurotrophic factor and nerve growth factor protein levels in a rat model of chronic stress. *J Neurosci Res,* **87,** 2551-2560.

Seifert, G., Huttmann, K., Binder, D. K., Hartmann, C., Wyczynski, A., Neusch, C. and Steinhauser, C. (2009) Analysis of astroglial K+ channel expression in the developing hippocampus reveals a predominant role of the Kir4.1 subunit. *J Neurosci,* **29,** 7474-7488.

Selye, H. (1973) The evolution of the stress concept. *Am Sci,* **61,** 692-699.

Selye, H. (1998) A syndrome produced by diverse nocuous agents. 1936. *J Neuropsychiatry Clin Neurosci,* **10,** 230-231.

Seri, B., Garcia-Verdugo, J. M., McEwen, B. S. and Alvarez-Buylla, A. (2001) Astrocytes give rise to new neurons in the adult mammalian hippocampus. *J Neurosci,* **21,** 7153-7160.

Seth, P. and Koul, N. (2008) Astrocyte, the star avatar: redefined. *J Biosci,* **33,** 405-421.

Sharma, H. S., Zimmer, C., Westman, J. and Cervos-Navarro, J. (1992) Acute systemic heat stress increases glial fibrillary acidic protein immunoreactivity in brain: experimental observations in conscious normotensive young rats. *Neuroscience,* **48,** 889-901.

Shevtsova, Z., Malik, J. M., Michel, U., Bahr, M. and Kügler, S. (2005) Promoters and serotypes: targeting of adeno-associated virus vectors for gene transfer in the rat central nervous system *in vitro* and in vivo. *Exp Physiol,* **90,** 53-59.

Silver, J. and Miller, J. H. (2004) Regeneration beyond the glial scar. *Nat Rev Neurosci,* **5,** 146-156.

Sofroniew, M. V. (2009) Molecular dissection of reactive astrogliosis and glial scar formation. *Trends Neurosci,* **32,** 638-647.

Song, H., Stevens, C. F. and Gage, F. H. (2002) Astroglia induce neurogenesis from adult neural stem cells. *Nature,* **417,** 39-44.

Stein, S., Thomas, E. K., Herzog, B., Westfall, M. D., Rocheleau, J. V., Jackson, R. S., 2nd, Wang, M. and Liang, P. (2004) NDRG1 is necessary for p53-dependent apoptosis. *J Biol Chem,* **279,** 48930-48940.

Steinhauser, C., Berger, T., Frotscher, M. and Kettenmann, H. (1992) Heterogeneity in the Membrane Current Pattern of Identified Glial Cells in the Hippocampal Slice. *Eur J Neurosci,* **4,** 472-484.

Stockmeier, C. A., Mahajan, G. J., Konick, L. C., Overholser, J. C., Jurjus, G. J., Meltzer, H. Y., Uylings, H. B., Friedman, L. and Rajkowska, G. (2004) Cellular changes in the postmortem hippocampus in major depression. *Biol Psychiatry,* **56,** 640-650.

Storck, T., Schulte, S., Hofmann, K. and Stoffel, W. (1992) Structure, expression, and functional analysis of a Na(+)-dependent glutamate/aspartate transporter from rat brain. *Proc Natl Acad Sci U S A,* **89,** 10955-10959.

Sullivan, R. M. and Gratton, A. (1999) Lateralized effects of medial prefrontal cortex lesions on neuroendocrine and autonomic stress responses in rats. *J Neurosci,* **19,** 2834-2840.

Sulston, J. E., Schierenberg, E., White, J. G. and Thomson, J. N. (1983) The embryonic cell lineage of the nematode Caenorhabditis elegans. *Dev Biol,* **100,** 64-119.

Tait, M. J., Saadoun, S., Bell, B. A. and Papadopoulos, M. C. (2008) Water movements in the brain: role of aquaporins. *Trends Neurosci,* **31,** 37-43.

Takahashi, K., Saitoh, A., Yamada, M., Iwai, T. and Inagaki, M. (2011) Dexamethasone indirectly induces Ndrg2 expression in rat astrocytes. *J Neurosci Res.*

Takahashi, K., Yamada, M., Ohata, H. and Honda, K. (2005a) Ndrg2 promotes neurite outgrowth of NGF-differentiated PC12 cells. *Neurosci Lett,* **388,** 157-162.

Takahashi, K., Yamada, M., Ohata, H., Momose, K., Higuchi, T. and Honda, K. (2005b) Expression of Ndrg2 in the rat frontal cortex after antidepressant and electroconvulsive treatment. *Int J Neuropsychopharmacol,* **8,** 381-389.

Takamatsu, N. (1998) [The new colorimetric assay (WST-1) for cellular growth with normal aging and Alzheimer's disease]. *Nihon Ronen Igakkai Zasshi,* **35,** 535-542.

Takeichi, T., Takarada-Iemata, M., Hashida, K. *et al.* (2011) The effect of Ndrg2 expression on astroglial activation. *Neurochem Int,* **59,** 21-27.

Thellin, O., Zorzi, W., Lakaye, B., De Borman, B., Coumans, B., Hennen, G., Grisar, T., Igout, A. and Heinen, E. (1999) Housekeeping genes as internal standards: use and limits. *J Biotechnol,* **75,** 291-295.

Theodosis, D. T., Poulain, D. A. and Oliet, S. H. (2008) Activity-dependent structural and functional plasticity of astrocyte-neuron interactions. *Physiol Rev,* **88,** 983-1008.

Tian, Q., Stepaniants, S. B., Mao, M. *et al.* (2004) Integrated genomic and proteomic analyses of gene expression in Mammalian cells. *Mol Cell Proteomics,* **3,** 960-969.

Towbin, H., Staehelin, T. and Gordon, J. (1979) Electrophoretic transfer of proteins from polyacrylamide gels to nitrocellulose sheets: procedure and some applications. *Proc Natl Acad Sci U S A,* **76,** 4350-4354.

Tramontina, A. C., Tramontina, F., Bobermin, L. D., Zanotto, C., Souza, D. F., Leite, M. C., Nardin, P., Gottfried, C. and Goncalves, C. A. (2008) Secretion of S100B, an astrocyte-derived neurotrophic protein, is stimulated by fluoxetine via a mechanism independent of serotonin. *Prog Neuropsychopharmacol Biol Psychiatry,* **32,** 1580-1583.

Tunbridge, E. M., Eastwood, S. L. and Harrison, P. J. (2010) Changed relative to what? Housekeeping genes and normalization strategies in human brain gene expression studies. *Biol Psychiatry,* **69,** 173-179.

Ulrich-Lai, Y. M. and Herman, J. P. (2009) Neural regulation of endocrine and autonomic stress responses. *Nat Rev Neurosci,* **10,** 397-409.

Uylings, H. B., Groenewegen, H. J. and Kolb, B. (2003) Do rats have a prefrontal cortex? *Behav Brain Res,* **146,** 3-17.

Valentine, G. W. and Sanacora, G. (2009) Targeting glial physiology and glutamate cycling in the treatment of depression. *Biochem Pharmacol,* **78,** 431-439.

Van den Berg, C. J., Krzalic, L., Mela, P. and Waelsch, H. (1969) Compartmentation of glutamate metabolism in brain. Evidence for the existence of two different tricarboxylic acid cycles in brain. *Biochem J,* **113,** 281-290.

Vandesompele, J., De Preter, K., Pattyn, F., Poppe, B., Van Roy, N., De Paepe, A. and Speleman, F. (2002) Accurate normalization of real-time quantitative RT-PCR data by geometric averaging of multiple internal control genes. *Genome Biol,* **3,** RESEARCH0034.

Verkman, A. S. (2005) More than just water channels: unexpected cellular roles of aquaporins. *J Cell Sci,* **118,** 3225-3232.

Vertes, R. P. (1991) A PHA-L analysis of ascending projections of the dorsal raphe nucleus in the rat. *J Comp Neurol,* **313,** 643-668.

Wallraff, A., Odermatt, B., Willecke, K. and Steinhauser, C. (2004) Distinct types of astroglial cells in the hippocampus differ in gap junction coupling. *Glia,* **48,** 36-43.

Walz, W. and Lang, M. K. (1998) Immunocytochemical evidence for a distinct GFAP-negative subpopulation of astrocytes in the adult rat hippocampus. *Neurosci Lett,* **257,** 127-130.

Wang, G., Lai, F. M., Lai, K. B., Chow, K. M., Kwan, C. H., Li, K. T. and Szeto, C. C. (2009) Discrepancy between intrarenal messenger RNA and protein expression of ACE and ACE2 in human diabetic nephropathy. *Am J Nephrol,* **29,** 524-531.

Wang, L., Liu, N., Yao, L. *et al.* (2008) NDRG2 is a new HIF-1 target gene necessary for hypoxia-induced apoptosis in A549 cells. *Cell Physiol Biochem,* **21,** 239-250.

Waniewski, R. A. and Martin, D. L. (1986) Exogenous glutamate is metabolized to glutamine and exported by rat primary astrocyte cultures. *J Neurochem,* **47,** 304-313.

Weber, B., Lewicka, S., Deuschle, M., Colla, M., Vecsei, P. and Heuser, I. (2000) Increased diurnal plasma concentrations of cortisone in depressed patients. *J Clin Endocrinol Metab,* **85,** 1133-1136.

Wielputz, M. O., Lee, I. H., Dinudom, A., Boulkroun, S., Farman, N., Cook, D. I., Korbmacher, C. and Rauh, R. (2007) (NDRG2) stimulates amiloride-sensitive Na+ currents in Xenopus laevis oocytes and fisher rat thyroid cells. *J Biol Chem,* **282,** 28264-28273.

Willner, P. (1995) Animal models of depression: validity and applications. *Adv Biochem Psychopharmacol,* **49,** 19-41.

Willner, P., D'Aquila, P. S., Coventry, T. and Brain, P. (1995) Loss of social status: preliminary evaluation of a novel animal model of depression. *J Psychopharmacol,* **9,** 207-213.

Willner, P. and Mitchell, P. J. (2002) The validity of animal models of predisposition to depression. *Behav Pharmacol,* **13,** 169-188.

Willner, P., Muscat, R. and Papp, M. (1992) Chronic mild stress-induced anhedonia: a realistic animal model of depression. *Neurosci Biobehav Rev,* **16,** 525-534.

Wood, G. E., Young, L. T., Reagan, L. P., Chen, B. and McEwen, B. S. (2004) Stress-induced structural remodeling in hippocampus: prevention by lithium treatment. *Proc Natl Acad Sci U S A,* **101,** 3973-3978.

Yee, N., Plassmann, K. and Fuchs, E. (2011) Juvenile stress impairs body temperature regulation and augments anticipatory stress-induced hyperthermia responses in rats. *Physiol Behav,* **104,** 408-416.

Yehuda, R., Giller, E. L., Southwick, S. M., Lowy, M. T. and Mason, J. W. (1991) Hypothalamic-pituitary-adrenal dysfunction in posttraumatic stress disorder. *Biol Psychiatry,* **30,** 1031-1048.

Zhang, J., Li, F., Liu, X. *et al.* (2006) The repression of human differentiation-related gene NDRG2 expression by Myc via Miz-1-dependent interaction with the NDRG2 core promoter. *J Biol Chem,* **281,** 39159-39168.

Zschocke, J., Bayatti, N., Clement, A. M., Witan, H., Figiel, M., Engele, J. and Behl, C. (2005) Differential promotion of glutamate transporter expression and function by glucocorticoids in astrocytes from various brain regions. *J Biol Chem,* **280,** 34924-34932.

.

# List of figures

# List of tables

# Acknowledgments

I would like to thank my supervisor, Prof. Dr. Gabriele Flügge, for her constant support and guidance during these years. I am especially grateful for the fact that you could always make time for me regardless your tight schedule. Also I would like to thank the members of my thesis committee: Prof. Dr. Swen Hülsmann and Prof. Dr. med. Christine Stadelmann-Nessler, for their help and suggestions. Special thanks to Prof. Dr. Eberhard Fuchs, for giving me the opportunity to be part of his group.

I would also like to thank our collaborators: Prof. Dr. Christoph Hiemke, Department of Psychiatry, University of Mainz, for quantification of citalopram levels in blood samples and

Dr. Mitsuhiko Yamada, Dept. of Neuropsychopharmacology, National Institute of Mental Health, National Center of Neurology and Psychiatry, Japan, for kindly providing us with the plasmids expressing two isoforms of Ndrg2. Special thanks go to the Dept. of Neurology, University of Göttingen, to Dr. Sebastian Kügler, for the production on the AAV vectors expressing NDRG2, Dr. Yuliya Tereshchenko for her time and methodological support and for Ulrike Schöll for showing me the basis of cell culture work. My gratitude goes also for Prof. Dr. Rüdiger Behr, (Dept. of Stem Cell Biology, German Primate Center, Göttingen) for letting me perform the cell culture experiments in his lab. Many thanks go for Dr. Katharina Debowski for her help and support, and to all the members of the group, for their collaboration and good disposition towards me.

I am also grateful to the DFG Research Center for Molecular Physiology of the Brain (CMPB) for financial support of my studies.

I want to specially thank all the members of the Clinical Neurobiology Department in the German Primate Center, since from the beginning I was welcomed in a nice atmosphere. Many thanks to Simone B. and Simone L. for their technical support and advice in the

laboratory. Also to Anna H. for introducing me to some basic molecular biology techniques. Ich möchte Simone Barsky besonders danken, denn sie seit den Anfängen freundlich mit mir war und sie hat auch die Geduld mit mir immer auf Deutsch zu sprechen. Das hat mich sehr motiviert, als ich mich in Deutschland willkommen füllte.

Thanks a lot to Cornelia, for being always ready to help me with the rats, and also Julia for technical assistance. Many thanks to Achim, Heino and Manuela for support with the rat experiments, and also to Andreas H. and Uschi for their help.

To the lunch break group (quite a changing group though, but always fun), among them: Quique, Marius, Nicole): I guess is not a secret that I wasn't joining you because of the first quality Mensa food; it was a nice pause in the middle of the day.

To the girls in the office (Nicole, Kerstin and Adema), you were a really nice company. I am glad you were there. Each of you with your strengths made the perfect combination to help me with my "little" questions and life issues. Again, thanks a lot for listening, you have no idea how much I appreciate that!. Special thanks go for Nicole, I am tremendously grateful that you took your time to check my thesis for more than just grammar mistakes! Vielen, vielen Dank Nicole!!. What would I do without you?.

Many thanks also to Aksana, because you helped me when I needed, without even having to ask. Also many thanks to Amilcar, for your understanding and support.

I would also like to express my gratitude to my family. Quiero agradecer especialmente a mi papá (Abraham), a mi mamá (Josefa), a mis hermanos (Tato, Elena y Alberto) y sus familias porque siempre me han dado su apoyo y se han preocupado por mi. Estoy muy orgullosa de todos ustedes. Gracias además por la visita, me alegró mucho que vinieran. And last but not least I would like to thank my friends, all nice people that happened to cross into my way and end up walking beside me.

# Curriculum Vitae

Carolina Araya Callís

Date and place of birth: 08/July/1982 in Costa Rica
Nationality: Costa Rican and Spanish
Contact information: email: carito_ac1@yahoo.com

## Academic background

2008-2012 Doctoral thesis in the GGNB Graduate Program "Molecular Physiology of the Brain" University of Göttingen. Performed at the German Primate Center in the Laboratory of Clinical Neurobiology. Laboratory head: Prof. E. Fuchs. Supervisor: Prof. Dr. G. Flügge

2004-2007 Master degree in Genetics and Molecular Biology, University of Costa Rica.

2000-2004 Bachelor degree in Biology, University of Costa Rica.

## Professional background

2008-2012 German Primate Center GmbH, (DPZ): Modulation of gene expression by chronic stress in astroglia in hippocampus and prefrontal cortex. Supervisor: Prof. G. Flügge.

2007 Institute of Clinical Medicine, University of Sassari, Italy: Analysis of candidate gene polymorphisms associated with longevity. Supervisor: Dr. Gianni Pes.

2005- 2006 Institute for Human Genetics at the University of Erlangen-Nürnberg: Study of the gene MED25, responsible of the hereditary peripheral neuropathy ARCMT2B. Supervisor: Prof. B. Rautenstrauss.

2005 Institute for Health Research (INISA) at the University of Costa Rica: Assistant in the area of molecular genetics. Supervisor: Dr. A. Leal Esquivel.

| | |
|---|---|
| 2003 – 2005 | Abnormal Hemoglobin and Related Disorders Research Center (CIHATA): Assistant in the area of Molecular Genetics. Supervisor: Dr. Walter Rodríguez and Lic. Gerardo Jimenez. |
| 2001 – 2002 | Cellular and Molecular Biology Research Center (CIBCM): Assistant in the laboratory of Molecular Biology of Plants. Supervisor: Dra. Pilar Ramírez. |

## Publications

**Araya-Callís, C.**, Hiemke, C., Abumaria, N., and Flügge, G. (2012). Chronic psychosocial stress and citalopram modulate the expression of the glial proteins NDRG2 and GFAP in the hippocampus. *Psychopharmacology*. Accepted for publication.

Schnell, C., Janc, O., Kempkes, B., **Araya-Callís, C.**, Flügge, G., Hülsmann, S. and Müller, M. 2012. Restraint stress intensifies interstitial $K^+$ accumulation during severe hypoxia. *Front. Neuropharmacol.3: 53.*

## Poster presentations

| | |
|---|---|
| Washington 2011 | Annual Meeting of the Society for Neuroscience (SfN) |
| Göttingen 2011 | 8$^{th}$ Göttingen Meeting of the German Neuroscience Society |
| Amsterdam 2010 | Forum of European Neuroscience (FENS) |
| Göttingen 2009 | Neurizons |

## Stipends

| | |
|---|---|
| 2000-2005 | University of Costa Rica stipend for students with outstanding academic performance. |
| 2005-2006 | DAAD scholarship. Six months internship in the Institute of Human Genetics, University of Erlangen-Nuremberg Supervisor: Prof. Bernd Rautenstrauss. |
| 2008-2012 | Ph.D. thesis stipend, Graduate Program "Molecular Physiology of the Brain" University of Göttingen. |